Pyrolysis Oils: Characterization, Stability Analysis, and Catalytic Upgrading to Fuels and Chemicals

PYROLYSIS OILS: CHARACTERIZATION, STABILITY ANALYSIS, AND CATALYTIC UPGRADING TO FUELS AND CHEMICALS

A Dissertation Presented

by

TUSHAR P. VISPUTE

Submitted to the Graduate School of the

University of Massachusetts Amherst in partial fulfillment

of the requirements for the degree of

DOCTOR OF PHILOSOPHY

February 2011

Chemical Engineering

PYROLYSIS OILS: CHARACTERIZATION, STABILITY ANALYSIS, AND CATALYTIC UPGRADING TO FUELS AND CHEMICALS

A Dissertation Presented

by

TUSHAR P. VISPUTE

Approved as to style and content by:

_____
George W. Huber, Chair

_____
W. Curt Conner, Member

_____
Scott M. Auerbach, Member

_____
T. J. (Lakis) Mountziaris, Department Head
Chemical Engineering

ACKNOWLEDGEMENTS

I would like to deeply acknowledge the help and support of my advisor Prof. George W. Huber on this fascinating research program. George is an excellent mentor and provides an outstanding research environment in the group for graduate students to work and develop. I am fortunate to be one of his first graduate students and witness him build his successful career. I am also very thankful to Prof. Curt Conner and Prof. Scott Auerbach, for being not only very helpful committee members but also invaluable mentors on several occasions. Being one of the first two members of the group, we had to build the Huber group labs from the scratch and Curt was a tremendous help for me in that. I cannot forget that in our first year he took me and Hakan down to New Jersey in his van to buy the used lab equipments to get us started. I would like to thank all the present and past group members of Huber research group for all the enlightening discussions we had in labs and group meetings. Specifically I would like to thank Hakan Olcay and Geoff Tompsett for their insight and help with equipment design. I would like to thank Torren Carlson for the collaboration on catalytic fast pyrolysis project. I would also like to thank Asad Javaid and Xiaoming Pan for the collaboration on bio-oil stabilization project and for carrying out bio-oil filtration and viscosity measurements experiments respectively. I would like to thank Aimaro Sanna and Huiyan Zhang for help with bio-oil hydroprocessing and zeolite upgrading experiments respectively. I would also like to thank Aniruddha Upadhye for help with bio-oil characterization.

I would like to thank all the people I met here at UMass that made my five years of stay happy and memorable. I would particularly like to thank Suresh Gupta, Sarvesh

Agrawal, Vishal Gaurav, Achyuta Teella, and Hakan Olcay for their friendship. My family has been a continuous source of encouragement and support for me. They have guided and supported me through all my decisions. I would like to thank my parents, my sister Prachi, and my brother Tejas for their unconditional love. Lastly I would like to acknowledge my funding agencies. This work was supported by the U. S. Department of Energy Office of Energy Efficiency and Renewable Energy, under grant DE-FG36-08GO18212 and by the Defense Advanced Research Project Agency through the Defense Science Office Cooperative Agreement HR0011-09-C-0075.

ABSTRACT

PYROLYSIS OILS: CHARACTERIZATION, STABILITY ANALYSIS, AND CATALYTIC UPGRADING TO FUELS AND CHEMICALS

FEBRUARY 2011

TUSHAR P. VISPUTE

B.Chem.Engg., INSTITUTE OF CHEMICAL TECHNOLOGY, UNIVERSITY OF MUMBAI

Ph.D., UNIVERSITY OF MASSACHUSETTS AMHERST

Directed by: Professor George W. Huber

There is a growing need to develop the processes to produce renewable fuels and chemicals due to the economical, political, and environmental concerns associated with the fossil fuels. One of the most promising methods for a small scale conversion of biomass into liquid fuels is fast pyrolysis. The liquid product obtained from the fast pyrolysis of biomass is called pyrolysis oil or bio-oil. It is a complex mixture of more than 300 compounds resulting from the depolymerization of biomass building blocks, cellulose; hemi-cellulose; and lignin. Bio-oils have low heating value, high moisture content, are acidic, contain solid char particles, are incompatible with existing petroleum based fuels, are thermally unstable, and degrade with time. They cannot be used directly in a diesel or a gasoline internal combustion engine.

One of the challenges with the bio-oil is that it is unstable and can phase separate when stored for long. Its viscosity and molecular weight increases with time. It is important to identify the factors responsible for the bio-oil instability and to stabilize the

bio-oil. The stability analysis of the bio-oil showed that the high molecular weight lignin oligomers in the bio-oil are mainly responsible for the instability of bio-oil. The viscosity increase in the bio-oil was due to two reasons: increase in the average molecular weight and increase in the concentration of high molecular weight oligomers. Char can be removed from the bio-oil by microfiltration using ceramic membranes with pore sizes less than 1 μm. Removal of char does not affect the bio-oil stability but is desired as char can cause difficulty in further processing of the bio-oil. Nanofiltration and low temperature hydrogenation were found to be the promising techniques to stabilize the bio-oil.

Bio-oil must be catalytically converted into fuels and chemicals if it is to be used as a feedstock to make renewable fuels and chemicals. The water soluble fraction of bio-oil (WSBO) was found to contain C2 to C6 oxygenated hydrocarbons with various functionalities. In this study we showed that both hydrogen and alkanes can be produced with high yields from WSBO using aqueous phase processing. Hydrogen was produced by aqueous phase reforming over Pt/Al_2O_3 catalyst. Alkanes were produced by hydrodeoxygenation over Pt/SiO_2-Al_2O_3. Both of these processes were preceded by a low temperature hydrogenation step over Ru/C catalyst. This step was critical to achieve high yields of hydrogen and alkanes. WSBO was also converted to gasoline-range alcohols and C2 to C6 diols with up to 46% carbon yield by a two-stage hydrogenation process over Ru/C catalyst (125 °C) followed by over Pt/C (250 °C) catalyst. Temperature and pressure can be used to tune the product selectivity.

The hydroprocessing of bio-oil was followed by zeolite upgrading to produce C6 to C8 aromatic hydrocarbons and C2 to C4 olefins. Up to 70% carbon yield to aromatics

and olefins was achieved from the hydrogenated aqueous fraction of bio-oil. The hydroprocessing steps prior to the zeolite upgrading increases the thermal stability of bio-oil as well as the intrinsic hydrogen content. Increasing the thermal stability of bio-oil results in reduced coke yields in zeolite upgrading, whereas, increasing the intrinsic hydrogen content results in more oxygen being removed from bio-oil as H_2O than CO and CO_2. This results in higher carbon yields to aromatic hydrocarbon and olefins. Integrating hydroprocessing with zeolite upgrading produces a narrow product spectrum and reduces the hydrogen requirement of the process as compared to processes solely based on hydrotreating. Increasing the yield of petrochemical products from biomass therefore requires hydrogen, thus cost of hydrogen dictates the maximum economic potential of the process.

TABLE OF CONTENTS

Page

LIST OF TABLES

Table **Page**

LIST OF FIGURES

Figure **Page**

CHAPTER 1

INTRODUCTION AND OBJECTIVES

1.1 Introduction

There is a growing need to develop the processes to produce renewable fuels and chemicals due to the economical, political, and environmental concerns associated with fossil fuels.[1, 2] The only economically sustainable source of renewable carbon is the carbon fixed in biomass by photosynthesis.[3] Lignocellulosic biomass is an excellent renewable feedstock because it is both abundant and inexpensive.[3-6] Currently no industrial process exists to economically convert lignocellulosic biomass to renewable fuels and chemicals. Several routes are being studied to convert lignocellulosic biomass to fuels and chemicals including fast pyrolysis[7-10], gasification[11, 12], catalytic fast pyrolysis[13, 14], and aqueous phase processing[15-17].

One of the most promising methods for the conversion of biomass into liquid fuels is fast pyrolysis. In fast pyrolysis, bio-oil (or pyrolysis oil) is produced by rapidly heating biomass to intermediate temperatures (450-600 °C) in the absence of any external oxygen followed by rapid quenching of the resulting vapors. Bio-oil can be produced in weight yields as high as 75 wt% of the original dry biomass[18] and bio-oils typically contain 60-75% of the initial energy of the biomass[1, 10]. The other products obtained from the fast pyrolysis of biomass are char (10-20 wt% of biomass) and non-condensable gases (10-25 wt% of biomass). A wide variety of feedstock can be used to produce bio-oil, including wood, corn stover, agricultural waste, switch grass, and forest waste.

Another advantage of fast pyrolysis technology is that it can be economical at a small scale (50 to 100 tons per day of biomass) hence avoiding the significant cost penalty of biomass transport.[19, 20] Biomass has low energy density due its low bulk density (~ 0.7 kg m^{-3}). Pyrolysis oil has same heating value has biomass (16 to 18 MJ kg^{-1}), but has higher energy density than biomass due to its higher bulk density (~ 1.2 kg m^{-3}).

Bio-oil is a complex mixture of more than 300 compounds resulting from the depolymerization of biomass building blocks, cellulose; hemi-cellulose; and lignin.[10] Typical oxygen content of bio-oil is about 40-50%, resulting in low calorific value of around 16-18 MJ kg^{-1}. It is also acidic in nature with pH of about 2.5. Bio-oil is highly viscous and its viscosity increases upon storage. The moisture content of bio-oil is about 25-35 wt%. Bio-oil typically contains micron sized char particles. Bio-oil is insoluble with petroleum based fuels. Due to these reasons bio-oil is a low quality fuel and cannot be used directly in a diesel or gasoline combustion engine. In this study we first develop techniques for the physical and chemical characterization of bio-oil. This will help us in developing the bio-oil stabilization approach as well as in designing cost-effective bio-oil conversion (to fuels and valuable chemicals) processes. As shown in this thesis, bio-oil can be upgraded to fuels and chemicals that fit seamlessly in our current fuels and chemicals infrastructure. In a typical biomass fast pyrolysis process based biorefinery the bio-oil produced from various small scale pyrolysis units can be transported to a common upgrading facility. The bio-oil may be needed to be stored in such a facility. It is hence essential to answer the storage stability problems of bio-oil.

We will study the instability of bio-oil and identify the factors responsible for it and to determine how bio-oil instability problems can be mitigated. The stability will be accessed by the accelerated stability method, where bio-oil is stored at 90 °C and its viscosity is measured over time at 40 °C. The rate of viscosity increase correlates with the bio-oil stability. Following are the factors believed to be contributing towards the unstable nature of bio-oil[21]:

- Presence of char
- Presence of acids
- Presence of high molecular weight lignin oligomers
- Polymerization reactions within various bio-oil functionalities

Char particles can aggregate over time in the bio-oil. The hydrophobic components of the bio-oil can also agglomerate with the char. Char particles can also act as catalyst or nucleation sites for the polymerization reactions between various bio-oil functionalities.[22, 23] Acids present in the bio-oil can also catalyze condensation polymerization reactions within bio-oil resulting in an increase in viscosity of bio-oil upon storage. The bio-oil components can also polymerize over time in the absence of any catalyst resulting in viscosity increase. The lignin oligomers present in the bio-oil can have molecular weight up to 10,000 and can contribute substantially towards the bio-oil instability. The oligomers are found to contain various reactive functional groups as well as free radicals and hence are highly susceptible to further polymerization.[24] In this study we have systematically evaluated the effects of various parameters discussed above on bio-oil instability. Char removal by microfiltration was done in Prof. David Ford's lab

at UMass-Amherst. The viscosity measurements were done at Prof. Surita Bhatia's lab at UMass-Amherst.

The majority of the past bio-oil upgrading efforts to date have revolved around catalytic hydrotreating and zeolite upgrading. These methods suffer from several drawbacks such as catalyst coking and low yields to valuable products. Hence it is imperative to develop alternative bio-oil upgrading technologies. Aqueous Phase Processing (APP) is a promising method to convert biomass based oxygenates to fuels such as hydrogen and alkanes. It is shown in the literature that hydrogen and alkanes can be produced with high yield from aqueous solutions of pure oxygenates such as glucose and sorbitol.[15, 16, 25-28] The aqueous solutions of pure oxygenates are not feasible feedstocks with the industrial point of view. Bio-oil is cheaply available and a large fraction of it is water soluble. Hence the aqueous fraction of the bio-oil can be an excellent feedstock to be treated by APP to produce hydrogen and alkanes. Our results show that we can produce hydrogen from the aqueous fraction of the bio-oil at moderate selectivity and conversion up to 60%. Alkane can be produced from the aqueous fraction of the bio-oil at high selectivity (up to 97%) and moderate conversion (up to 60%).[29] Aqueous fraction of the bio-oil can potentially be used to produce valuable chemicals including polyols such as ethylene glycol, propylene glycol and butanediols.

Hydroprocessing can also be used to produce fuels and chemicals from bio-oil. The majority of the past bio-oil hydroprocessing efforts have revolved around using conventional sulfided CoMo and NiMo based catalysts.[30, 31] The current

hydroprocessing processes suffer from drawbacks such as high hydrogen consumption, catalyst deactivation, reactor plugging, and use of sulfided catalysts. Zeolite upgrading has also been studied extensively for bio-oil upgrading to aromatic hydrocarbons and olefins but suffer from drawbacks such has high coke yield and low valuable product yields.[32, 33] The past bio-oil upgrading processes are discussed later in detail in Sections 6.2 and 7.1.We want to combine the advantages of hydroprocessing and zeolite upgrading and eliminate the drawbacks. In this study we will develop the hydroprocessing and zeolite upgrading based processes to convert bio-oil to tangible fuels and chemicals. I will specifically study the hydrogenation of water soluble fraction of bio-oil over noble metal catalyst. Effect of operating parameters such as temperature, space velocity, and pressure are studied in detail to determine the optimum reaction conditions required to maximize the carbon yield to valuable products. Zeolite upgrading of bio-oil and its aqueous fraction will be studied and will be integrated with the hydroprocessing to maximize the aromatics and olefins yield from bio-oil. Some economic considerations will also be presented.

1.2 Objectives

The objective of this thesis is to develop realistic catalytic processes for the conversion of bio-oil into fuels and chemicals. In order to develop these catalytic processes, we first need to understand what bio-oil is, which requires the development of techniques to characterize the bio-oil. We also need to understand what makes bio-oil unstable and how the bio-oil can be stabilized. This thesis has five main objectives including:

1. Physical and chemical characterization of bio-oil.

2. Investigation of the factors responsible for the instability of bio-oil. The factors that will be studied are char, acids, and high molecular weight lignin. Various bio-oil stabilization approaches will also be investigated.

3. Conversion of aqueous fraction of bio-oil to hydrogen and alkanes by aqueous phase processing.

4. Study the single and two stage hydroprocessing of aqueous fraction of bio-oil and whole bio-oil. Study the effect of operating conditions including temperature, pressure, and space velocity to maximize the yield of desired products.

5. Study the integration of hydroprocessing and zeolite upgrading to produce aromatics and olefins from bio-oil with high yields.

CHAPTER 2

MATERIALS AND METHODS

2.1 Bio-oil

Three different kinds of bio-oils were used in this study. The oak wood bio-oil (OWBO) was obtained from the Renewable Oil International (ROI). It was produced using ROI's proprietary fast pyrolysis process where they use auger reactor to pyrolyze the biomass.[34, 35] OWBO was used for bio-oil characterization data described in Chapter 3 and for the low temperature hydrogenation (LTH) studies in batch reactor (Chapter 5), as well as for the production of hydrogen and alkanes (Chapter 5). The 2nd kind of bio-oil used in our studies is Pine Wood Bio-oil (PWBO). It was obtained from Mississippi State University. PWBO was used for the bio-oil stability studies (Chapter 4), for the low temperature hydrogenation studies in flow reactor (Chapter 6), for the 2-stage hydrogenation in flow reactor (Chapter 6), and its aqueous fraction was used for the integrated hydroprocessing and zeolite upgrading studies (Chapter 7). The 3rd kind of bio-oil used in our studies was supplied by the US Department of Energy and was manufactured by National Renewable Energy Laboratory, Golden, Colorado using the Thermochemical Process Development Unit from white oak pellets. It is called DOE-BO in this thesis. We used the aqueous fraction of DOE-BO for some of the 2-stage hydrogenation studies in the flow reactor (Chapter 6), and for the whole bio-oil studies in the integrated hydroprocessing and zeolite upgrading (Chapter 7). All of the bio-oils were stored in the refrigerator to minimize ageing.

2.2 Elemental Analysis, Ash Content, Viscometry, Accelerated Stability Testing, Water Analysis, TAN Measurement, Catalyst Characterization and TOC Analysis

Elemental analysis (C, H and O) of the bio-oil and its various fractions was done at either Schwarzkopf Microanalytical Laboratory, Woodside, NY or at Galbraith Laboratories, Knoxville, TN. Ash content of the bio-oil samples was found by heating about 1 gm of sample in a muffle furnace in the presence of air at 600-750 °C for 6 hours. The temperature was raised in stages so as to prevent the excessive boiling of bio-oil. The amount of ash remained was measured at the end of the run. The viscosity of the OWBO and its various fractions was measured in a capillary glass viscometer (from Cannon Instrument Company). Viscosity measurement of the water insoluble bio-oil (WIBO) was carried out in a TA instrument, AR2000 using a concentric cylinders geometry. All the viscosity measurements were done at 25 °C. Viscosity measurements for the accelerated stability tests were carried out by Prof. Bhatia's group at University of Massachusetts, Amherst. For the accelerated stability test, bio-oil is stored in an oven at 90 °C. Samples of this bio-oil are taken at various times. The bio-oil is allowed to cool down and the viscosity is measured at 40 °C at different shear rates. The data is reported in the form of a viscosity vs. incubation time graph. For viscous bio-oil samples, ARES G2 viscometer with 40 mm parallel plate geometry was used with a solvent trap. For diluted samples, rheometer AR2000 with concentric cylinder geometry was used. All the measurements followed the standard procedure, equilibrium for 10 minutes at desired temperature and then steady state flow test at shear rates 0.001-10 s^{-1}. Water content of the bio-oil was

determined using a Mettler-Toledo volumetric Karl-Fischer titrator V20. Total Acid Number (TAN) of the bio-oil was determined by titrating bio-oil solution in methanol with KOH solution in methanol of known concentration. Catalysts were characterized by hydrogen chemisorption in a Quantachrome Autosorb 1C. The liquid samples were analyzed for the carbon content by a Shimadzu 5000A Total Organic Carbon (TOC) analyzer. The aqueous samples were further diluted by distilled water to the concentration below 1000 ppm carbon for the TOC analysis. The TOC analyzer was standardized by sorbitol or potassium hydrogen phthalate solutions of known carbon concentrations.

2.3 Thermogravimetric Analysis

Thermogravimetric analysis (TGA) experiments were carried out with a SDT Q600 TGA system (TA Instruments). Ultra-high-purity helium (Airgas Company) was used as the sweep gas with a flow rate of 100 cm^3 min^{-1}. Approximately 15 mg of sample was loaded into an aluminum pan. An aluminum cap was placed on the sample crucible to avoid any vaporization of sample prior to starting the temperature ramp. The temperature of the sample was programmed from room temperature to 700 °C at 1.5 °C min^{-1}, followed by an isothermal period of 30 min at 700 °C.

2.4 Gel Permeation Chromatography

Gel Permeation Chromatography (GPC) experiments were carried out on a Shimadzu HPLC system with an UV detector (frequency 254 nm). Varian MesoPore

column (Part No. 1113-6325) was used with stabilized tetrahydrofuran (THF) as mobile phase flowing at 0.5 cm^3 min^{-1}. Samples for GPC were prepared by dissolving bio-oil in THF at 1 wt% concentration. The bio-oil solution in THF was then filtered with 0.45 μm filter and used for GPC. The GPC column was standardized using polystyrene molecular weight standards in the range of 162 to 38640 Da. Hence the molecular weight of bio-oil as determined by GPC will be polystyrene equivalent molecular weight.

2.5 Bio-oil Extraction and Pre-treatment

Bio-oil was mixed with distilled water to separate into two phases: an aqueous rich phase (WSBO: water soluble fraction of bio-oil) and an organic rich phase (WIBO: water insoluble fraction of bio-oil). The mixture was then centrifuged in a Marathon 2100 centrifuge (Fisher Scientific) at 10,000 rpm for 30 minutes to ensure the phase separation. The two phases, aqueous (top) and non-aqueous (bottom), were then separated by decanting. The weight of the aqueous faction was measured to determine the amount of bio-oil that dissolved in water. It was assumed that no externally added water would go into WIBO during the extraction process. Bio-oil and water were mixed in 1:4 weight ratio to get an aqueous solution with about 12-13 wt% water soluble bio-oil in water, which is about 4-5 wt% carbon in water. This aqueous solution was used in the batch as well as flow hydrogenation (single stage and 2-stage) experiments. The product of batch hydrogenation was further diluted to about 2 wt% carbon in water. This solution was then used as the feed for further aqueous phase processing experiments. Concentrated WSBO solution was used in some of the 2-stage hydrogenation studies and it was made by mixing bio-oil and water in 1:1 weight ratio. The resulting WSBO solution is about 38%

WSBO in water. The WSBO and WIBO phases of a particular bio-oil was named according to abbreviations used for those bio-oils. For example, water soluble fraction of oak wood bio-oil (OWBO) is called WS-OWBO, whereas water insoluble fraction of OWBO is called WI-OWBO. Similarly, water soluble fraction of DOE bio-oil (DOE-BO) is called WS-DOE-BO and so on.

2.6 Low Temperature Hydrogenation (LTH) of the Aqueous Fraction of Bio-oil

2.6.1 Batch Reactor

The low temperature hydrogenation was carried out in batch as well as flow reactor. In the case of batch reactor, about 80 ml of the aqueous fraction of the bio-oil (with about 5 wt% carbon) was loaded in the reactor along with 3-4 gm (50 wt% moisture content) of 5 wt% Ru / activated C catalyst (Strem Chemicals, Product No. 44-4059). The reactor was then purged at least 4-5 times with helium gas to get rid of the air present in the reaction vessel. The reactor was then purged with hydrogen at least 4-5 times to replace all the helium with hydrogen. The reactor pressure was set to 700 psi by adding hydrogen and the heating and stirring were started. Once the temperature reached the desired value, the reactor pressure was increased to 1000 psi total by adding more hydrogen. Additional hydrogen was added to the reactor during the course of reaction to compensate for the hydrogen consumption. The total pressure was maintained at 1000 psi. Amount of hydrogen consumed during the reaction was calculated from the decrease in pressure. Liquid samples were withdrawn during the run from the liquid sampling tube. The liquid samples were filtered before analysis to remove the catalyst particles.

Typical operating temperature and pressure were 175 °C and 1000 psi respectively. The product and feed compositions were measured with a Shimadzu Gas Chromatograph (GC) (model 2010) and a High Performance Liquid Chromatograph (HPLC). Flame ionization detector (FID) was used on the GC to quantify all the reactants and products except sugars, sugar alcohol and levoglucosan. The reactants and products were also verified by GCMS. Restek Rtx-VMS (Catalog No. 19915) column was used with constant column linear velocity of 31.3 cm s^{-1}. Ultra high purity helium was used as the carrier gas. Injector and detector were both held at 240 °C. The GC oven was programmed with following temperature regime: Hold at 35 °C for 5 min, ramp to 240 °C at 10 °C min^{-1} and hold at 240 °C for 5 min. On HPLC, RI detector (held at 30 °C) was used to quantify sugars, sugar alcohol and levoglucosan in the feed and product of batch hydrogenation. Bio-Rad's Aminex HPX-87H column (Catalog No. 125-0140) was used with distilled water as the mobile phase with the flow rate of 0.5 to 1 ml min^{-1}. The column oven temperature was held constant at 30 °C.

2.6.2 Flow Reactor

A gas and liquid down-flow reactor was built to study the hydrogenation of the bio-oil. Typically a ¼" diameter and 1 foot long stainless steel tube was loaded with the 5 wt% Ru/C catalyst. Both the sides were plugged with glass wool to ensure that catalyst bed stays at its place. No voids were left in the reactor tube to avoid any homogeneous reactions. An empty reactor tube was used to study the homogeneous reactions. An High Performance Liquid Chromatography (HPLC) pump (Eldex Lab Model 1SM) was used

to pump the aqueous fraction of the bio-oil. A mass flow controller was used to maintain the flow rate of hydrogen at 150 ml min^{-1}. The catalyst was reduced *in-situ* in flowing hydrogen prior to the reaction with following temperature regime: Room temperature to 260 °C at 30 °C h^{-1} and then hold at 260 °C for 2 h. The Ru/C catalyst came in the wet form, and was dried at 100 °C for 4 hour in an oven before loading in the reactor. The liquid and gas phase products flow to a gas-liquid (G-L) separator. The gaseous products continue to flow to a back pressure regulator which is used to maintain the pressure of the entire reaction system. The gaseous products are collected in a gas bag and analyzed by Gas Chromatograph-Flame Ionization Detector (GC-FID) and GC-Thermal Conductivity Detector (GC-TCD). The G-L separator is drained periodically and the liquid sample is analyzed offline by TOC analysis and by GC-FID, and HPLC as described in Section 2.6.1. The schematic of the reactor is shown in Figure 2-1. The steady state is achieved in the reactor within 4-6 h and at least 3 samples were collected to ensure that the steady state is achieved. The feed line can be heated to up to 60 °C if required.

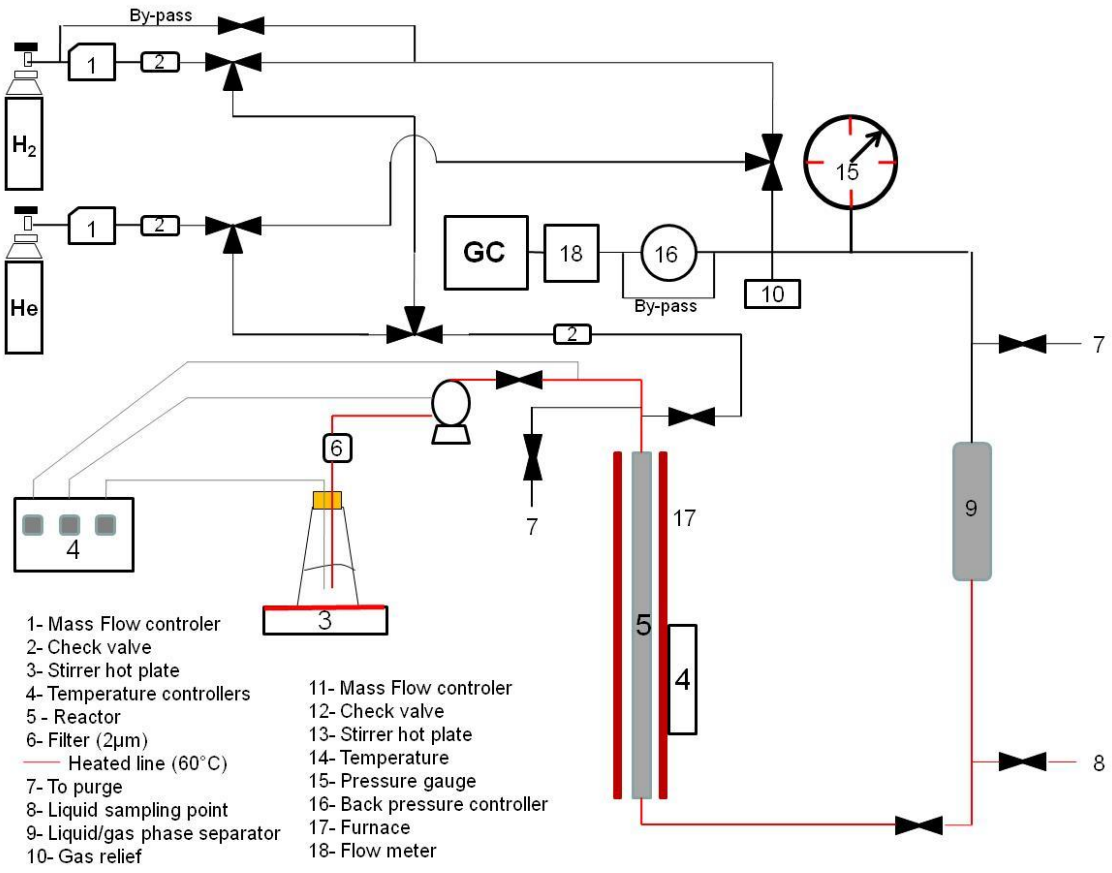

Figure 2-1 Schematic of the single stage flow reactor system used for the hydrogenation

2.7 Aqueous Phase Processing

The batch hydrogenated aqueous fraction of the bio-oil was diluted by the addition of distilled water to about 2 wt% carbon in water. This diluted product was used as the feed for the further liquid phase processing. The hydrogenation of the aqueous fraction of bio-oil was carried out at 175 °C and 1000 psi total pressure for 3 hours in a batch reactor as described earlier. A ¼" or ½" stainless steel tube was packed with the reforming or dehydration/hydrogenation catalyst with glass wool plugs on both the sides.

The catalyst used for reforming was 1 wt% Pt/Al_2O_3, and was obtained from the UOP research center (Product No. 4761-137). The dehydration/hydrogenation catalyst was 4 wt% Pt/SiO_2-Al2O_3 and was prepared by the insipient wetness method. The appropriate amount of the solution of tetraammineplatinum (II) nitrate (Strem Chemicals, Product No. 78-2010) in distilled water was added drop wise to the silica-alumina powder (SiO_2 to Al_2O_3 ratio = 4, Davison SIAL 3125) with continuous mixing. The wet catalyst was then dried in an oven at 80 °C for 7-8 h. The catalyst was then calcined in air flowing at 300 ml min^{-1}. The temperature regime for calcining was: room temperature to 260 °C in 3 h, then hold at 260 °C for 2 h. Both the catalysts (Pt/Al_2O_3 and Pt/SiO_2-Al_2O_3) were reduced in the flow reactor with hydrogen flowing from the bottom at 200 ml min^{-1}. The temperature regime used for reduction of Pt/SiO_2-Al_2O3 catalyst was: room temperature to 450 °C at 50 °C h^{-1}, then hold at 450 °C for 2 h. The temperature regime used for reducing Pt/Al_2O_3 catalyst was: room temperature to 260 °C at 30 °C h^{-1}, then hold at 260 °C for 2 h.

The reactor tube was heated by a Lindberg (type 54032) furnace. The liquid feed was fed to the reactor from the bottom (*i.e.* up-flow mode) with the help of a JASCO PU980 HPLC pump. A gas-liquid separator was employed after the reactor tube. Helium was supplied from top as the carrier gas at the flow rates from 30 ml min^{-1} to 60 ml min^{-1}. The gaseous products from the reactor (and helium carrier gas) flow through a back pressure regulator, used to maintain the pressure of the reaction system. External hydrogen, required for catalyst reduction or for the reaction was supplied from the bottom

of the reactor (flow rate: ~100 ml min^{-1}) and no carrier gas was used in such a case. The gaseous products were further analyzed by two online gas chromatographs (HP 5890 series II). Permanent gases in the gaseous product (CO_2 and H_2) were analyzed by a Thermal Conductivity Detector (TCD). Alltech HAYESEP DB 100/120 packed column (Part no. 2836PC) was used with the oven temperature held constant at 75 °C. The TCD and the injection port were held at 160 °C and 120 °C respectively. The column flow rate was 1 ml min^{-1} with helium carrier gas. Alkanes in the gaseous product were analyzed on a FID with Alltech AT-Q capillary column (Part no. 13950). Helium was used as the carrier gas with the column flow rate of 1 ml min^{-1}. The injection port and the detector were both held at 200 °C. Following GC oven temperature regime was used: Hold at 40 °C for 6 min, ramp to 180 °C at 5 °C min^{-1} and hold at 180 °C for 25 min. Carbon selectivity to a particular alkane was calculated by dividing the carbon moles in that particular alkane by total carbon moles in all of the alkanes. For a particular catalyst loaded in the reactor, liquid feed was started at time t = 0. Steady state was usually reached within 8 hours. At least 3 gas samples were analyzed to ensure the steady state. Liquid product accumulated in the gas-liquid separator was drained then. Liquid product was analyzed for the carbon content. Reactions parameters were then changed for further studies. Time on stream for a particular catalyst from the start of reaction (t = 0) was noted for each sample and was denoted by Time On Stream (TOS) for that catalyst.

2.8 Two Stage Hydrogenation of Water Soluble Bio-oil

For the two stage hydrogenation a 2nd tubular reactor (30 cm length, 6.35 mm outer diameter) was added in series after the first (low temperature) hydrogenation reactor with all of the other reaction system remaining the same as single stage operation. Dry 5 wt% Pt/C (Strem Chemicals Product No. 78-1509) was as the catalyst used in this reactor and the catalyst was reduced *in-situ* prior to the reaction with the same temperature regime as that used for Ru/C catalyst. Pt/C catalyst was also dried in an oven at 100 °C for 4 hours before loading in the reactor. Same amount of catalyst was loaded in both the reactors. Pressure was 1450 psi typically foe both reactors and the low temperature hydrogenation step was operated at 125 °C. Various temperatures were studied for the 2nd high temperature stage. While operating with 2 reactors, the first reactor was heated using a heating tape and the second reactor was heated using the tubular furnace. A type K thermocouple was placed next to the reactor wall and reactor temperature was controlled at 125 °C using an Omega temperature controller. The products were analyzed by TOC, GC-FID, and HPLC as described in previous sections.

2.9 Zeolite Upgrading of Bio-oil, Water Soluble Bio-oil and Hydrogenated Water Soluble Bio-oil

The zeolite upgrading was done using H-ZSM-5 catalyst obtained from Zeolyst (CBV 3024E, SiO_2/Al_2O_3 = 30). All the pure compounds used in the zeolite upgrading were > 99% pure (from Fisher Scientific) and were used without further purification. Prior to loading in the reactor, the ZSM-5 catalyst was sieved to 425-800 μm size. A

quartz tube (1.27 cm outer diameter) was packed with a quartz wool plug. Quartz beads (700 mg, 250-425 μm particle size) were placed on the quartz wool plug to act as a catalyst bed support. The sieved ZSM-5 catalyst (26 mg typically) was then loaded in the reactor. The catalyst was then calcined *in situ* in flowing air (60 ml min^{-1}, dehumidified by passing through a drierite tube) at 600 °C for 6 hours. The reactor temperature was measured using a type K thermocouple inserted into the catalyst bed. Reactor tube was heated using a Lindberg tubular furnace and temperature was controlled using an Omega temperature controller. Once the calcination was complete, helium carrier gas flow was started over the catalyst at 204 ml min^{-1}. The catalyst was maintained at reaction temperature. All the experiments were carried out at atmospheric pressure and no significant pressure drop was observed across the catalyst bed. The liquid feed was then started at 2.7 ml $hour^{-1}$ for WSBO, low temperature hydrogenated WSBO and high temperature hydrogenated WSBO which corresponds to the WHSV of 11.7 $hour^{-1}$ on the bio-oil content basis (excluding the added water). The liquid feed rate of 0.34 ml $hour^{-1}$ (0.06 ml $hour^{-1}$ for furan) was used for DOE-BO and low temperature hydrogenated DOE-BO, which corresponds to the WHSV of 11.7 $hour^{-1}$ (1.97 $hour^{-1}$ for furan). Liquid was pumped using a syringe pump (KD Scientific, Model No. 780100). For pure compounds (except furan), 12.5 wt% solution in water was used as feed. This is to keep the partial pressure of water the same for pure compounds and WSBO (and its hydrogenated products). Pure furan was used as feed as it is water insoluble.

The reactor effluent is carried by the helium carrier gas to an ice-water cooled condenser where heavy products are condensed. The effluent gas was then collected in a

gas bag. The heavy products in the condenser were collected by washing the condenser with 10 cm^3 of ethanol. Liquid product was analyzed by an Agilent 7890A GC-FID system with an Agilent capillary column (Catalog No. 19091J-413). Helium was used as carrier gas with the FID detector maintained at 250 °C. Following column temperature regime was used: hold at 40 °C for 5 min, ramp to 250 °C at 20 °C min^{-1}, and hold at 250 °C for 20 min. The gaseous product was analyzed using a Shimadzu 2014 GC system. Restek Rtx-VMS capillary column (Catalog No. 19915) was used to quantify aromatic hydrocarbons (with FID detector) and HAYSEP D packed column from Supelco was used to analyze CO and CO_2 (with TCD detector). Both FID and TCD detectors were maintained at 240 °C. Helium was used as the carrier gas. Following column temperature regime was used with both the columns: hold at 35 °C for 5 min, ramp to 140 °C at 5 °C min^{-1}, ramp to 230 °C at 50 °C min^{-1} and hold at 230 °C for 8.2 min. The coke yield was measured by burning the coke and measuring the amount of CO_2 produced. After the reaction is complete, dry air (60 cm^3 min^{-1}) was flown over the spent catalyst (600 °C) for 2 hours to burn off the coke formed during the reaction. The resulting effluent gas was then passed in series through a copper converter (to convert CO to CO_2), a moisture trap and a CO_2 trap. Copper converter (Sigma Aldrich, Part No. 417971) contained 13 wt% CuO on alumina catalyst and was operated at 250 °C. The coke yield was determined from the difference in the mass of the fresh and spent CO_2 adsorbent.

2.10 Bio-oil Microfiltration and Nanofiltration

Membralox® TI-70 microfiltration membranes with nominal pore sizes of 0.5 µm and 0.8 µm were obtained from Pall Fluid Dynamics, Deland FL. These tubular

membranes were 25 cm in length with an outer diameter of 10mm and an inner diameter of 7 mm. Each membrane consists of a filtering layer which is about 10–15 μm thick. The filtering layer is supported by two layers; an under layer with an approximate pore size of 10 μm and the macroporous support layer.[36, 37] The total surface area available for filtration was 98.55 cm^2. The microfiltration experiments were conducted by placing the membrane in a stainless steel housing (part # S700-00141) also obtained from PALL Fluid Dynamics. Rubber O-rings, metal and Teflon gaskets and stainless steel screws were used at both ends to secure the membrane inside the holder. The DOE bio-oil was used for these studies. Methanol, sodium hydroxide and acetic acid all of purity > 99% (from Fischer Scientific) were used for cleaning the membrane. Figure 2-2 shows the schematic of the microfiltration permeation setup. The fluid was pumped into the tube side of the membrane using a positive displacement gear pump obtained from Cole Parmer. The pressure differential across the membrane was measured using a pressure gauge at the inlet side of the module. Since the outlet was at atmospheric pressure the gauge reading directly provided the pressure difference for the permeation experiment. Stainless steel tubing of 1/4 in. diameter was used at the inlet and the outlet tubing diameter was reduced to 1/8 in. A needle valve was used at the outlet to control the trans-membrane pressure. All experiments were conducted in the cross-flow mode to reduce the fouling effects. The retentate flow was kept at nearly 90% of the total feed flow for both water and bio-oil permeation experiments. The retentate was collected and recycled back to the feed tank. The water permeation experiments were conducted at room temperature. However, due to the high viscosity of bio-oil, microfiltration of bio-oil was carried out at elevated temperatures near 40 °C; more precisely, temperature was

maintained within in the range of 38–45 °C during the course of an experiment. For this purpose the bio-oil feed tank was placed on a heating mantle with a magnetic stirrer. The feed and retentate temperatures were monitored by using thermocouples placed at the two ends. To maintain the temperature across the module a heating tape covered with an insulation tape was wrapped around the tubing and the membrane housing. The same experimental set-up was used for bio-oil nanofiltration. The membranes with an additional 5 nm or 10 nm pore size filtering layer were used.

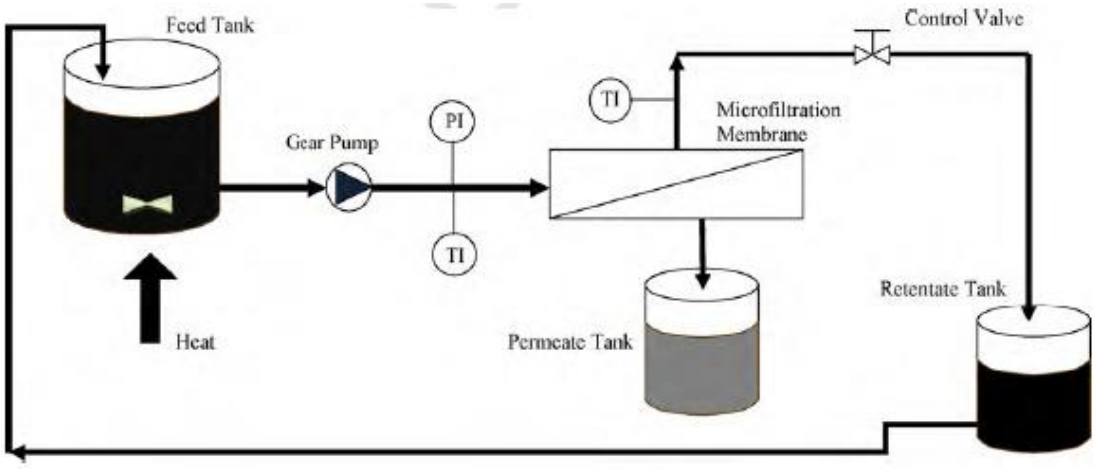

Figure 2-2 Schematic of the bio-oil microfiltration process

CHAPTER 3

CHARACTERIZATION OF BIO-OIL

3.1 Introduction

It is important to characterize the bio-oil that is used in the studies as every bio-oil has different composition depending on its biomass source and the pyrolysis conditions used. We have used various characterization techniques to characterize the bio-oil. Physical characterization was done by the viscosity and solubility measurements. GC-MS was used to identify the components. GC-MS, GC-FID and HPLC were used for the quantification of the components.

A large part of bio-oil literature is devoted to its characterization. Typical bio-oil properties are shown in Table 3-1 with comparison to heavy fuel oil.[7] Bio-oil has low heating value due to its high oxygen and moisture content. Bio-oil has acidic pH. It is thermally unstable and leaves up to 50 wt% residue upon distillation. Peacocke *et al.* gives a detailed documentation of the physical properties of the bio-oil.[38] Chemically bio-oil is a complex mixture of various components. Not all of the bio-oil constituents are identifiable by common analytical techniques such as GC and HPLC. Typical important fractions of bio-oil are shown in Figure 3-1.[10] Only about 30-40% of the bio-oil is said to be quantifiable by GC.[10, 39] Another 15% can be identified by HPLC.[10] Bio-oil contains high molecular weight lignin up to 30-35 wt% which is difficult to analyze by GC.

Table 3-1 Typical physical properties of bio-oil and heavy fuel oil*

Physical Property	Bio-oil	Heavy fuel oil
Moisture content (wt%)	15-30	0.1
pH	2.5	-
Specific gravity (gm ml^{-1})	1.2	0.94
Elemental composition (wt%)		
Carbon	54-58	85
Hydrogen	5.5-7.0	11
Oxygen	35-40	1.0
Nitrogen	0-0.2	0.3
Ash (wt%)	0-0.2	0.1
HHV (MJ/kg)	16-19	40
Viscosity (cP) at 50 °C	40-100	180
Solids (wt%)	0.2-1.0	1
Distillation residue (wt%)	up to 50	1

*Data taken from reference (*7*)

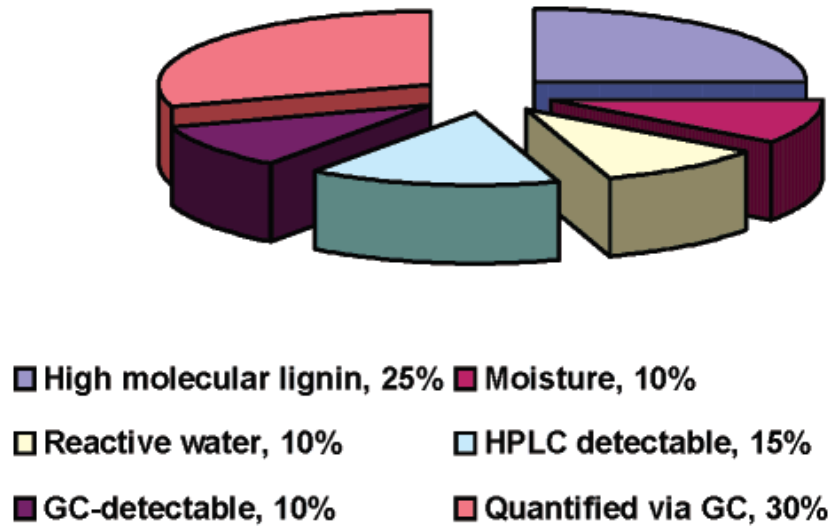

Figure 3-1 Bio-oil fractions classification. Data taken from reference (*10*)

The solubility of bio-oil in various solvents varies. It is almost completely miscible with solvents such as methanol, iso-propanol and acetone. Sipila *et al*. describes a bio-oil characterization technique where they extract three different bio-oils in water.[(40)]

The aqueous fraction is then extracted in diethyl ether. The water solubility of various bio-oils was found to be in the range of 60-80 wt%, whereas ether solubility was in the range of 40-60 wt%. The ether insoluble fraction mainly consisted of polysaccharides that are present in the water soluble fraction.

3.2 Experimental

The experimental methods and materials used for this work are described in Sections 2.1, 2.2, 2.4, and 2.5.

3.3 Elemental Analysis

Elemental analysis of the OWBO was found to be 47.0 wt% carbon, 8.2 wt% hydrogen and the rest oxygen. Nitrogen was not detected. The oxygen content of 44.8 wt% is higher as compared to other bio-oils. Typical bio-oil oxygen content is in the range of 35 to 40 wt%.[41] In addition to carbon, oxygen and hydrogen, nitrogen (0 to 0.2 wt%) can be present in the bio-oil.[7] Mineral components of the biomass (including potassium, sodium, calcium and magnesium) also end up in the bio-oil in trace quantities.[10] Typical ash content of bio-oils is 0-0.2 wt%.[7] The ash content of OWBO was 0.3 wt%.

3.4 Solubility Studies and Chemical Composition

Upgrading of the bio-oil without using any solvent is preferred if possible. However, this route has many problems such as high viscosity and thermal instability of

bio-oil, clogging of reactors, considerable coking, and catalyst deactivation due to coking. Bio-oil can be dissolved in a suitable solvent and then treated for upgrading to help ease these problems. The oak wood bio-oil (OWBO) used in this study was found to be almost completely miscible in methanol, iso-propanol and acetone with small amounts of solid residue. About 14 wt% of the bio-oil was found to be soluble in toluene, which is a gasoline like solvent. Solubility of this bio-oil in diesel fuel was about 4 wt%. The solubility were measured by mixing bio-oil and solvent in a 1:1 w/w ratio at room temperature and the two layers formed were separated by decanting after centrifugation. Toluene and diesel fuel fractions were found to be consisting of guaiacol and its derivatives. Low solubility of bio-oil in toluene and diesel fuel signifies its incompatibility with conventional liquid transportation fuels. An ideal solvent for hydroprocessing of the bio-oil should dissolve a considerable fraction of bio-oil and should be inert to hydrogenation. Alcohols such as methanol and iso-propanol are not inert to the hydrogenation. Whereas gasoline or diesel fuel range saturated liquid alkane are relatively unreactive during hydrogenation, but are incompatible with the bio-oil.

Two phases form, when OWBO is mixed with water at water to bio-oil weight ratio of greater than 1 to 4. About 60 to 65 wt% of the OWBO is soluble in water irrespective of the amount of water added. The two phases can be separated by centrifuging and then decanting. Water is inert for hydrogenation. Furthermore, a significant fraction of the bio-oil is water soluble, making water an ideal solvent for the hydroprocessing of bio-oil. The elemental balance for mixing OWBO with water is shown in Figure 3-2 for water to bio-oil weight mixture of 1:1. As can be seen in this

figure the WS-OWBO has higher oxygen content than the WI-OWBO. About 62 wt% of the original bio-oil is in the aqueous phase. This also includes water that was present in the bio-oil. Our findings are similar to those of Sipila et al., where 60 wt% of the bio-oil (made from mixed maple and oak wood) was found to be water soluble.[40]

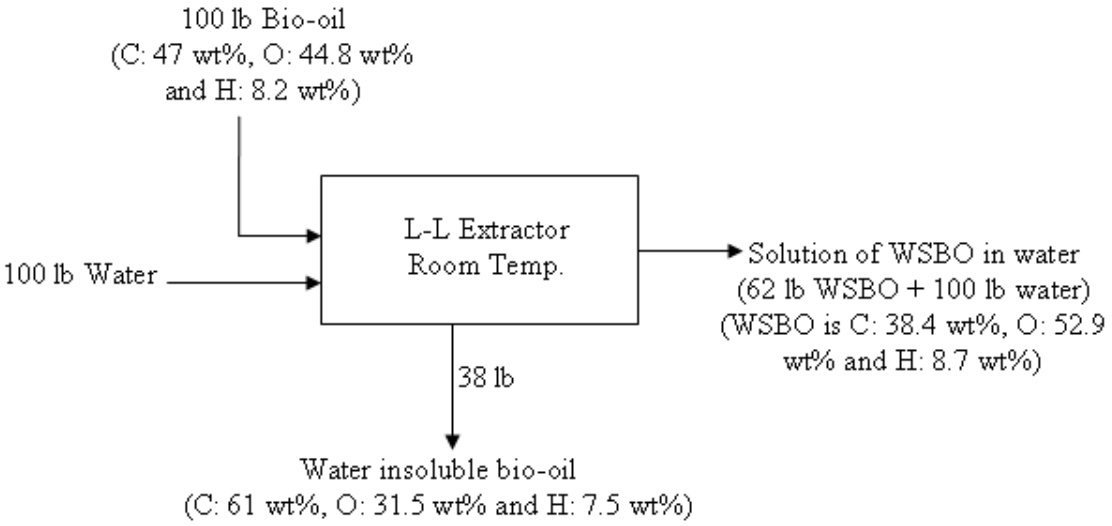

Figure 3-2 Extraction of oak wood bio-oil in water

The WSBO was analyzed with GC-MS, GC-FID, HPLC and TOC as shown in Figure 3-3. The major components of the aqueous fraction are levoglucosan > sugars (glucose + xylose) > acetic acid > hydroxyacetone > furfural + 2-furanone > guaiacols > hydroxyacetaldehyde. We were only able to identify 60% of the carbon in the aqueous fraction of the bio-oil with our methods used in this study. This did however help us in understanding some of the bio-oil conversion reactions.

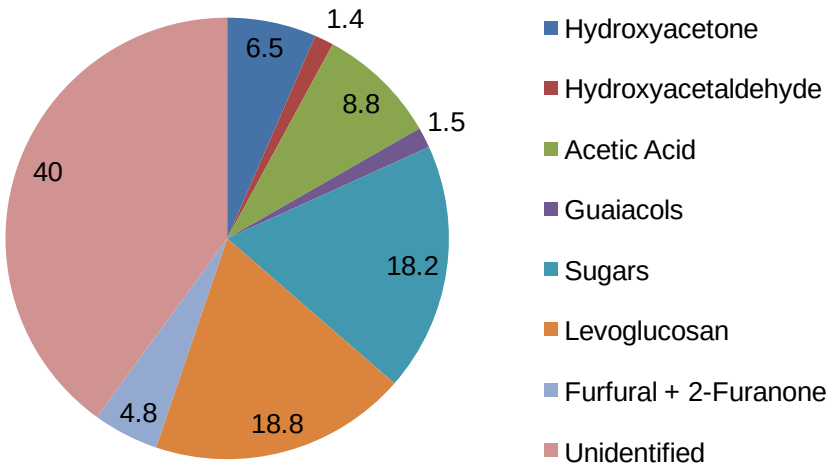

Figure 3-3 Identification of the major components of water soluble fraction of oak wood bio-oil. The aqueous fraction was made by mixing 9 gm of oak wood bio-oil with 80 gm water.

The rest of the carbon is probably present in the form of compounds like formic acid, various furans, and higher molecular weight sugars (e.g. cellobioses and trioses). The column used in HPLC can separate sugar, sugar alcohols and anhydrosugars. This column cannot separate various sugars from each other. A broad peak was observed for sugars in HPLC. Various sugars may be present including glucose, xylose, fructose, mannose and galactose. Piskorz *et al.* have identified hydroxyacetaldehyde up to 10 wt% in the bio-oil.[42] We found that only 1.5% of the carbon in WSBO was from hydroxyacetaldehyde. Formic acid could not be observed in our solution due to the large amounts of water we used and hence is not quantified here. High molecular weight degradation products of pentoses, hexoses are also present in the bio-oil[10] and were not detected by our analytical methods. Cellobiosan is known to be present in the bio-oil in a significant amount.[40, 43] Luo *et al.* have identified phenolic compounds (phenol and its alkyl derivatives) up to 20 wt% in the bio-oil made from *P. indicus*.[44] Phenol and its

alkyl derivatives were also not detected in significant amounts in the bio-oil we used for this study.

The composition of the bio-oil, the storage conditions and storage time are the factors affecting the bio-oil phase separation. Some bio-oils can phase separate during the storage without the addition of external water. The extent of separation of bio-oil in the two phases can also depend on the method of addition of water to it.[40] The oak wood bio-oil used in our studies phase separates upon addition of small amount of water. The minimum water to bio-oil ratio required for phase separation was 1:4 (weight ratio). The amount of bio-oil extracted in water was independent of the amount of water added as long as water to bio-oil ratio was above 1:4. This ensures that concentrated aqueous solutions of water soluble bio-oil can be used in our process. However, dilute WSBO solutions were used in our studies primarily because of the lack of large amounts of bio-oil.

The composition of pine wood bio-oil (PWBO), DOE bio-oil and their water soluble fractions will be presented in the later part of the thesis wherever relevant.

3.5 Viscosity Measurements

The various bio-oil fractions have a wide range of viscosities, which are probably due to both intramolecular and intermolecular interactions. Bio-oils are also known to undergo viscosity changes during ageing and bio-oil upgrading.[21, 30] Table 3-2 shows the viscosity of bio-oil, bio-oil mixtures and bio-oil fractions prior to upgrading. The oak

wood bio-oil used in our studies was found to have the viscosity of 153 cP at 25 °C. Typical viscosity values of the bio-oil reported in the literature depicts an order of magnitude variation. According to Bridgwater *et al.* the viscosity of bio-oils ranges from 30 to 200 cP at 40 °C.[9] The viscosity can be as high as 1000 cP at 40 °C depending on the feedstock and process conditions.[7] The viscosity of the bio-oil decreases exponentially upon addition of small amount of solvents. As shown in Table 3-2 addition of 20 wt% of methanol to bio-oil results in an order of magnitude decrease in the viscosity.

Table 3-2 Viscosity of the oak wood bio-oil and its fractions

	Viscosity[a] *(cP)*
Oak Wood Bio-oil (OWBO)	153
80wt% OWBO in methanol	17.1
50wt% OWBO in methanol	2.93
20wt% OWBO in methanol	1.01
Water insoluble OWBO[b]	50000
80wt% water insoluble OWBO in methanol	95.1
50wt% water insoluble OWBO in methanol	5.1
20wt% water insoluble OWBO in methanol	1.04
Water soluble OWBO solution[c]	1.65

[a]All the viscosity measurements are done in a capillary glass viscometer (except for water insoluble bio-oil) at 25 °C
[b]TA instrument AR2000 used with concentric cylinders geometry
[c]Solution was 50 wt% water soluble oak wood bio-oil in water

The water insoluble bio-oil from OWBO is highly viscous sticky brown liquid with the viscosity of more than 50000 cP. Its viscosity also decreases exponentially upon addition of methanol. The phenolic compounds originating from lignin are present in the bio-oil as both monomeric and oligomeric compounds.[10] These phenolic compounds are present in significantly higher concentrations in the WIBO than in the WSBO. These high molecular weight oligomers can form a network due to intermolecular interactions resulting in high viscosity of the bio-oil. A rheological study of bio-oil obtained from the soft wood bark residue indicates the existence of self-aggregating intermolecular interactions forming long-range network structures.[45] These interactions will be stronger in the water insoluble bio-oil due to its concentrated nature, explaining the very high viscosity observed for it. Addition of methanol to bio-oil or WIBO results in disrupting of the intermolecular network due to solvation, significantly reducing the viscosity.

Some of the bio-oils that we used were further characterized for their instability by accelerated stability test followed by measurement of viscosity and molecular weight distribution by GPC. That characterization will be presented in Chapter 4.

3.6 Gel Permeation Chromatography

Only a fraction of carbon in bio-oil is detectable using analysis techniques such as gas chromatography and liquid chromatography. The GC and HPLC undetectable carbon in bio-oil is present in the form of lignin and sugar oligomers. Gel permeation chromatography (GPC) can be used to determine the molecular weight distribution of bio-oil. Figure 3-4 depicts the GPC chromatographs of DOE bio-oil and its aqueous and

organic (water insoluble) fractions. It can be seen that bio-oil contains oligomers with molecular weight up to 6000. The concentration of oligomers is higher in water insoluble fraction as these oligomers are mostly derived from lignin and hence are water insoluble. Some of the highly functionalized oligomers can be water soluble and hence water soluble bio-oil also shows the presence of oligomers with molecular weight up to 1000, although at considerably less concentration than bio-oil and water insoluble bio-oil.

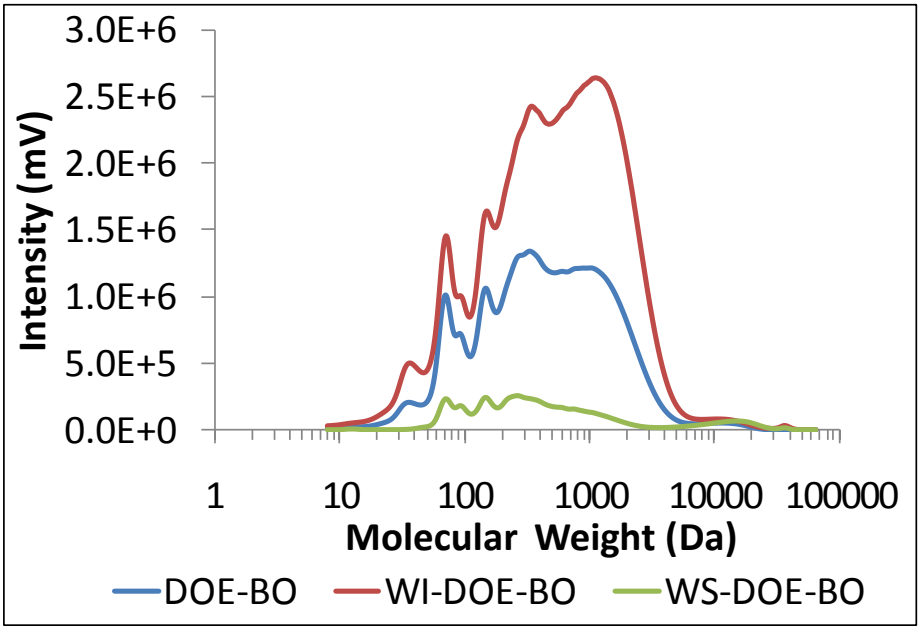

Figure 3-4 Gel permeation chromatographs of DOE bio-oil, water soluble DOE bio-oil (WS-DOE-BO) and water insolubel DOE bio-oil (WI-DOE-BO)

3.7 Conclusion

Bio-oil is a complex mixture of oxygenated hydrocarbons of various functionalities including aldehydes, ketones, acids, sugars and anhydro-sugars. Only about 35-40% carbon in bio-oil is detectable by GC and HPLC and is present in C2 to C6

oxygenated hydrocarbons. Bio-oil is highly soluble in water. With water being ideal solvent for hydroprocessing, water soluble bio-oil would be an ideal candidate for hydroprocessing to produce valuable fuels and chemicals. Only about 10-15% carbon is detectable in water insoluble bio-oil and is present mostly in the form of guaiacols and its derivatives. The rest of the carbon as ensured by gel permeation chromatography is present in the form of high molecular weight oligomers. Hence along with GC and HLPL, GPC should be a core bio-oil analysis technique as it enables us to see the GC and HPLC undetectable carbon in bio-oil. The aqueous fraction of bio-oil also contain high molecular weight oligomers with molecular weight up to 1000, but at low concentration compared to that in bio-oil and in water insoluble bio-oil.

Bio-oil contains a wide variety of compounds and it would be challenging although crucial to convert it to valuable fuels and/or chemicals with high selectivity so as to reduce downstream processing costs such as separation cost. Another important finding is that the water soluble bio-oil and water insoluble bio-oil have significant physical and chemical differences. Hence different processing techniques might be required to convert water soluble and water insoluble fractions of bio-oil to tangible fuels and chemicals.

CHAPTER 4

STABILIZATION OF BIO-OIL

4.1 Introduction

Bio-oil stability is of importance for its transport, storage and further processing. Bio-oil is a complex mixture of compounds which is not at equilibrium due to the rapid quenching in pyrolysis process. Due to this, the mixture changes chemically and physically towards the equilibrium during the storage.[21]

Different theories have been proposed to explain the causes of the instability of bio-oils. Proposed mechanisms include agglomeration of char and reactions of unsaturated or reactive chemicals, such as polymerization, esterification, acetalization, oxidization, dimerization, etc.[46-48] The minerals can also concentrate in the chars and catalyze the aging reactions.[21, 22, 49] Char particles also may attract low polarity molecules on to their surface and work as condensation nuclei.[22, 23] Czernik et al. reported the evidence of esterification and etherification as the mechanisms for condensation of bio-oils.[7] Diebold proposed that the acids could work as catalysts by accelerating the polymerization reactions within bio-oil compound.[21, 49] Fratini et al. reported that the condensation and polymerization of lignin in bio-oils could cause viscosity increase and phase separation.[50]

The change in viscosity of bio-oil over time can be a direct measure of bio-oil stability. The viscosity of the bio-oil increase over time and this can be related to the

molecular weight increase if volatiles are not allowed to escape during the storage.[49] Thus viscosity indirectly is a measure of polymerization reactions taking place in bio-oil. Water content of the bio-oil also typically increases with time due to the formation of water in condensation polymerization reactions that occur within bio-oil. The rate of viscosity increase is proportional to the storage temperature of bio-oil. Typical bio-oil stability studies are hence done at elevated temperatures such as 60-90 °C. Czernik et al. incubated the oak wood bio-oil at 90 °C and measured its viscosity, water content and apparent weight average molecular weight (M_w) with time.[51] The data is tabulated in Table 4-1. The authors also show that there exists a linear correspondence between weight average molecular weight and viscosity of bio-oil.

Table 4-1 Viscosity, water content and weight average molecular weight changes in oak wood bio-oil at 90 °C

Time (days) at 90 °C	Water Content (wt%)	Time (h) at 90 °C	Viscosity (cP) at 40 °C	M_w
0	16.2	0	144	530
7	16.2	1	152	560
17	16.6	2	167	600
28	17.3	4.5	210	690
56	17.5	8	286	790
84	17.7	15	326	860

Data taken from reference (*51*)

Diebold has compiled the viscosity versus time data for four different kinds of bio-oil in his report.[21] He plotted the rate of viscosity increase versus the inverse of storage temperature and found a linear Arrhenius like correlation. This indicates towards the chemical reactions as the reason for the viscosity increase in bio-oils. Following are the major reactions that can occur within the bio-oil:[21]

- Organic acids + alcohols → esters + water.
- Organic acids + olefins → esters.
- Aldehydes + water → hydrates.
- Aldehydes + alcohols → hemiacetals + acetals + water.
- Aldehydes → oligomers + resins.
- Aldehydes + phenolics → resins + water.
- Unsaturated compounds → polyolefins.

Not much literature is available on the actual chemical changes taking place within the bio-oil. Diebold reports that the amount of hydroxyacetaldehyde, propenal (acrolein), 2-methoxy-4-propenylphenol, and 5-methylfurfural in bio-oil quickly decreases during ageing at 90 °C.[21]

In this study, we treated the bio-oils using filtration, water extraction, solvent extraction and hydrogenation to test the effects of chars, acids, unsaturated chemicals, and lignin on the rate of viscosity increase in pyrolysis oils.

4.2 Material and Methods

The experimental procedure and materials used in this study are described in Sections 2.1, 2.2, 2.10, and 2.11.

4.3 Stability Analysis of Bio-oil and its Fractions

To establish the base case for the stability of bio-oil, pine wood bio-oil (PWBO) was incubated in a tightly sealed container in an oven at 90 °C. Samples were withdrawn at various times and the viscosity was measured at 40 °C at the shear rates of 1 s^{-1} and 10 s^{-1}. The results of this study are shown in the Figure 4-1. The viscosity of the bio-oil increases upon incubation at 90 °C. The viscosity increase with the incubation time is exponential in nature. The viscosity increase can be more prominently observed at low shear rate than high. The data for viscosity increase at the shear rate of 10 s^{-1} can be fitted with a straight line as shown in Figure 4-1. The initial viscosity of the PWBO is about 0.078 Pa-s (78 cP). The rate of viscosity increase for incubation time less than 250 h is about 0.0026 Pa-s h^{-1}, which is about 3 % h^{-1}. We saw an order of magnitude increase in viscosity within 250 h. The reason for the viscosity increase can be the polymerization reactions taking place in the bio-oil when stored at high temperature. The polymerization may or may not be catalyzed by char and/or acids in bio-oil.

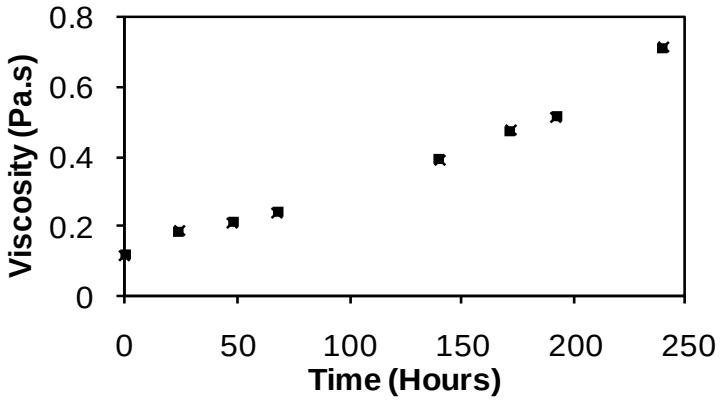

Figure 4-1 Viscosity of pine wood bio-oil versus incubation time at 90 °C.

The stability of aqueous and non-aqueous phases of the PWBO was also studied. The accelerated stability data for the Water Insoluble PWBO (WI-PWBO) is shown in Figure 4-2. The WI-PWBO was incubated at 90 °C only for about 32 h. The initial viscosity of the water insoluble fraction is about 1.4 Pa-s which is about 20 times of the viscosity of whole bio-oil. The WI-PWBO shows an exponential rise in viscosity when incubated at high temperature. Averaging over the two shear rates, there is about 25% increase in viscosity of WI-PWBO over the incubation time of 32 h.

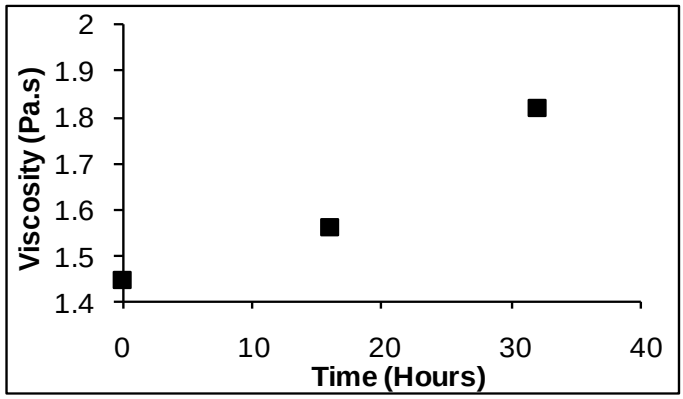

Figure 4-2 Viscosity of Water Insoluble – Pine Wood Bio-oil versus incubation time at 90 °C.

The accelerated stability test data for the aqueous fraction of the PWBO (WS-PWBO) is shown in Figure 4-3. The aqueous fraction was made by mixing 75 gm of PWBO with 60 gm of water and the two layers are separated by decanting after centrifugation. The resulting aqueous fraction was about 39.5 wt% WS-PWBO in water. The viscosity increase upon incubation at 90°C is apparent for WS-PWBO only at low shear rate of 1 s^{-1} as seen in Figure 4-3. The viscosity of WS-PWBO almost doubles in about a day upon incubation. The viscosity rise is linear for the time period studied as

opposed to PWBO and WI-PWBO which show an exponential rise in viscosity as seen earlier. The aqueous fraction of the bio-oil do not contain any char particles as all the char particles tend to go in water insoluble part upon centrifugation. This implies that the polymerization reactions that cause the viscosity increase in various bio-oil fractions can proceed even in the absence of the char particle. The rate of viscosity increase is lower for the WS-PWBO as compared to that for PWBO and WI-PWBO. This can be due the diluted nature of the WS-PWBO.

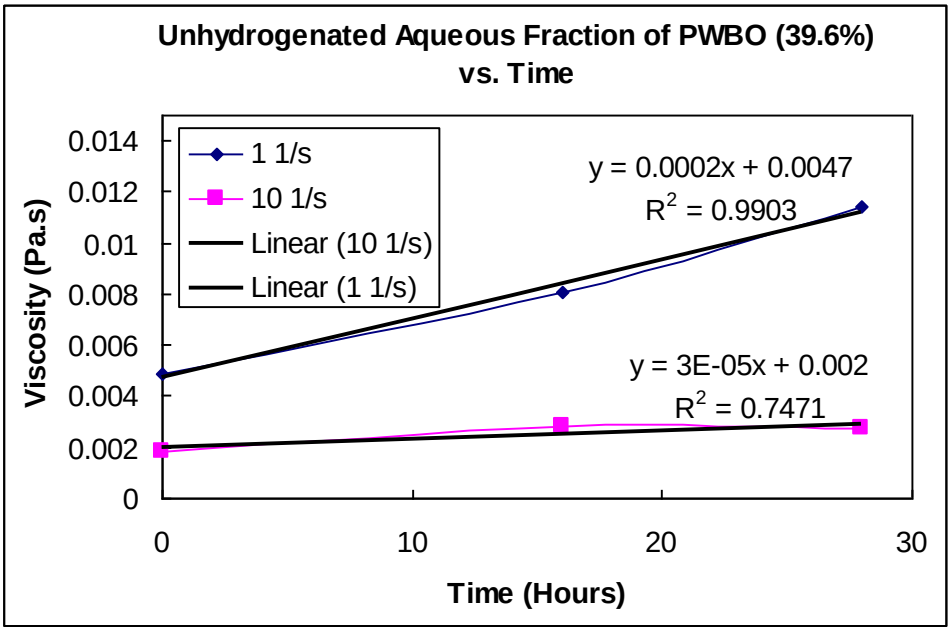

Figure 4-3 Viscosity of water soluble pine wood bio-oil versus incubation time at 90 °C.

The aqueous fraction of the Pine wood bio-oil (WS-PWBO) discussed in above study was hydrogenated in the Parr batch reactor at 125 °C and 1000 psi for 4 hours with 5 wt% Ru/C catalyst. Upon hydrogenation all the thermally unstable functionalities (aldehydes, ketones, sugars) in the WS-PWBO are converted to corresponding alcohols. Acetic acid is resilient to the hydrogenation at the reaction conditions we used. The

hydrogenated WS-PWBO was then subjected to the accelerated stability tests and the results are depicted in Figure 4-4. The viscosity of the hydrogenated aqueous fraction of the bio-oil does not increase upon incubation at 90 °C. The viscosity is constant at high shear rate and shows a decrease at low shear rate as seen in Figure 4-4. This behavior can be attributed to the stable, non-reactive nature of the chemicals present in the hydrogenated WS-PWBO. Since we eliminate all the reactive functionalities from the WS-PWBO by hydrogenation, the polymerization reactions that cause the viscosity to increase upon incubation are suppressed. Hence low temperature hydrogenation treatment can be used to stabilize the aqueous fraction of the bio-oil.

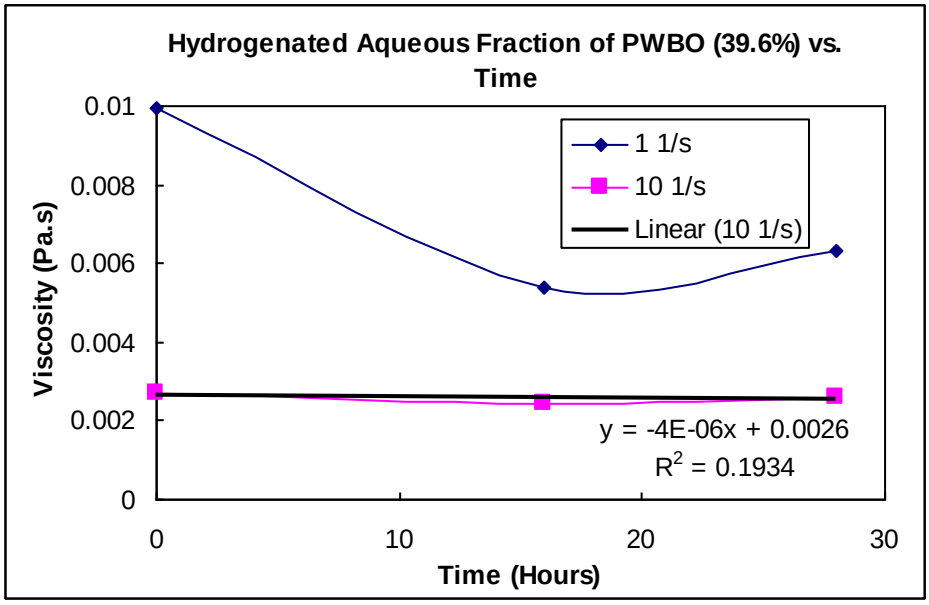

Figure 4-4 Viscosity of hydrogenated water soluble pine wood bio-oil versus incubation time at 90 °C.

4.4 Stability Analysis of the Model Bio-oil Systems

It is evident that the chemical changes taking place in the bio-oil and its various fractions during the high temperature incubation, are responsible for the increase in their viscosities. It would be of great importance to track and identify these changes to better understand the mechanism of bio-oil ageing. Bio-oil being a complex mixture of more than 300 compounds, it is difficult to track all the chemical changes taking place in it during the accelerated stability testing. Hence we have decided to study the stability of model bio-oil systems. The model bio-oil is based on the composition of the aqueous fraction of the bio-oil (see Figure 3-3). Hence the model system resembles the aqueous fraction of the bio-oil rather than entire bio-oil. The first model system we studied consisted of glucose, acetic acid, hydroxyacetone, formic acid, furfural, guaiacol, catechol and water. Hydroxyacetaldehyde and levoglucosan were not added to the model bio-oil as they are very expensive and hence cannot be bought in large quantities. The exact composition is depicted in Table 4-2.

Table 4-2 Composition of model bio-oil system 1

Compound	Wt%
Glucose	15.0
Formic acid	2.5
Acetic acid	7.5
Hydroxyacetone	7.5
Furfural	2.5
Guaiacol	2.5
Catechol	1.5
Water	61.0

The accelerated stability test data for the Bio-oil Model System 1 is shown in Figure 4-5. The viscosity increases upon incubation at high temperature and this increase in more evident for the low shear measurement. The viscosity shows linear increase over the time period studied with the rate of about 0.001 centi Pa-s h^{-1}. This model bio-oil system contains 39 wt% of organics. Hence the rate of viscosity increase can be directly compared to that for 39.6 wt% WSBO solution discussed in previous section. The rate of viscosity increase is only $1/20^{th}$ of that for water soluble fraction of bio-oil.

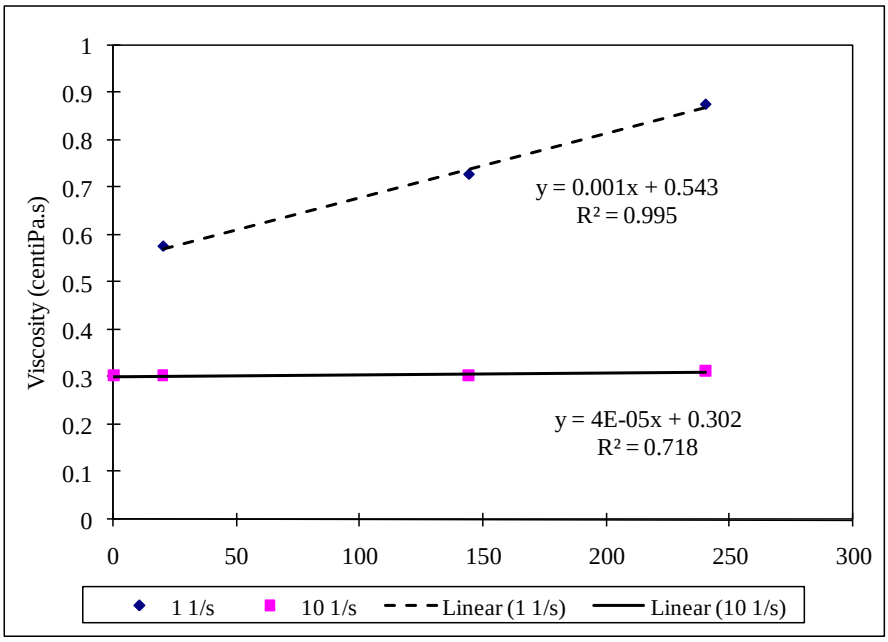

Figure 4-5 Viscosity of bio-oil model system -1 versus incubation time at 90 °C.

One of the hypotheses is that the acids present in the bio-oil facilitate the polymerization reactions within its components at high temperature. To study this, model bio-oil system – 2 was made without any acetic acid and formic acid. The exact composition is depicted in Table 4-3. The accelerated stability data for this system is

shown in Figure 4-6. A linear rise in viscosity is seen over the incubation time period. The rate of viscosity increase is double of that for Bio-oil model system - 1. This implies that acids do not play role in the stability of the model bio-oil system. It will be imperative to study the role of acids on stability of bio-oil and aqueous fraction of bio-oil. We also tracked the chemical changes in the model bio-oil but no solid conclusion could be reached from the data.

Table 4-3 Composition of model bio-oil system 2

Compound	Wt%
Glucose	16.7
Hydroxyacetone	8.3
Furfural	2.8
Guaiacol	2.8
Catechol	1.7
Water	67.7

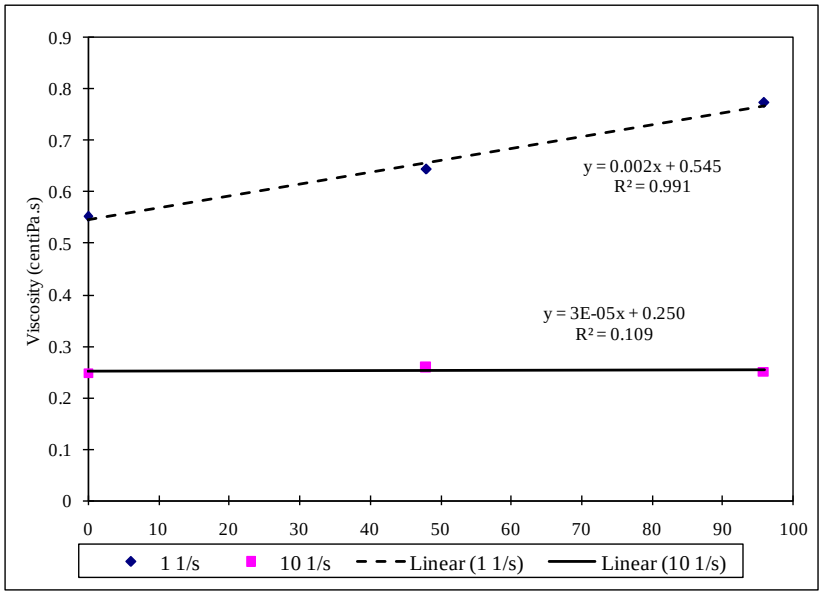

Figure 4-6 Viscosity of bio-oil model system - 2 versus incubation time at 90 °C.

4.5 Effects of lignin on the bio-oil viscosity

Pyrolytic lignin occupies about 20-40 wt% of the bio-oil and has many reactive functional sites.[48, 52, 53] On extraction with water most of the large molecular weight lignin species stay in the water insoluble bio-oil (WIBO) phase while the smaller lignin units can go to the water soluble phase. Lignin is a complex polymer with aromatic backbone. Since WIBO has significantly high viscosity and instability, the oligomeric lignin in the bio-oil could be the major viscosity and instability contributor in bio-oil. Fratini et al. investigated the structural changes in bio-oils upon aging and verified that the lignin oligomers polymerize during storage.[50] To investigate the contribution of lignin towards instability of bio-oils, DOE-BO was used since we ran out of PWBO. The DOE-BO had a much lower initial viscosity (0.0638 Pa·s, Figure 4-7) than the PWBO (0.1165 Pa·s, Figure 4-1). The rate of viscosity increase for the DOE-BO was also lower than the rate of viscosity increase for the PWBO (0.0007 ± 0.0001 Pa·s hr^{-1} compared to 0.0017 ± 0.0003 Pa·s hr^{-1}). The GPC results show that there is increase in the molecular weight DOE bio-oil during the incubation at 90 °C as shown in Figure 4-8. There was also phase separation in the DOE-BO after 144 hours of incubation. Phase separation occurs due the formation of water from condensation polymerization reactions. As seen in this figure, oligomers with wide molecular weight distribution are present in the DOE bio-oil. The oligomers molecular weight ranges from about 200 to up to 10000. Since the dependence of viscosity on molecular weight is exponential, It is possible that oligomers with high molecular weight (say > 2500) contribute more towards the absolute viscosity of bio-oil and also towards the viscosity increase upon incubation more than the

oligomers with low molecular weight. To test this we separated the lignin fraction of DOE bio-oil in low and high molecular weight lignins.

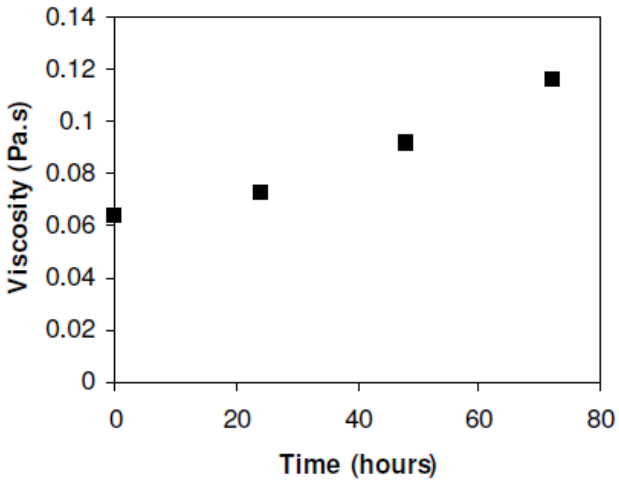

Figure 4-7 Viscosity of DOE bio-oil versus incubation time at shear rate 10 s^{-1}. The samples were incubated at 90 ºC and the viscosity was measured at 40ºC.

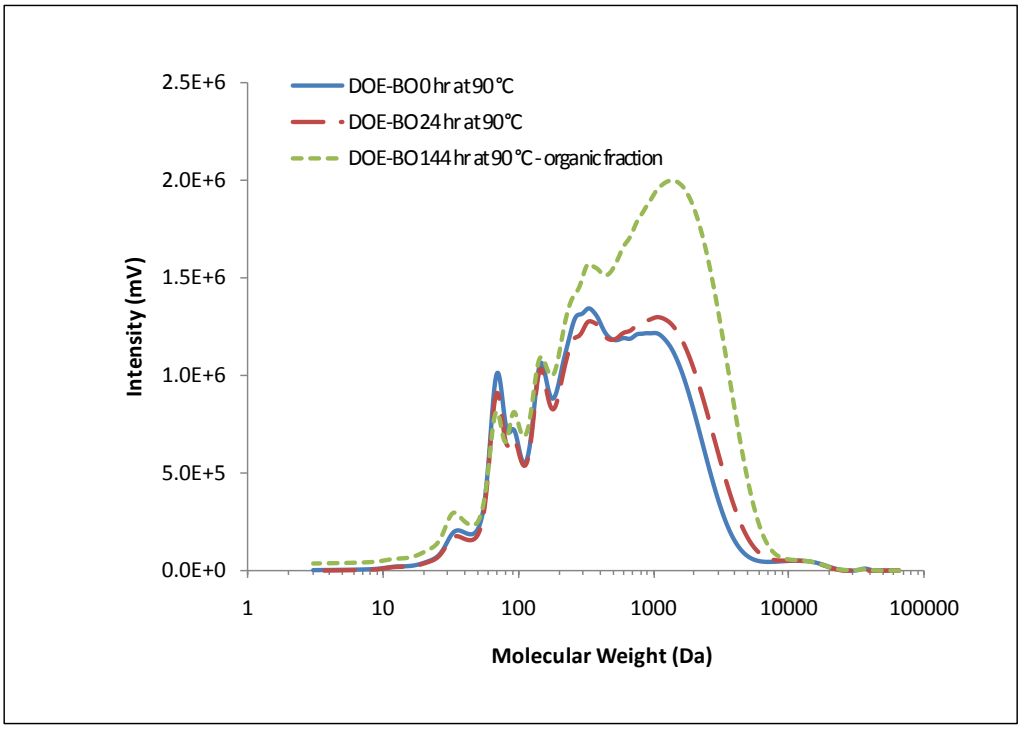

Figure 4-8 GPC analysis results of DOE-BO. Phase separation occurs after 144 hours, GPC results at this time point are for the bottom phase.

The lignin fraction (water insoluble bio-oil) was separated from the bio-oil by extraction bio-oil with water and decanting out the water soluble fraction. The water to bio-oil weight ratio of 5:1 was used for extraction. According to the procedure used by Oasmaa et al., dichloromethane can be used to extract low molecular weight (LMW) lignin from the water insoluble fraction of bio-oil.[52-54] Dichloromethane is evaporated to recover LMW lignin. The dichloromethane insoluble fraction of water insoluble bio-oil is called high molecular weight (HMW) lignin. We used the same procedure to separate WI-DOE-BO in LMW and HMW lignins. We then subjected the LMW and HMW lignin to accelerated stability testing through GPC analysis. Viscosity was measured for accelerated stability samples of LMW lignin but not for HMW lignin samples. Viscosity measurements and GPC analysis suggest that the LMW lignin continued to polymerize during incubation (Figures 4-9 and 4-10). The LMW lignin predominantly has oligomers with molecular weight up to 3000 Da. The HMW lignin also continues to polymerize during incubation (Figure 4-11). HMW lignin contains oligomers with molecular weight up to 10000 Da. The weight average molecular weight of DOE bio-oil and LMW and HMW lignin from DOE bio-oil are plotted in Figure 4-12. The rate of increase of molecular weight with incubation time is highest for the HMW lignin followed by DOE bio-oil and is lowest for the LMW lignin. The weight average molecular weight data along with the area under curve for the highest molecular weight peak in GPC (absolute areas as well as area normalized to 0 hr incubation samples) are tabulated in Table 4-4. The molecular weight increased by 23.6% over 24 hour incubation at 90 °C for DOE bio-oil and HMW lignin. The rate of molecular weight increase is significantly lower for

LWM lignin with only a 14.5% increase in molecular weight over the same time period. Also the rate of change of area under the highest molecular weight peak in GPC is in the order: HMW lignin > DOE bio-oil > LMW lignin. This is in agreement with the viscosity increase that was observed (Figure 4-12). The viscosity of incubated sample increases due to two reasons: increase in average molecular weight of sample due to self-polymerization reactions, and increase in the concentration of high molecular weight oligomers. The concentration of high molecular weight oligomers increase due the condensation of two low molecular weight oligomers forming a high molecular weight oligomer. For the LMW lignin the increase in the area under the highest molecular weight peak in GPC is only about 10% even after 58 hr of incubation and this is because not enough lower molecular oligomers are available in this sample that can polymerize and increase the area under the highest molecular weight peak in GPC significantly. Hence in LMW lignin only the increase in molecular weight of oligomers is responsible for the viscosity increase. The rate of viscosity increase is hence lower for LMW lignin compared to that for HMW lignin. In HMW lignin the rate of molecular weight increase as well as concentration (or under the peak) increase slows down after the first day of incubation.

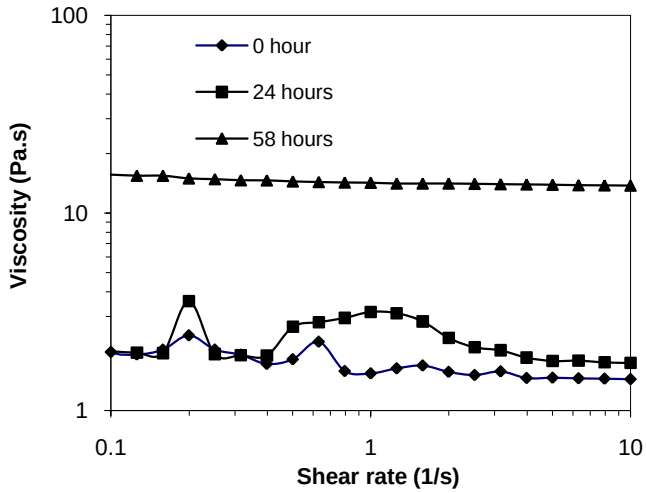

Figure 4-9 Viscosity of LMW lignin at 40 °C. The lines are guides for the eye. Hours is the incubation time at 90 °C.

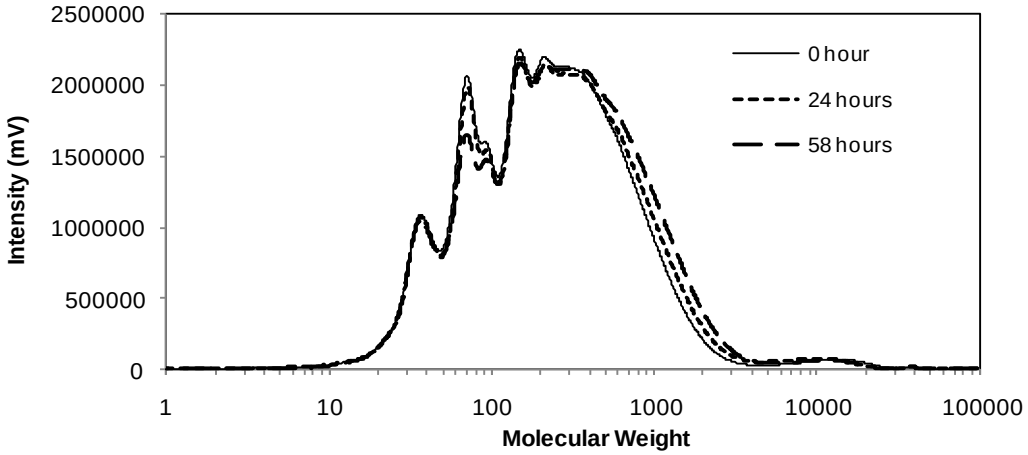

Figure 4-10 GPC analysis LMW lignin fraction of DOE-BO incubated at 90 °C.

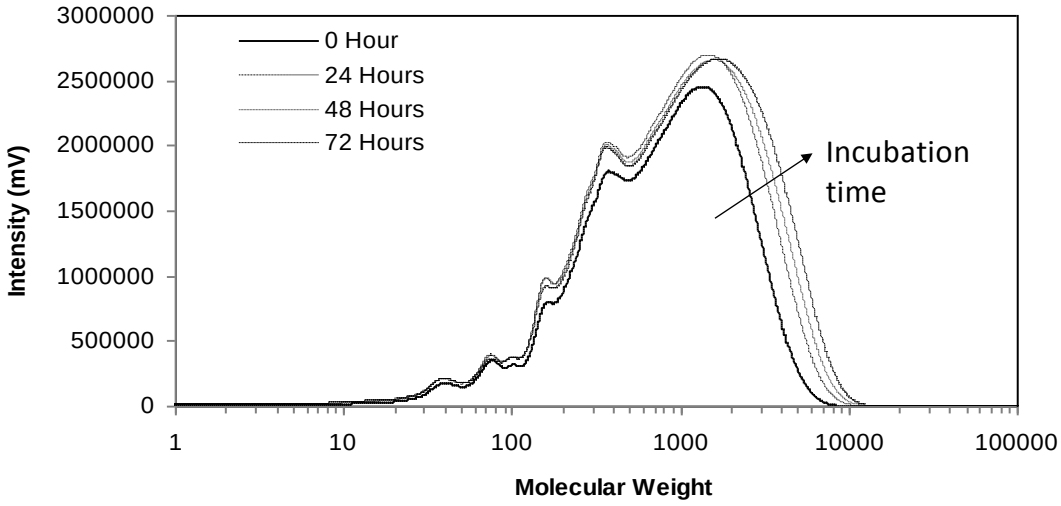

Figure 4-11 GPC analysis of HMW lignin fraction of DOE-BO incubated at 90 °C.

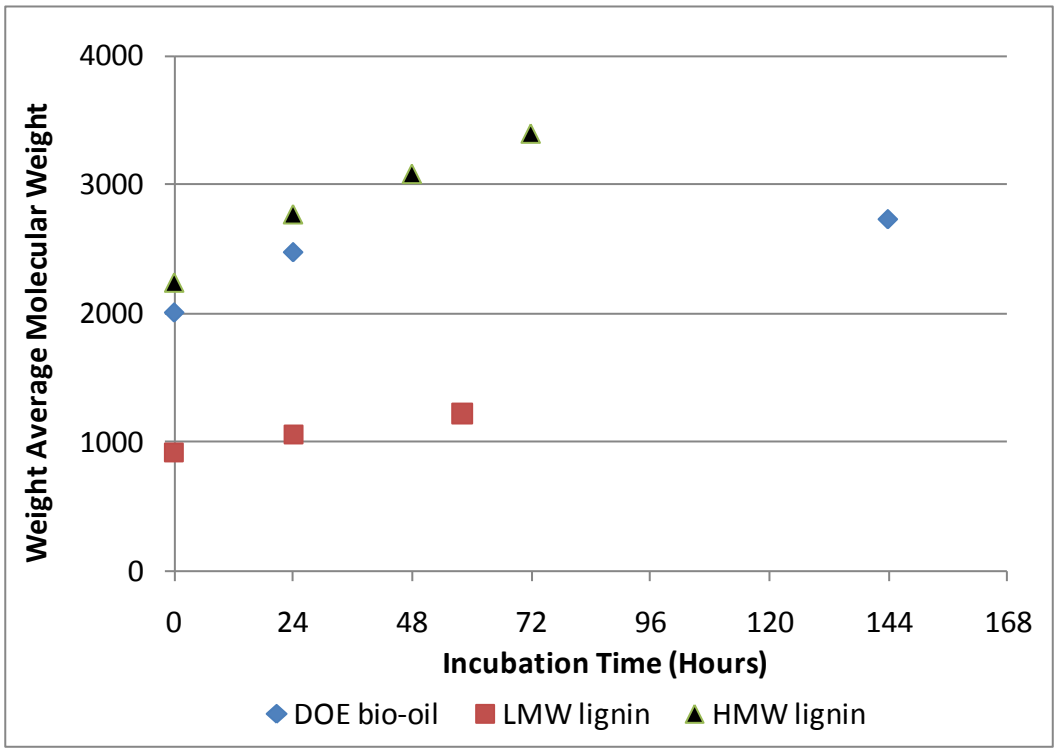

Figure 4-12 Weight average molecular weight for DOE bio-oil, low molecular weight lignin and high molecular weight lignin from DOE bio-oil against the incubation (at 90 °C.) time.

Table 4-4 Molecular weight and area under the peak data from GPC for DOE bio-oil, and low and high molecular weight lignin from DOE bio-oil.

	DOE bio-oil		LMW lignin			HMW lignin			
	Incubation Time (hr)		Incubation Time (hr)			Incubation Time (hr)			
	0	24	0	24	58	0	24	48	72
Mw of highest mol. wt. peak*	2003	2477	920	1054	1221	2244	2774	3088	3401
% Change in mol. wt. over 0 hr sample	-	23.6	-	14.5	32.7	-	23.6	37.6	51.6
Area under GPC curve for highest mol. wt. peak (million units)	3278	4110	3086	3351	3378	6709	9567	10757	12212
Area under curve normalized to 0 hr sample	100	125.4	100	108.6	109.5	100	142.6	160.3	182.0

* Mw is weight average molecular weight

These results imply that the high molecular weight lignin in bio-oil can mainly be responsible for the increase in the viscosity of bio-oil upon storage. In order to improve bio-oil stability, one can either take steps to prevent polymerization during aging, or to eliminate the presence of lignin derived oligomers prior to storage and aging. Separation of lignin prior to storage using processes such as ultrafiltration, extraction, and refining have been widely explored in the paper industry.[55, 56] There is much scope for the improvement of upstream pyrolysis process especially the bio-oil vapor condensation system. A selective condensation system can be developed where the high molecular

weight lignin is condensed out separately than the rest of the bio-oil. Such a bio-oil would exhibit better stability.

4.6 Bio-oil Microfiltration

The char particles as discussed earlier can cause problems with respect to bio-oil stability as well as char can clog the downstream bio-oil upgrading reactors. Hence it is desirable to remove the char from bio-oil. Bio-oil was subjected to microfiltration using membranes with pore diameter less than a micron to remove the fine char particles that get entrained in bio-oil. Figures 4-13 and 4-14 show the microscopic images of bio-oil feed, 0.5 µm permeate and 0.8 µm permeate at magnification levels 20X and 50X. The microscopic analysis was conducted within 5 days of carrying out the microfiltration. The feed image shows the presence of a large number of char particles of varying sizes with some particles larger than 25 µm. Some of the particles appear to be agglomerates of smaller particles. Similar aggregation of char particles in the bio-oil have been previously reported by Tzanetakis et al.[57] They found that char particles, being hydrophobic in nature, tend to bind to the organic phase in the bio-oil, which then agglomerate to form larger structures. The permeate images from the 0.5 µm membrane show that while the majority of the char particle have been removed by microfiltration we still observe some micron size particles especially at higher magnification. Since the tubular Membralox membrane have a pore size distribution, with some pores larger than the nominal pore size, the presence of a few particles in this size range is not surprising. The 0.8 µm membrane permeate shows similar microfiltration characteristics as observed in the 0.5 µm permeate. Based on microscopic images it is evident that the microfiltration using

both pore size membranes has successfully removed the majority of the char particles, with only a small fraction of the smaller size char particles retained in the permeate. Ash characterization experiments were carried out within 7 days after the microfiltration. Fig. 6 shows the ash weight percent of the feed and the filtered bio-oil. The feed has nearly 0.1 wt% ash. The weight percent of ash in bio-oil can be as high as 0.2%[8, 58], therefore, our bio-oil sample has a moderate level of ash content. The ash content after microfiltration is reduced by approximately 60%, to about 0.03 wt% (Figure 4-15). Both pore size membranes achieve similar levels of ash reduction after filtration. The residual bio-oil ash in permeate can be attributed to the small amount of micron level char particles observed in the microscopic images of the permeate streams and also perhaps to the presence of inorganic compounds dissolved in the liquid-phase that cannot be removed by a microfiltration process.

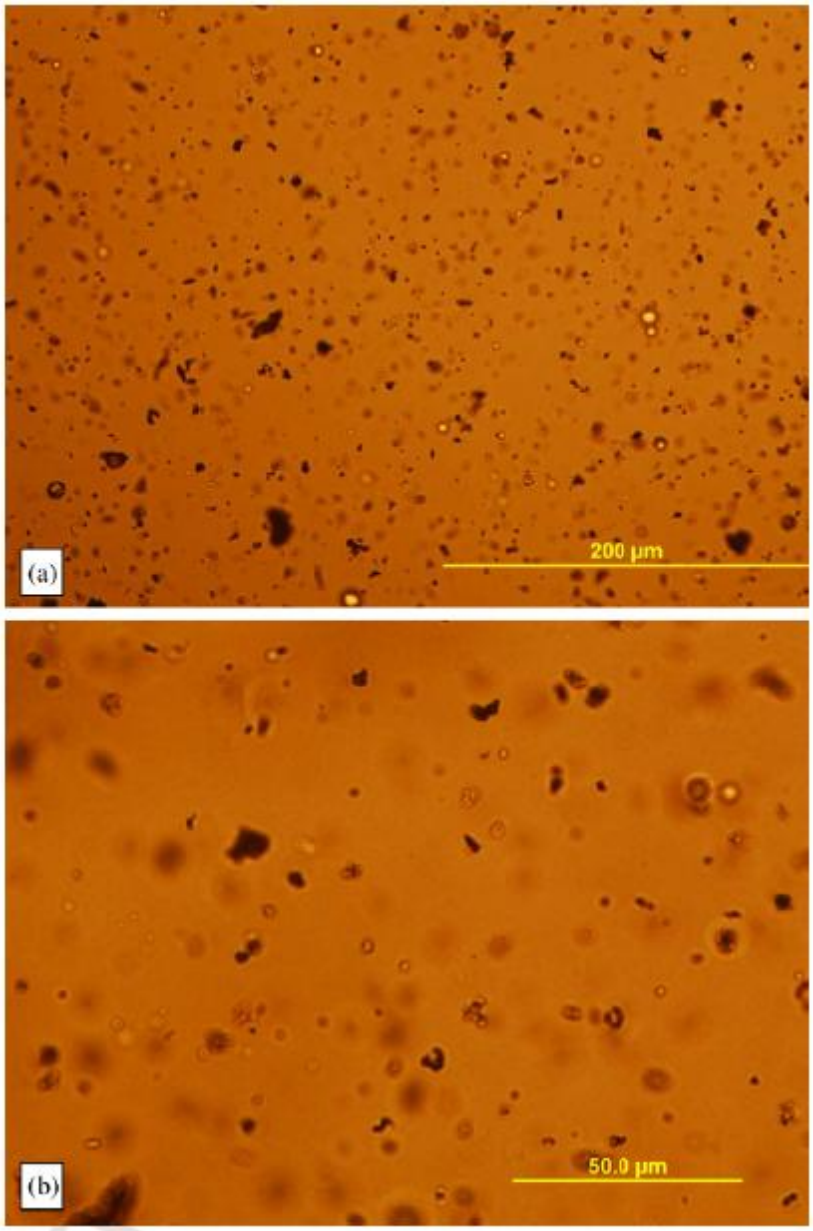

Figure 4-13 Microscopic image of DOE bio-oil feed at different magnification levels: a=20X and b=50X.

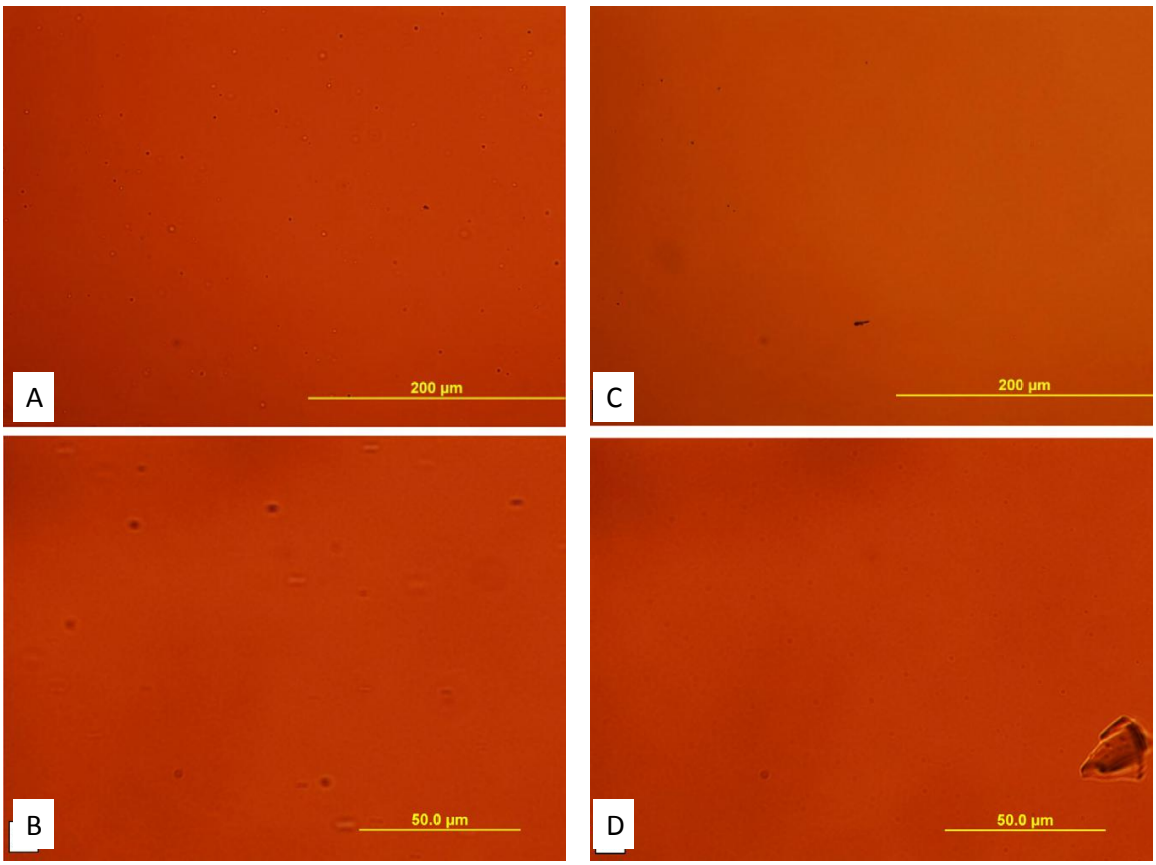

Figure 4-14 Microscopic images of membrane permeate of DOE bio-oil. A: 0.5 µm, 20X, B: 0.5 µm, 50X, C: 0.8 µm, 20X, and D: 0.8 µm, 50X.

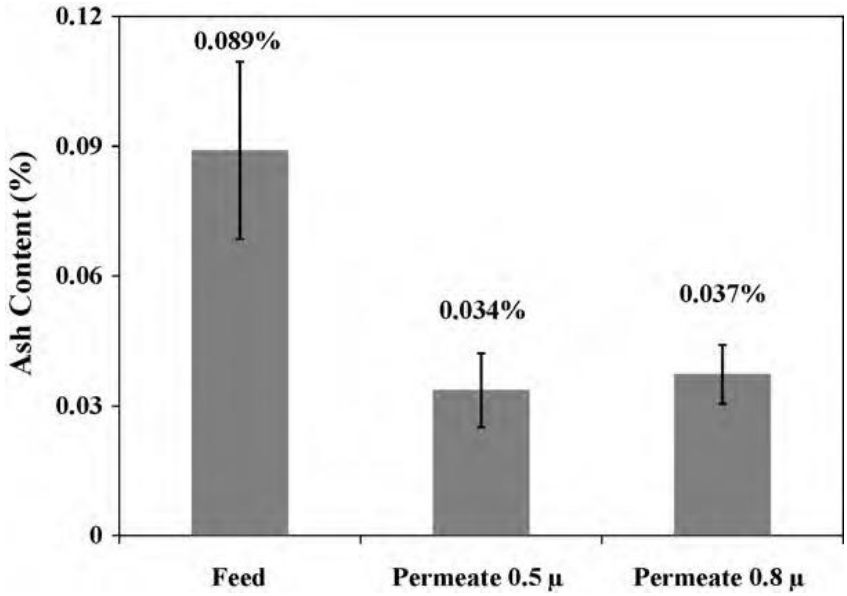

Figure 4-15 Ash content of DOE bio-oil feed, 0.5 µm permeate and 0.8 µm permeate.

Six months after the microfiltration was carried out, samples of the feed and permeate streams were removed from refrigerated storage and subjected to the GC and water extraction experiments to probe for possible chemical differences. The time lapse is notable because bio-oil is known to undergo significant physico-chemical changes, commonly referred to as ageing, over time scales of months under ambient conditions. The GC data are given in Table 4-5. The weight percents are based on the total bio-oil. There is no significant difference in the concentration of the key components in the unfiltered and microfiltered bio-oil with the exception of hydroxyacetaldehyde, for which the concentration is more than two times higher in the filtered samples as compared to the feed. At this time we do not have an explanation for this exception. Microfiltration also does not seem to have any significant impact on the composition of bio-oil in terms of the water and water-soluble content as observed in Table 4-6. There is a slight decrease in the water-insoluble fraction, on the order of one or two percent, after filtration; this may be attributed to the removal of the solid chars which are themselves water insoluble (char content is typically on the order of one percent by weight). It should be noted that the typical water-soluble content of fresh bio-oil is well above 50%, so the corresponding percentages in Table 4-6 are much lower than expected. This may be attributed to the aging process, which is known to increase the concentration of the water-insoluble fraction over time.[*(50)*] In one case, for the 0.8 μm membrane permeate, the water-soluble fraction was also measured very soon after the permeation experiment (6 months before the measurements used to generate the data reported in Table 4-6), the water-soluble fraction was 55% at that time, as compared to 27.2%. Although such time-dependent data are not available for the other samples, it is likely that similar aging phenomena occurred

in all of them. Interestingly, the microfiltration process itself had little influence on the aging, with unfiltered feed and filtered permeate samples having similar water content and water-soluble fraction at the same point in time.

Table 4-5 Composition of DOE bio-oil before and after microfiltration.

Compound	Weight Percent		
	Unfiltered	0.8 µm permeate	0.5 µm permeate
Hydroxyacetaldehyde	3.16	8.21	7.70
Acetic acid	8.66	9.59	9.11
Hydroxyacetone	1.13	1.45	1.33
1-Hydroxybutanone	0.40	0.44	0.40
Furfural	0.47	0.47	0.42
2-Furanone	0.33	0.32	0.33
Levoglucosan	11.95	10.22	10.38

Table 4-6 Impact of microfiltration on the total water content and water soluble and insoluble content of DOE bio-oil.

	Weight Percent		
	Unfiltered	**0.8 µm permeate**	**0.5 µm permeate**
Water	28.1	25.8	26.3
Water soluble fraction	25.6	26.1	27.2
Water insoluble fraction	74.4	73.9	72.8

4.7 Bio-oil Nanofiltration

In Section 4.5 we saw that the high molecular weight lignin has higher rate of viscosity increase than the bio-oil. Solvent extraction of the high molecular weight lignin from bio-oil may not be economical at an industrial scale. Hence the idea was to remove the very high molecular weight oligomers from the bio-oil using nanofiltration technology. We filtered bio-oil using membranes with nominal pore sizes of 5 nm and 10

nm. The GPC chromatographs for the feed, retentate and permeate are shown in Figure 4-16. It can be seen that the nanofiltration affects the bio-oil composition over the molecular weight range > 120 Da. The permeates have lower concentrations than feed, which has lower concentration than retentates. Table 4-7 depicts the weight average molecular weight and normalized concentration (of the highest molecular weight peak in GPC) data for DOE bio-oil feed and the 5 nm and 10 nm permeates and retentates. The nanofiltration by 10 nm filter does not affect the weight average molecular weight of bio-oil. The concentration of the highest molecular weight peak in permeate is only about 6% less than in the feed and 6.7% more in the retentate than in the feed. Since molecular weight and concentration of oligomers are the main factors in determining the bio-oil viscosity and possibly to its instability, the nanofiltration by 10 nm membrane is not expected to improve the bio-oil properties substantially. In the case of 5 nm permeate there is a noteworthy drop (2003.3 to 1859.6) in the weight average molecular weight as well as in the normalized concentration (100 to 69.9), implying that it can be used to improve the bio-oil stability.

Table 4-7 Molecular weight and concentration data for DOE bio-oil and its nanofiltration permeates and retentates.

	DOE-Bio-oil	10 nm permeate	10 nm retentate	5 nm permeate	5 nm retentate
Weight average molecular weight for the last peak in GPC	2003.3	1995.6	1999.2	1859.6	2005.5
Normalized concentration of last peak in GPC	100	94.0	106.7	69.9	118.4

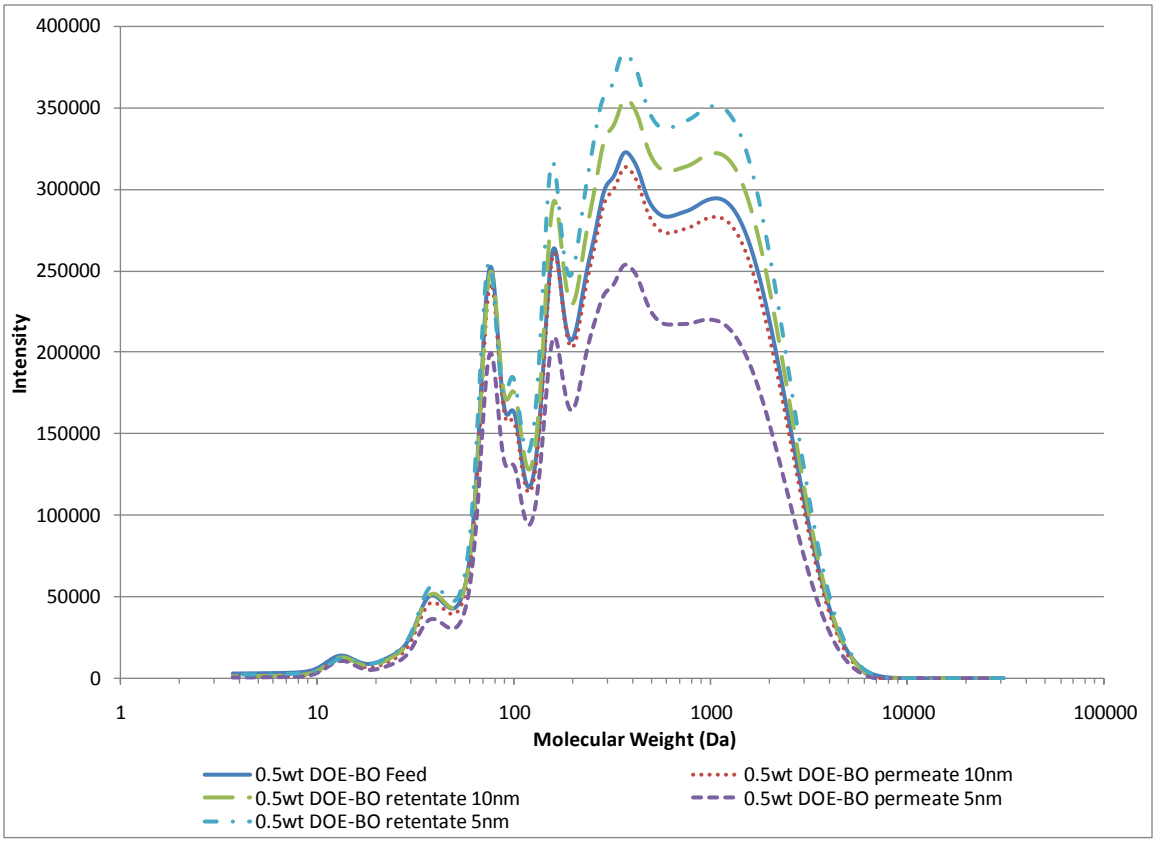

Figure 4-16 GPC data for DOE bio-oil feed and permeates and retentates from 5 nm and 10 nm filters.

The permeates and retentates obtained after the filtration were subjected to the accelerated stability testing. The viscosity and GPC weight average molecular weight data of the accelerated stability testing are depicted in Figures 4-17 and 4-18 respectively. The viscosity data here for the DOE bio-oil feed was gathered about six months before the permeates and retentates data were gathered. The feed was significantly more stable six months ago than at the time when these experiments were carried out. During the microfiltration and nanofiltration experiments the feed was repeatedly heated to filtration temperature (~ 45 °C) and cooled down again at the end of the experiments. This might

have accelerated the degradation of feed resulting in the molecular weight and viscosity increase. We do not have viscosity and molecular weight data available for this degraded feed which should be compared with the permeate and retentate data and not the original feed. Due to this reason, even the permeate viscosity is higher than the DOE bio-oil feed viscosity in Figure 4-17 which should not be the case. The 10 nm permeate, 10 nm retentate, and 5 nm permeate viscosities can be compared to each other. It can be seen that the 10 nm permeate has a slightly lower rate of viscosity increase than 10 nm retentate, implying that some stabilization has occurred due to nanofiltration, although not significant. The viscosity of 5 nm permeate increases at substantially lower rate that 10 nm permeate and retentate. Nanofiltration hence is a promising bio-oil stabilization method. The stabilization in 5 nm permeate is due to the reduction in the average molecular weight of bio-oil and the reduction in the concentration of oligomers.

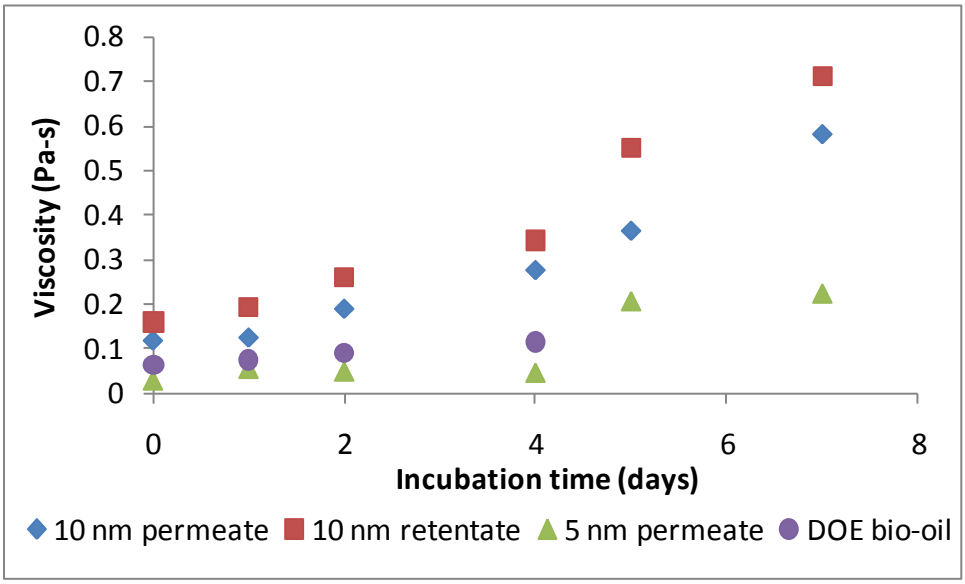

Figure 4-17 Accelerated stability viscosity data for DOE bio-oil and permeates and retentates from nanofiltration.

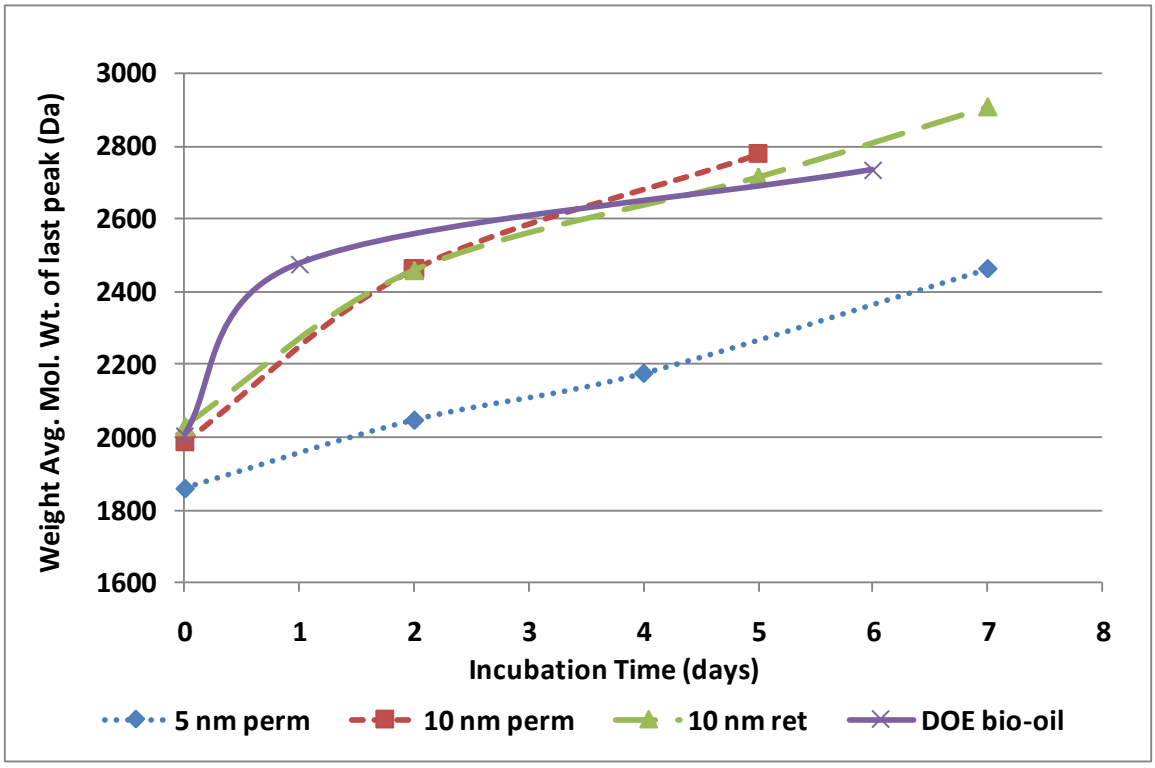

Figure 4-18 Accelerated stability GPC data for DOE bio-oil and its permeates and retentates from nanofiltration.

4.8 Conclusion

The general conclusion from this study is that in its original form bio-oil is unstable, that is its viscosity and molecular weight increases upon storage. The self-polymerization reactions within the bio-oil components are the reason for the increase in the molecular weight, which results in the increase in viscosity. The rate of viscosity increase is higher for the water insoluble fraction of bio-oil (WIBO) than that for bio-oil than that for the water soluble fraction of bio-oil (see Table 4.8). The WIBO contains a

high concentration of high molecular weight lignin oligomers, implying that these oligomers are largely responsible for the bio-oil instability.

Table 4-8 Initial viscosity and rate of viscosity increase for bio-oil and different fraction from bio-oil.

Sample	Initial Viscosity* at 40 °C (Pa-s)	Rate of Viscosity Increase† (Pa-s h^{-1})
Pine wood bio-oil	0.117	1.70×10^{-3}
Water insoluble pine wood bio-oil	1.46	1.16×10^{-2}
Water soluble pine wood bio-oil	1.85×10^{-3}	3×10^{-5}
Hydrogenated water soluble pine wood bio-oil	2.72×10^{-3}	0
DOE bio-oil	0.064	7×10^{-4}
LMW lignin from DOE-BO	1.44	0.22
HMW lignin from DOE-BO	66.3	N/A‡

* at shear rate of 10 s^{-1}.

† rate of viscosity increase when incubated at 90 °C. A linear equation is fit to the viscosity data to get the rate of viscosity increase.

‡ HMW lignin solidified during the incubation.

For the aqueous fraction of the bio-oil (WSBO), low temperature hydrogenation can be used for the stabilization. Low temperature hydrogenation converts the reactive aldehyde, ketone, and carbohydrate functionalities to corresponding alcohols, which are thermally stable. The hydrogenation hence prevents any further polymerization in the WSBO. The viscosity of hydrogenated WSBO was found to be stable during the incubation at 90 °C. Bio-oil model compound studies indicated that the acids do not affect the rate of viscosity increase in model systems.

Char is postulated to catalyze the polymerization reactions within the bio-oil or it can also act as nucleation sites for the forming of second phase during the storage of bio-oil. We were able to remove char particles above 1 μm in size from fast pyrolysis bio-oil by microfiltration using ceramic membranes. Microfiltration had little impact on the composition of the bio-oil. The microfiltration did not improve the stability of bio-oil. Ash content of the bio-oil can be reduced by microfiltration as the majority of the ash is trapped in char, which is removed upon microfiltration. Never the less, microfiltration of bio-oil is beneficial for the further processing of bio-oil such as hydrogenation and zeolite upgrading. Future work should focus on developing the pilot and industrial scale microfiltration processes for the bio-oil.

The high rate of viscosity increase of water insoluble bio-oil shows that the high molecular weight oligomers are mainly responsible for the instability of bio-oil. The water insoluble bio-oil was further separated into low molecular weight (LMW) lignin and high molecular weight (HMW) lignin by extraction with dichloromethane. The HMW lignin was found to be significantly more unstable than LWM lignin and the whole bio-oil with respect to average molecular weight increase and increase in the concentration of high molecular weight species. Hence it can be concluded that the HMW lignin is the major contributor to the bio-oil instability. The future work for this reason should be focused on the selective removal of HMW lignin from bio-oil. The dichloromethane extraction method may not be feasible at the industrial level. Upstream modifications in the pyrolysis vapors condensation system such that HMW lignin is condensed separately from rest of the bio-oil needs to studied. Nanofiltration of bio-oil

with 5 nm pore size membrane was found to stabilize bio-oil to some extent. The stabilization is by reduction in the average molecular weight of bio-oil and in the concentration of high molecular weight oligomers. More work needs to be done to understand the effects of bio-oil nanofiltration on its stability and chemical composition. The economic feasibility of the nanofiltration also needs to be evaluated.

Chapter 5

AQUEOUS PHASE PROCESSING OF WATER SOLUBLE BIO-OIL

5.1 Introduction

The existing bio-oil upgrading processes suffer from various drawbacks such as coking of the catalyst, low yield to desired products, and use of sulfided catalysts. The existing bio-oil upgrading processes are discussed in detail in Sections 6.2 and 7.1. It is hence necessary to find the alternate efficient bio-oil processing technologies. We process the aqueous fraction of oak wood bio-oil (water soluble oak wood bio-oil or WS-OWBO) by Aqueous Phase Processing (APP). Aqueous phase processing, developed by Dumesic and co-workers, involves the selective conversion of sugars and polyols to hydrogen and targeted alkanes.[15, 25] The major advantage of this approach is that targeted products can be selectively produced by controlling the chemistry that occurs in the aqueous phase. Other advantages of aqueous phase processing include: (1) liquid fuels can be made that can be used with gasoline and diesel engines, (2) high thermal efficiencies because the process occurs in the liquid phase, (3) no energetically-intense distillation steps, and (4) have high rates of production per reactor volume. Liquid-phase catalytic processing of biomass-derived compounds offers unique opportunities for achieving high yields of specific, and well-defined, liquid fuels from biomass.

Hydrogen is an important reactant in a majority of refinery processes to make liquid fuels and biofuels.[59] Hydrogen can be produced in our process by aqueous-phase reforming (APR) which is a part of APP. APR involves C-C bond cleavage (to

produce CO) followed by the water gas shift reaction over supported metal catalysts.[15] The overall reaction for APR of sorbitol is shown in Equation (5-1). Side reactions such as methanation and dehydration/hydrogenation take place to produce C1 to C6 alkanes as by-products.

$$C_6H_{14}O_6 + 6H_2O \rightarrow 6CO_2 + 13H_2 \quad (5\text{-}1)$$

Alkanes ranging from C1 to C6 can be produced more selectively by aqueous phase dehydration/hydrogenation (APDH), also a subset of APP. This involves passing the aqueous solution of oxygenated hydrocarbon over a bi-functional catalyst containing metal and acidic sites such as Pt supported on SiO_2-Al_2O_3. Hydrogen can be either produced in-situ on metal sites according to the Equation (5-1) or supplied externally. The alkanes are produced by dehydration reactions on solid acid sites to produce dehydrated products, and hydrogenation reactions on metal sites as shown in Equation (5-2). If the alkane and hydrogen production reactions are balanced then alkanes can be directly produced from a sugar with CO_2 and H_2O as the byproducts as shown in Equation (5-3). Smaller alkanes are obtained as by-products due to the C-C bond cleaving reactions.

$$C_6H_{14}O_6 + 6H_2 \rightarrow C_6H_{14} + 6H_2O \quad (5\text{-}2)$$

$$(19/13)\ C_6H_{14}O_6 \rightarrow (36/13)\ CO_2 + C_6H_{12} + (42/13)\ H_2O \quad (5\text{-}3)$$

Figure 5-1 shows the reactions taking place during APP of sorbitol. The majority of the previous APP work was done with pure compounds such as ethylene glycol, glycerol and sorbitol.[15, 25-27] A substantial fraction of bio-oil is water soluble as discussed in Chapter 3 the aqueous fraction of the bio-oil consists of various oxygenated hydrocarbons. Hence the aqueous fraction of the bio-oil can be an excellent feedstock for the APP to produce hydrogen and alkanes. We thus proposed a new route for production of renewable liquid fuels from biomass by combining fast pyrolysis with aqueous phase processing.

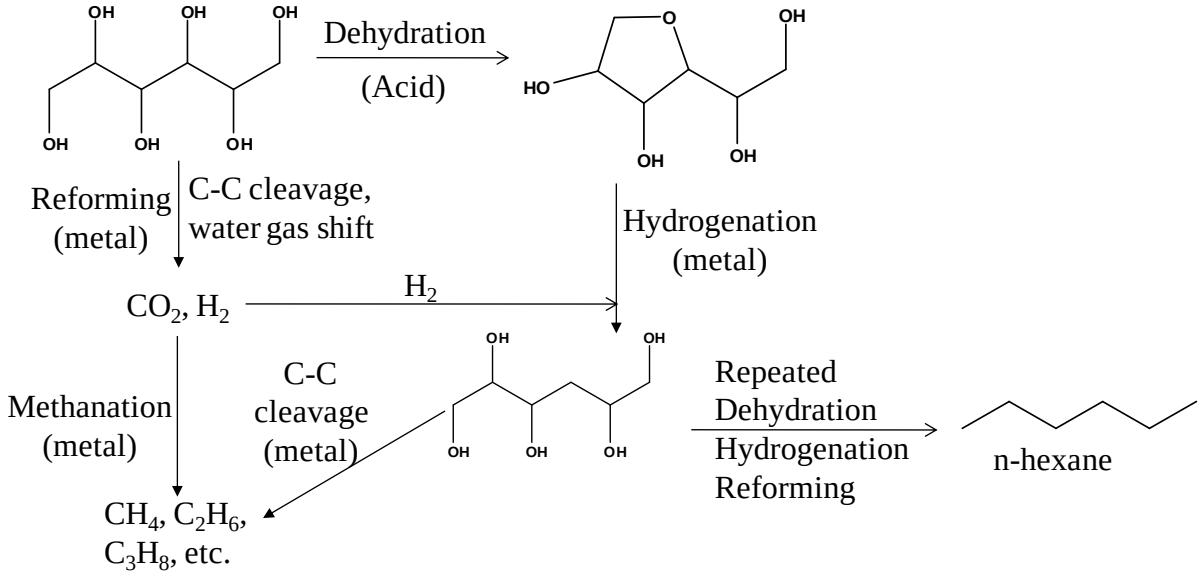

Figure 5-1 Aqueous phase processing of sorbitol (from reference (*25*))

5.2 Experimental

The material and methods for this chapter are described in Sections 2.1, 2.5, 2.6.1, and 2.7. Only oak wood bio-oil has been used for gathering the data presented in this chapter. Hence abbreviation WSBO is used sometimes to describe water soluble oak wood bio-oil (WS-OWBO) in this chapter.

5.3. Proposed Process, Reaction System and Theoretical Yields

The proposed process for the aqueous phase processing of bio-oil is depicted in the form of a simplified block diagram in Figure 5-2. The bio-oil is first phase separated in water soluble and water insoluble fractions. The water soluble fraction is then subjected to low temperature hydrogenation on Ru/C catalyst. Methane is formed as by-product in this step. The hydrogenated WSBO can then be fed to either APR (Pt/Al_2O_3 catalyst) or APDH (Pt/SiO_2-Al_2O_3 catalyst) reactor. In APR, H_2 and CO_2 are obtained as major products with light alkanes as by-products. From APDH reactor, C1-C6 alkanes and CO_2 are obtained as major products. Hydrogen can be supplied externally to APDH reactor. In that case C1-C6 alkanes are major products with CO_2 being a by-product.

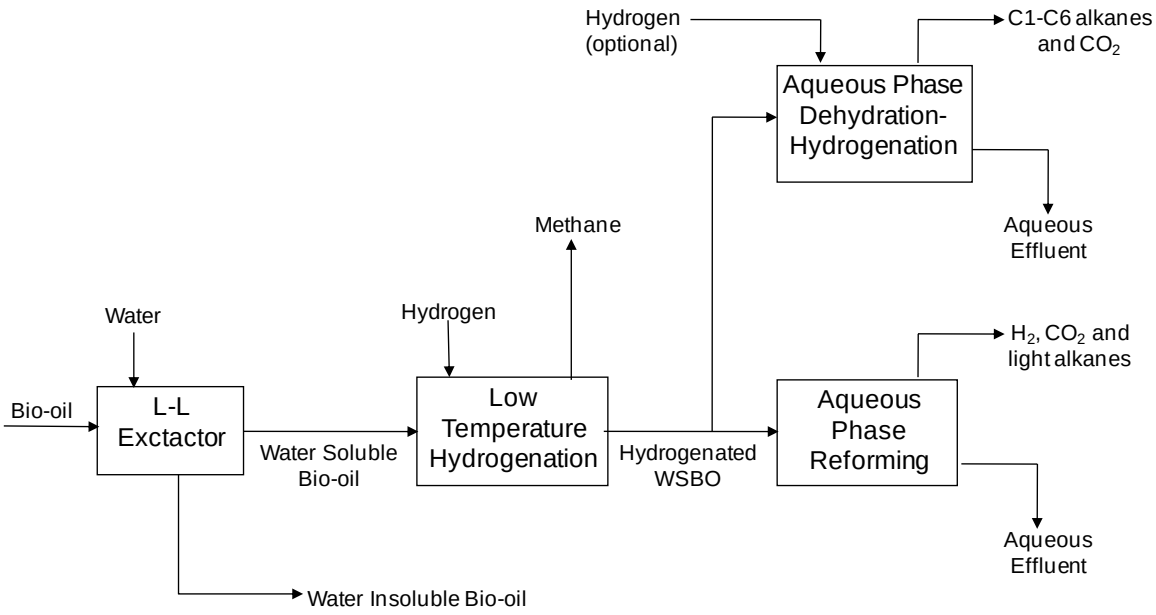

Figure 5-2 Block diagram of the aqueous phase processing of bio-oil

From the elemental analysis data, the WS-OWBO can be represented by a molecular formula $C_2H_{5.4}O_{2.05}$ with an arbitrary molecular weight of about 62. The amount of hydrogen in water soluble bio-oil increases during the hydrogenation step and depends on the hydrogen consumption in this step. About 25% of the carbon is converted to CH_4 in the hydrogenation step under the conditions of 175 °C and 1000 psi in batch reactor. Clearly, reducing the amount of methane formed in the hydrogenation step is of critical importance in obtaining commercially relevant yields. Methane can form by the hydrogenation of CO produced upon decarbonylation of bio-oil compounds. A mole of water is also formed when a mole of CH_4 is obtained from hydrogenation of CO. The hydrogen consumption in this step is about 0.06 gm /gm WS-OWBO for reaction temperature and time of 175 °C and 3 h respectively. For 0.06 gm H_2 consumed per gram of WSBO, the hydrogenated WS-OWBO (H-WS-OWBO) can be represented by a molecular formula $C_{1.5}H_{6.1}O_{1.55}$ with the molecular weight of 48.9 (see Equation 5-4).

$$C_2H_{5.4}O_{2.05} + 1.87\ H_2 \rightarrow C_{1.5}H_{6.1}O_{1.55} + 0.5\ CH_4 + 0.5\ H_2O \qquad (5\text{-}4)$$

WS-OWBO H-WS-OWBO

Hydrogen is produced by Equation (5-5) from the H-WS-OWBO and water by aqueous-phase reforming. The hydrogen can react with the bio-oil to produce alkanes (pentane is shown as an example) as shown in Equation (5-6) (No carbon-carbon bond forming reactions are taking place in Equation (5-6)). Addition of Equation (5-5) and (5-6) so that the hydrogen produced in Equation (5-5) is consumed in Equation (5-6) gives Equation (5-7). From Equation (5-5) it can be seen that the theoretical highest yield of

hydrogen is 0.184 gm hydrogen per gm of H-WS-OWBO or 0.145 gm hydrogen per gm of WSBO (non-hydrogenated). The net hydrogen production accounting for hydrogen consumption in hydrogenation step is 0.085 gm hydrogen per gm WS-OWBO. The selectivity of alkanes produced from the water soluble bio-oil depends upon its composition. However if we assume that pentane is the major product, the theoretical highest yield of pentane that can be produced from hydrogenated WS-OWBO is 0.326 gm per gm of WS-OWBO (Equation 5-7).

$$C_{1.5}H_{6.1}O_{1.55} + 1.45\ H_2O \rightarrow\ 1.5\ CO_2 + 4.5\ H_2 \qquad (5\text{-}5)$$

$$C_{1.5}H_{6.1}O_{1.55} + 0.3\ H_2 \rightarrow\ 1.55\ H_2O + (1.5/5)\ C_5H_{12} \qquad (5\text{-}6)$$

$$16\ C_{1.5}H_{6.1}O_{1.55} \rightarrow\ 1.5\ CO_2 + 21.8\ H_2O + 4.5\ C_5H_{12} \qquad (5\text{-}7)$$

In our experiments we were only able to obtain 0.031 gm H_2 per gm of WS-OWBO. This is only about 21% of the maximum possible yield (0.145 gm). This yield could be increased by recycling the un-reacted product and decreasing the amount of methane we produce in the low-temperature hydrogenation step. The hydrogen production in reforming step is less than the hydrogen consumption in the hydrogenation step. Better reforming catalysts are required to increase the hydrogen production. If higher hydrogen production is achieved the excess hydrogen produced can be used for the low temperature hydrogenation reaction and to hydrogenate the WIBO. The water insoluble fraction of the bio-oil can be hydrotreated with the hydrogen produced from the aqueous fraction of the bio-oil to produce aromatic fuel. WIBO also has the potential to

replace phenol in phenol-formaldehyde resins.[7] WIBO can also be converted to aromatic gasoline through catalytic cracking on zeolite.[60]

5.4 Low Temperature Hydrogenation (LTH) of the Aqueous Faction of Bio-oil in Batch Reactor

The aqueous fraction of bio-oil contains thermally unstable compounds (*e.g.* glucose, levoglucosan) that decompose when heated to high temperature. These compounds must be converted into thermally stable compounds prior to APP.[15, 25] If they are not converted to thermally stable compounds then they can cause deactivation of the catalyst by coke formation. The thermally unstable compounds can be converted to thermally stable compounds by a low temperature aqueous phase hydrogenation. In the low temperature hydrogenation, compounds such as hydroxyacetaldehyde, hydroxyacetone, and furfural are converted to corresponding alcohols such as ethylene glycol, propylene glycol and tetrahydrofurfuryl alcohol respectively. The challenge with the low temperature aqueous phase hydrogenation step is to selectively hydrogenate targeted C=O bonds and not break the C-C or C-O bonds. Cleavage of C-C and C-O bonds results in formation of lighter products including undesired methane. The aqueous phase hydrogenation was studied in a batch as well as in a flow reactor in this study.

Batch hydrogenation of the aqueous fraction of bio-oil was done in the temperature range of 125-175 °C with a 5 wt% Ru/Carbon catalyst. The hydrogen uptake of this catalyst was 33.2 μmol H atoms/gm dry catalyst, which corresponds to surface to bulk Ru ratio of 6.7%. Table 5-1 depicts the data gathered for batch hydrogenation where

temperature is increased in steps from 125 °C to 150 °C to 175 °C. Ethylene glycol, propylene glycol, butanediols, tetrahydrofurfuryl alcohol, ϒ-butyrolactone and 1,2-cyclohexanediol all reach their respective maximum concentrations within 2.5 hours at 125 °C. All the hydroxyacetone is also consumed during this same period. Acetic acid does not react at the reaction conditions used.

Table 5-1 Hydrogenation of the aqueous fraction of bio-oil with initial carbon concentration of 24900 mg L^{-1} (by TOC) in batch reactor, Catalyst: 3 gm of 5 wt% Ru/C (wet basis), total pressure: 1000 psi.

	Temperature (°C)	*25*	*125*	*125*	*125*	*125*	*150*	*150*	*150*	*175*	*175*
Method	**Minutes →**	*0*	*30*	*60*	*150*	*210*	*270*	*320*	*360*	*400*	*455*
		Concentration (mmole C L^{-1})									
GC-FID	Hydroxyacetone	135.5	55.7	24.5	0.0	0.0	0.0	0.0	0.0	0.0	0.0
GC-FID	Hydroxyacetaldehyde	28.1	0.0	0.0	0.0	0.0	0.0	0.0	0.0	0.0	0.0
GC-FID	Ethylene Glycol	0.0	90.6	172.3	212.2	216.9	198.9	191.6	204.6	222.6	210.9
GC-FID	Propylene Glycol	0.0	25.4	113.1	159.0	164.1	154.9	163.0	172.5	186.6	182.7
GC-FID	Butanediols[a]	0.0	13.3	36.6	52.7	55.5	51.8	59.1	63.0	64.3	61.1
GC-FID	THFA[b]	0.0	9.9	12.5	15.7	14.9	13.5	11.4	13.3	12.0	15.0
GC-FID	ϒ-Butyrolactone	0.0	24.7	31.7	30.4	29.4	30.5	30.3	30.7	30.8	29.8
GC-FID	Guaiacols[c]	30.8	28.8	0.0	0.0	0.0	0.0	0.0	0.0	0.0	0.0
HPLC	Sugars	377.4	242.5	232.6	N.A.	174.7	140.4	125.9	117.7	80.4	67.3
HPLC	Sorbitol	0.0	0.0	0.0	N.A.	56.6	89.8	117.1	141.2	186.7	204.7
HPLC	Levoglucosan	390.6	274.8	271.4	N.A.	276.7	235.8	216.0	212.9	150.7	132.0
GC-FID	Acetic Acid	182.2	126.1	192.6	170.9	167.1	186.0	196.3	201.1	206.8	210.2
	Total mmole-C L^{-1} identified	1144	891.8	1087	N. A.	1155	1101	1110	1157	1141	1114
	% C identified in liquid	55.2	50.5	59.8	N. A.	63.8	59.6	61.8	61.7	64.6	63.8
	% C in liquid by TOC	100.0	85.1	87.6	86.1	87.3	89.2	86.7	N.A.	85.1	84.2
	H_2 Consumption (gm/gm WSBO)	0	0.007	0.016	0.024	0.034	0.038	0.048	0.061	0.070	0.091

[a]1,2 and 1,4-butanediol, [b] tetrahydrofurfuryl alcohol, [c] contains guaiacol and methyl guaiacol, N.A. = not analyzed.

Sugars and levoglucosan do not undergo complete conversion at 125 °C. Levoglucosan has a very slow rate of hydrogenation at 125 °C. Initially levoglucosan concentration decreases rapidly from 390.6 mmol-C L^{-1} to about 275 mmol-C L^{-1} at 125°C. However, it then stays the same for 3 h. The levoglucosan concentration does decrease when the temperature is increased further. This implies that the high reaction temperature is required for the hydrogenation of levoglucosan. Levoglucosan is converted to sorbitol in two steps, hydrolysis of levoglucosan to glucose, followed by hydrogenation of glucose to sorbitol.[43] The first reaction is an acid catalyzed reaction, whereas the second reaction is catalyzed by a hydrogenation catalyst, in this case Ru/C. In the absence of any externally added acid in the reaction mixture, it is possible that the first reaction is catalyzed by acids that are present in the aqueous fraction of bio-oil. Disappearance of the sugars follows a similar but less obvious trend as levoglucosan. At 125 °C, sugars (377 mmol-C L^{-1} to 175 mmol-C L^{-1}) disappear twice as fast as levoglucosan (390 mmol C L^{-1} to 275 mmol-C L^{-1}) does in 3.5 hours. This implies that the first step (levoglucosan to glucose) is the slower one and hence the rate limiting step in the conversion of levoglucosan to sorbitol. Increasing the acidity of the feed could therefore help expedite the conversion of levoglucosan to sorbitol.[43]

It is desirable to minimize carbon loss from liquid in the form of methane in LTH step. About 25% carbon is converted to methane at 175 °C, whereas at 125 °C, only about 10% carbon is converted to methane. However, sugars and levoglucosan are not completely converted to corresponding alcohols at 125 °C for shorter reaction time (< 3.5 h). Thus, there requires some optimization of reaction temperature and time. At high

temperature, shorter reaction times (just sufficient to convert all the reactants to desired products), should be used to keep carbon loss to methane low. At low temperature, longer reaction time may be required to convert the reactants to respective alcohols. Hydrogen consumption during the LTH step increases with the temperature and is tabulated in Table 5-1.

Hydrogen consumption is about 0.034 gm/gm WS-OWBO at 125 °C and doubles for every 25 °C rise in the temperature. Hydrogen consumption at the end of the run was found to be 0.12 gm/gm WS-OWBO. Hydrogen consumption should be minimized by using as low temperature as possible. At low temperature unwanted reactions, such as saturation of aromatic rings, which consume a considerable amount of hydrogen, are suppressed. The hydrogen consumption at low temperature (125 °C) is comparable to that reported by Elliott for the two stage hydroprocessing process, where 0.034 gm H_2 is consumed per gm of bio-oil.[30]

We selected Ruthenium on activated carbon catalyst for LTH as it is known to exhibit high activity and stability for similar hydrogenation reactions in the aqueous phase.[61-63] The temperature and reaction time both influence the products that are formed. Strong acid (*e.g.* H_2SO_4, HCl) can be added to the reaction mixture to increase the rate of acid catalyzed hydrolysis of levoglucosan to glucose. Helle *et al.* showed that increasing the concentration of sulfuric acid increases the rate of hydrolysis of levoglucosan in water at 110 °C.[43]

The hydrogen consumption in LTH step is up to 0.12 gm/gm WS-OWBO at 175 °C (Table 5-1). At high hydrogenation temperature large amounts of undesired methane is produced. This results in significant increase in hydrogen consumption during this step. Methane formation also results in reduced hydrogen production in APR. Theoretically, a maximum of 0.15 gm of hydrogen can be produced per gm of WS-OWBO. We have studied the LTH in down-flow reactor in details and those results are discussed in Chapter 6. We were able to reduce the carbon loss to the gas phase and hydrogenate all the bio-oil functionalities at the same time. Reactions taking place during the LTH are identified in Chapter 6.

5.5 Aqueous Phase Reforming of the Aqueous Fraction of Bio-oil

We produced hydrogen from the aqueous fraction of the oak wood bio-oil by passing it over 1 wt% Pt/Al_2O_3 catalyst as shown in Table 5-2 and Figure 5-3. The Pt/Al_2O_3 catalyst had a hydrogen uptake of 40.6 μmol H/gm catalyst which corresponds to a surface to bulk metal ratio of 79.2%. The concentration of the WSBO in water was 4-5 wt% which corresponds to 1.5-2 wt% carbon in water. The concentration varied depending on the pretreatment of the bio-oil. Prior to each run the exact carbon content of the feed was measured with TOC. The liquid phase carbon content was measured by TOC analysis of the feed and liquid products. The gas phase contained C1 to C6 alkanes, CO_2 and H_2 for all products tested.

Table 5-2 Aqueous-phase reforming of H-WSBO (from OWBO) and 5 wt% sorbitol solution with a 1 wt% Pt/Al_2O_3 catalyst. Reaction conditions: 265 °C and 750 psi. The H-WSBO contains 1.5-2 wt% carbon and is prepared by hydrogenation of the aqueous fraction of bio-oil at 175 °C and 1000 psi with a 5 wt% Ru/C catalyst for 3 h.

Run Code	Pre-treatment on WSBO	WHSV (h^{-1})[a]	Hours Catalyst on Stream	H_2 Selectivity[b] (%)	Alkane Selectivity[c] (%)	% Carbon in gas phase effluent[d]	% Carbon in liquid phase effluent
H-WSBO-A	Hydrogenation	0.73	75	60	21	21	73
H-WSBO-B	Hydrogenation	0.13	20	50	35	41	43
WSBO-C	None	0.73	10	36	30	32[e]	26
Sorbitol	None	0.73	34	64	16	44[f]	51

[a] WHSV = flow rate of the aqueous fraction of bio-oil (gm h^{-1}) divided by grams of catalyst in the reactor.
[b] H_2 Selectivity = (molecules H_2 produced / C atoms in gas phase) × (1/Reforming Ratio) × 100, Reforming Ratio (RR) is the ratio of molecules of H_2 produced to C atoms in gas phase assuming that all the water soluble bio-oil goes to H_2 and CO_2 only, for hydrogenated water soluble bio-oil RR is 3, RR for sorbitol is 13/6.
[c] Alkane selectivity = (total moles of carbon atoms in alkane products) / (total moles of carbon atoms in the feed) × 100.
[d] Gas phase contains C1 to C6 alkanes, CO_2 and H_2.
[e] Decreases to 23% with the catalyst on stream for 22 h.
[f] Decreases to 38% with the catalyst on stream for 48 h.

Table 5-3 Production of alkanes from H-WS-OWBO and sorbitol at 260 °C and 750 psi with a 4 wt% Pt/SiO_2-Al_2O_3 catalyst. (The WSBO feed contains 1.5-2 wt% carbon and are prepared by hydrogenation of the aqueous fraction of bio-oil at 175 °C and 1000 psi with a 5 wt% Ru/C catalyst for 3 h).

Run Code	Feed	WHSV[a] (h^{-1})	Hours Catalyst on Stream	Alkane Selectivity[b] (%)	% Carbon in Gas Phase Effluent[c]	% Carbon in Liquid Phase Effluent
H-WSBO-D	H-WSBO	0.96	48	45	35[d]	38
H-WSBO-E	H-WSBO	0.20	25	42	40-50	43
H-WSBO-D-H_2	H-WSBO + H_2	0.96	80	77	18	59
H-WSBO-E-H_2	H-WSBO + H_2	0.20	55	85	56	37
H-WSBO-HCl	H-WSBO + HCl	0.20	200	55-60	40-45	47
H-WSBO-HCl-H_2	H-WSBO + HCl + H_2	0.20	215	97	55-60	32
Sorbitol	Sorbitol	0.96	24	42	72	19

[a] WHSV = flow rate of the aqueous fraction of bio-oil (gm h^{-1}) divided by grams of catalyst in the reactor.
[b] Alkane selectivity = (total moles of carbon atoms in alkane products) / (total moles of carbon atoms in the feed) × 100.
[c] Gas phase contains C1 to C6 alkanes and CO_2.
[d] Decreases to 30% with the catalyst on stream for 60 h.

The carbon conversion to gas phase products was just above 20% for the hydrogenated aqueous fraction of bio-oil (H-WSBO-A) at WHSV of 0.73 h^{-1}. The H_2 and alkane selectivities were 60% and 21% respectively. This indicates that at low conversion high hydrogen selectivity can be obtained from the aqueous fraction of bio-oil. At similar

conditions sorbitol showed the carbon conversion of 44% and H_2 and alkane selectivity of 64% and 16% respectively. Decreasing the WHSV to 0.13 h^{-1} for the H-WSBO (run code H-WSBO-B in Table 5.2) increases the gas phase conversion to 41%. At this higher conversion the hydrogen selectivity decreases to 50%. Thus the hydrogen and alkane selectivities are a function of the gas phase conversion. When H-WSBO-B data is compared to sorbitol (both have similar conversion), it can be concluded that aqueous fraction of the bio-oil is less active than sorbitol. The alkane selectivity for the WSBO and sorbitol are significantly different as shown in Figure 5-3. The WSBO more selectively produces the heavier alkanes as compared to the sorbitol.

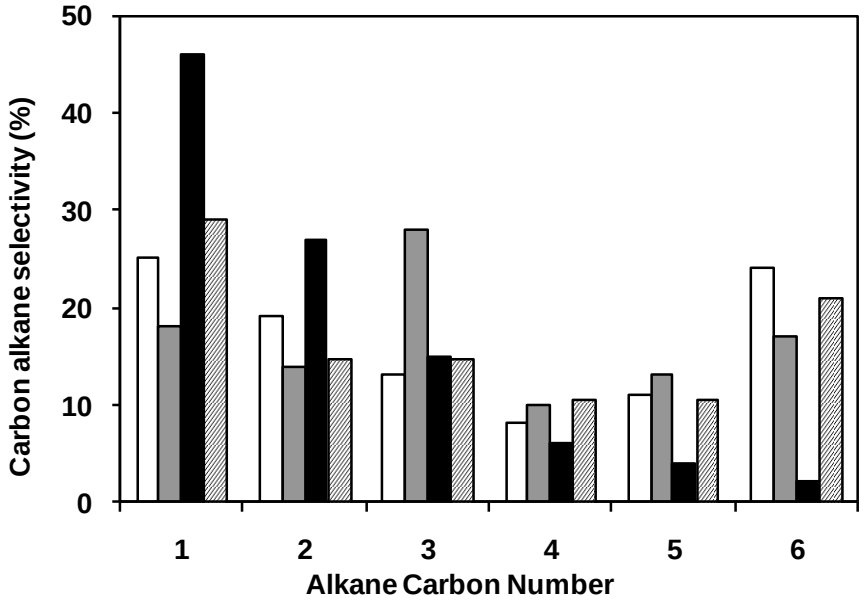

Figure 5-3 Alkane distribution for aqueous-phase reforming of WSBO and 5 wt% sorbitol solution at 265 °C and 750 psi with 1 wt% Pt/Al_2O_3 catalyst. Feed and reaction key (see Table 5-2) (□) H-WSBO-A, (■) H-WSBO-B, (▨), (■) Sorbitol, (▨) WSBO-C.

Our results are similar to that of Cortright *et al.* who produced hydrogen from 1 wt% sorbitol solution at 265 °C and 800 psi with a 3 wt% Pt/Al_2O_3.[(15)] Carbon

conversion to gas phase, CO_2 selectivity and hydrogen selectivity of 90%, 68% and 46% respectively, were reported. The difference between our runs and that of Cortright *et al.* is that our catalyst had significantly fewer surface sites (40.6 μmol H/gm catalyst of hydrogen uptake vs. 105 μmol gm^{-1} catalyst of CO uptake). Also the sorbitol space velocity used by Cortright et al. is 0.008 gm sorbitol per gram catalyst as compared to our 0.0365 gm sorbitol per gram catalyst. To compare our catalyst to that of Cortright *et al.,* we fed our reactor with 5 wt% sorbitol in water with same operating conditions. Conversion to gas phase, CO_2 selectivity and hydrogen selectivity for sorbitol were 44%, 84% and 64% respectively. We see low activity for sorbitol due the low catalyst concentration we used. Reforming of a non-hydrogenated aqueous fraction of the bio-oil (WSBO-C) was also studied at WHSV of 0.73 h^{-1}. The gas phase conversion decreased from 32% at 10 h to 23% at 22 h. The hydrogen selectivity of only 36% was observed with non-hydrogenated water soluble bio-oil, demonstrating the necessity of the hydrogenation step.

A process flow diagram that shows how bio-oil could be converted into liquid fuels and chemicals is shown in Figure 5-4 with mass balances for the different reaction assuming that 100% of the theoretical yield and 25% carbon loss to methane. In the first step in this process the bio-oil is mixed with water (1:1 weight mixture) and separated into a water soluble fraction (WSBO) and a water insoluble bio-oil (WIBO). Approximately 62 wt% of the initial bio-oil goes into the WSBO and 38 wt% of the initial bio-oil goes into the WIBO. The WSBO is then sent to a low temperature hydrogenation unit where the hydrogen consumption is up to 0.12 gm/gm bio-oil. In

Figure 5-4, hydrogen consumption of 0.06 gm/gm non-hydrogenated WS-OWBO is shown. The purpose of this unit is to stabilize the bio-oils. The hydrogenated WS-OWBO is then sent to an aqueous-phase reformer where hydrogen is produced. The maximum amount of hydrogen that can be produced from 100 kg h^{-1} of bio-oil is 9 kg h^{-1}. In the process, 66 kg h^{-1} CO_2 and 8 kg $h^{-1}$of methane will also form. The hydrogen consumption is 3.7 kg h^{-1} in hydrogenation step. The net hydrogen production for this process is 5.3 kg h^{-1}. After the hydrogenation step, the polyols can be separated out if desired. The unreacted bio-oil can be re-concentrated and recycled back to the reactor.

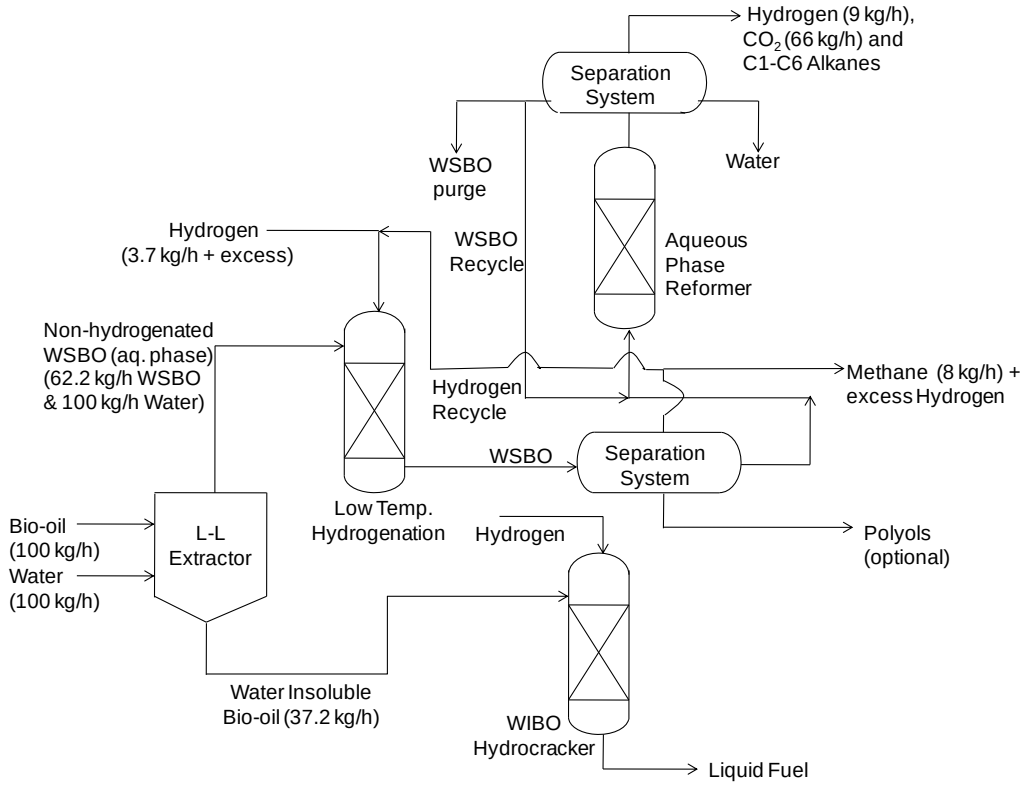

Figure 5-4 Process flow diagram for aqueous phase reforming of bio-oil.

In our experiments, hydrogen is produced from the aqueous fraction of the bio-oil with high selectivity (50-60%). The major challenge is that the bio-oils have low activity.

This could be due to poisoning of the catalyst surface by acids or other impurities. Lower hydrogen selectivity is observed for bio-oil (50%) as compared to sorbitol (64%) at similar conversions. Bio-oil exhibits low reforming activity though with moderate hydrogen selectivity. The moderate hydrogen selectivity can be attributed to the presence of smaller oxygenated hydrocarbons in the aqueous fraction of bio-oil. Smaller oxygenates present in bio-oil are converted to diols such as ethylene glycol and propylene glycol upon hydrogenation. These diols can produce hydrogen in high yield as compared to larger polyols such as sorbitol. These polyols also have higher rates of reaction than sorbitol.[15, 26] Even though it contains diols, the aqueous fraction shows lower hydrogen selectivity as compared to sorbitol. This can be due the presence of unreacted bio-oil components and other unidentified compounds in the aqueous fraction.

Theoretically about 0.085 gm hydrogen can be produced from a gram of non-hydrogenated WS-OWBO when about 25% of the carbon is converted to methane in hydrogenation step. We were able to produce 0.031 gm of hydrogen from a gram of non-hydrogenated WS-OWBO while consuming 0.06 gm hydrogen in the hydrogenation step. The low hydrogen production is due to two reasons (a) high carbon loss and hence the hydrogen loss to gas phase during hydrogenation and (b) low activity of bio-oil in reforming. About 0.032 gm hydrogen per gm non-hydrogenated WSBO is lost in the form of methane during hydrogenation at 175 °C. To reduce the carbon loss, optimization of reaction temperature and time is necessary as discussed earlier. Catalyst with low decarbonylation activity is desired for the hydrogenation step. For reforming, catalyst with high activity for bio-oil is desired. The low reforming activity seen for Pt/Al_2O_3

catalyst can also be due to various impurities in bio-oil. Effects of the bio-oil impurities (*e.g.* alkali salts of organic acids) on the reforming process needs to be studied. Bi-metallic catalysts are known to be highly active for the reforming of ethylene glycol[26] and can potentially be used for reforming of aqueous fraction of bio-oil.

5.6 Aqueous Phase Dehydration/Hydrogenation of the Aqueous Fraction of Bio-oil

Alkanes can be produced from the aqueous fraction of the bio-oil by aqueous-phase dehydration/hydrogenation with a bi-functional catalyst.[25] Platinum supported on silica-alumina is the catalyst used in these studies. The reactions that occur on Pt include hydrogenation; reforming and water gas shift reactions. The acidic silica-alumina catalyzes dehydration reactions. The data gathered with 4wt% Pt/Al_2O_3-SiO_2 catalyst are depicted in Table 5-3 and in Figures 5-5 and 5-6. This data was collected on the hydrogenated WSBO with hydrogen as a co-feed and without hydrogen as a co-feed. The concentration of WSBO in water was 4-5 wt% which corresponds to 1.5-2 wt% carbon in water.

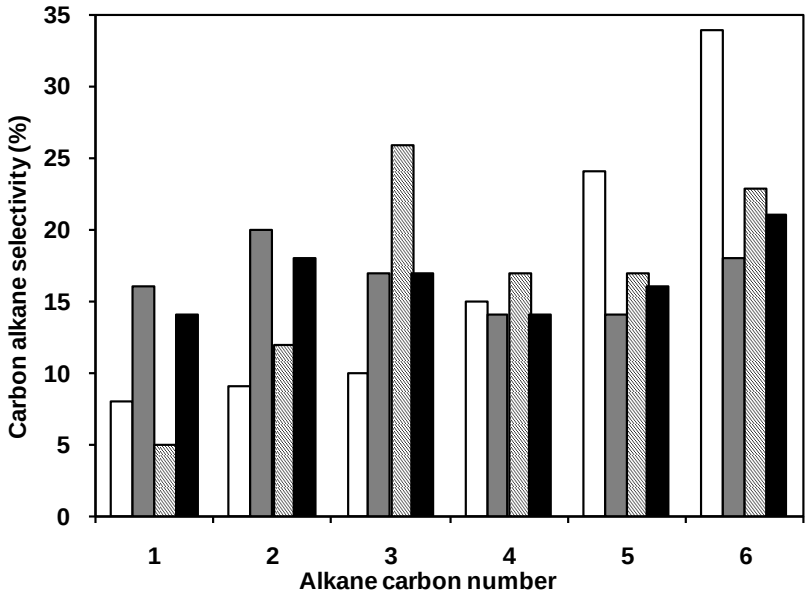

Figure 5-5 Alkane distribution for the liquid phase dehydration/hydrogenation of H-WS-OWBO and 5 wt% sorbitol solution at 260 °C and 750 psi with 4 wt% Pt/SiO_2-Al_2O_3 catalyst. Feed and reaction key (see Table 5-3): (□) H-WSBO-D, (■) H-WSBO-E, (▨) H-WSBO-HCl, (■) Sorbitol.

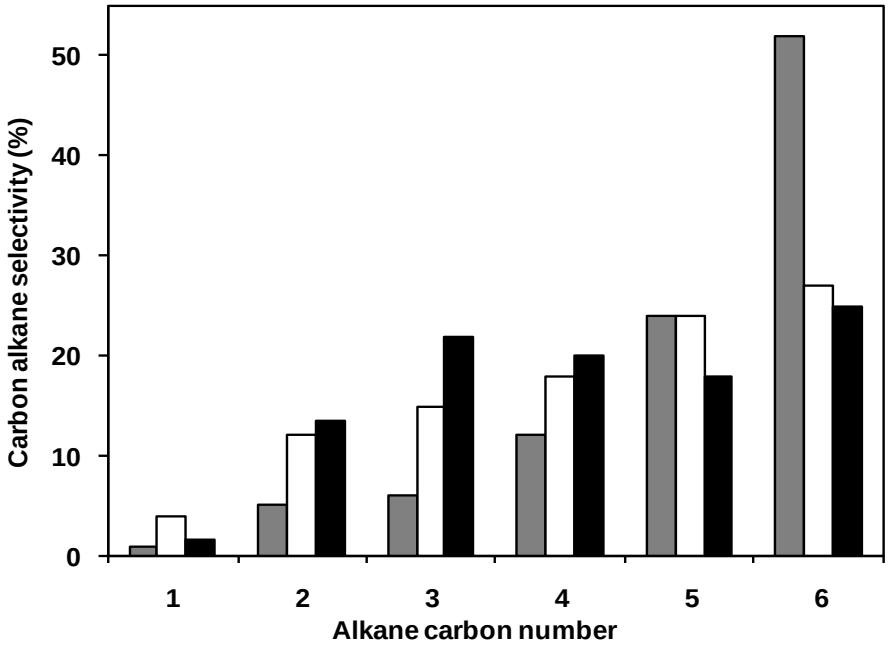

Figure 5-6 Alkane distribution for the liquid phase dehydration/hydrogenation of H-WS-OWBO at 260 °C and 750 psi with 4 wt% Pt/SiO_2-Al_2O_3 catalyst. Feed and reaction key (see Table 5-3): (■) H-WSBO-D-H_2, (□) H-WSBO-E-H_2, (■) H-WSBO-HCl-H_2.

The H-WSBO was tested at two different space velocities (H-WSBO-D and H-WSBO-E) without adding hydrogen as a feed. The carbon conversion to gas phase products increased from 35% to 40-50% when the WHSV decreased from 0.96 h^{-1} to 0.2 h^{-1}. The alkane carbon selectivity was 45% for H-WSBO-D with hexane and pentane being the most abundant alkanes (see Figure 5-5). A similar (42%) alkane selectivity is observed at both the space velocities. However, the alkane distribution shifts towards lower alkanes at higher conversions (see Figure 5-5). At similar operating conditions to the H-WSBO, sorbitol had a carbon conversion of 72% with the alkane selectivity of 42%. The sorbitol shows a similar distribution of C1-C6 alkanes as the WSBO. For sorbitol (72% conversion) and H-WSBO-E (up to 50% conversion), similar alkane selectivity (42%) is observed. Bio-oil clearly is less active than pure sorbitol for alkane production, but comparable alkane selectivities can be achieved. Huber *et al.* reported 95% conversion with 60% alkane selectivity for the sorbitol with the same temperature, pressure, catalyst and the WHSV of 1.3 h^{-1}.[25] Our catalyst is less active for dehydration/hydrogenation as compared to that of Huber *et al.* As the time of on stream increases from 48 h to 60 h the conversion decreases from 35% to 30% indicating catalyst deactivation.

Hydrogen was supplied externally to improve the carbon selectivity towards alkanes (H-WSBO-D-H_2 and H-WSBO-E-H_2). The alkane selectivity increases when hydrogen is added from 42-45% to 77-85%. This is due to the suppression of hydrogen producing reforming reactions in the presence of external hydrogen. Catalyst deactivation can be the reason for the low conversion observed as the H-WSBO-D-H_2 data was

gathered on the same catalyst after the collection of H-WSBO-D data. At low WHSV ($0.2\ h^{-1}$) carbon conversion was 56% with 85% alkane selectivity when the hydrogen was supplied externally (H-WSBO-E-H_2). When hydrogen is supplied externally, very high hexane and pentane selectivities are observed with almost complete suppression of methane formation (Figure 5-6). Moreover, the hexane and pentane carbon selectivity does decrease with increasing conversion.

The alkane selectivity is a function of relative rates of dehydration and hydrogenation reactions. Hydrochloric acid was added to the reaction mixture to increase the rate of dehydration reactions. HCl was added to the aqueous fraction of bio-oil before the hydrogenation step to a HCl concentration of 1 wt%. The product was then subjected to the aqueous phase dehydration/hydrogenation. The gas phase carbon conversion did not increase when HCl was added. However, the alkanes carbon selectivity increased with and without hydrogen being co-fed to the reactor (see H-WSBO-HCl-H_2 and H-WSBO-HCl). Low methane selectivity and a fairly even distribution of C2 to C6 alkanes is observed in case of the acidified feed (see Figures 5-5 and 5-6). Up to 97% selectivity alkanes was observed when HCl was added to the feed and hydrogen was supplied externally. HCl addition especially suppresses the methane formation. However it also increase the selectivity to propane. Hydrochloric acid might catalyze the retro-aldol condensation reactions of sorbitol producing C3 alcohols and hence increasing the propane selectivity.

The process flow diagram for the production of alkanes from the aqueous fraction of the bio-oil is shown in Figure 5-7. The amount of alkanes produced is shown with 100% carbon conversion to alkanes. The process is essentially the same as that for APR, except that the APR reactor is replaced by the APDH reactor. Theoretically when hydrogen is not supplied externally, about 18.0 to 20.4 kg h^{-1} of C1 to C6 alkanes mixture can be produced from 100 kg h^{-1} of bio-oil (62.2 kg h^{-1} WS-OWBO). At the same time, 3.5 to 16.0 kg h^{-1} of CO_2 and 8 kg h^{-1} of CH_4 will be produced. The composition of the alkane mixture produced depends on the composition of WSBO. Hydrogen can be supplied externally to the APDH reactor to increase the carbon selectivity towards alkanes.

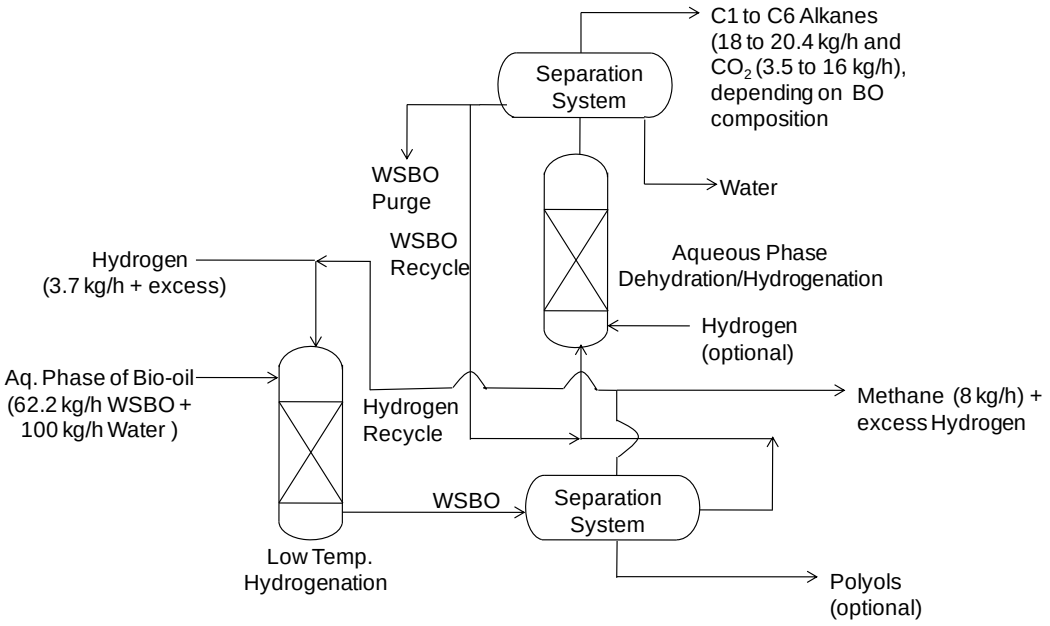

Figure 5-7 Process flow diagram for the aqueous phase dehydration/hydrogenation of bio-oil.

In our experiments, alkanes are produced at modest yields from the aqueous fraction of bio-oil over a bi-functional catalyst. Conversion for bio-oil is almost half of that for sorbitol. From Figure 5-7 it can be seen that, 0.289 to 0.328 gm alkanes can be produced per gram of WS-OWBO. We were able to produce up to 0.139 gm alkanes per gram of WS-OWBO, which is 42-48% of the theoretical yield. The alkane selectivity and the heavier alkane distribution are better for the bio-oil than the sorbitol. The alkane selectivity can be altered by supplying hydrogen externally or by adding a strong acid to the feed. External hydrogen suppresses the C-C bond breaking reactions that produce CO and CH_4 as the by-products. The near absence of methane when hydrogen is supplied externally implies that the methane is a result of C-C bond breaking reactions and not of dehydration/hydrogenation reactions of bio-oil component containing a single carbon atom (*e.g.* methanol). The strong acid can act as dehydration catalyst and hence can expedite the dehydration reactions resulting in higher alkanes selectivity.

The theoretical selectivities for the individual alkanes from WSBO and H-WSBO can be calculated from the composition shown in Figure 5-8. These theoretical selectivities assume that no carbon-carbon bond cleavage occurs in aqueous-phase dehydration hydrogenation. This provides an upper limit for alkane production by APDH. In Figure 5-8 the theoretical selectivities are compared with the actual selectivities observed for H-WSBO-E-H2. Theoretically no methane should be produced from the H-WSBO but in actuality up to 16% methane selectivity is observed for H-WSBO (see Figure 5-5). This implies the presence of C-C bond cleaving reactions during APDH. The actual ethane selectivity is lower than the theoretical value, implying that C2 compounds

are involved in the production of methane. Butane and pentane selectivities are higher than what is expected theoretically, implying that other than the respective C4 and C5 compounds, these alkanes are also produced from the C6 compounds.

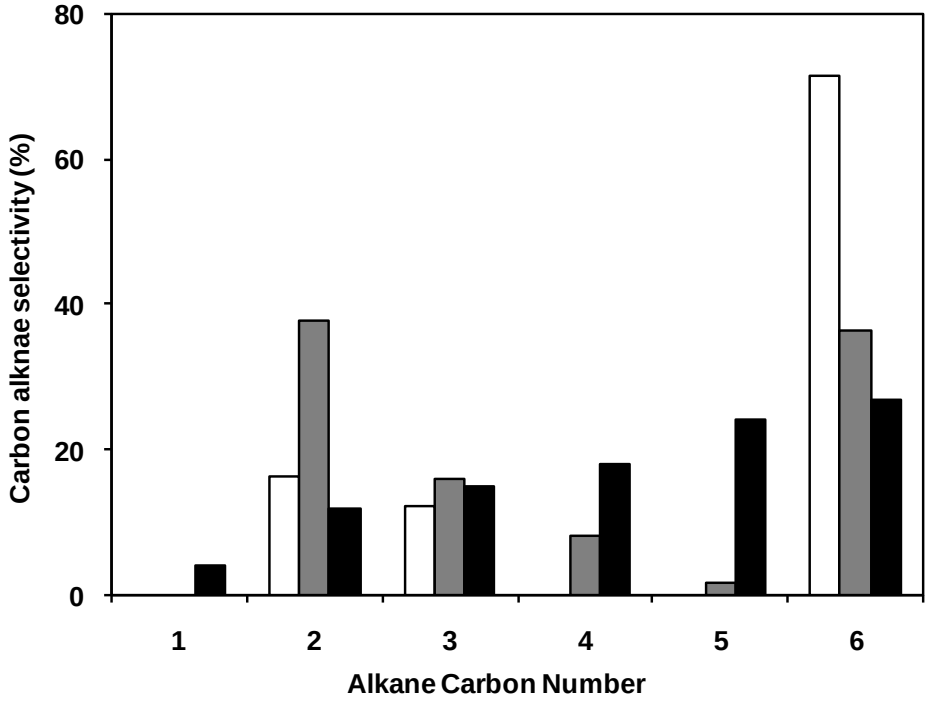

Figure 5-8 Theoretical and actual alkane selectivities for the production of alkanes from the aqueous fraction of the bio-oil. Legend (refer Table 5-3): (□) WSBO - theoretical, (▩) H-WSBO - theoretical, (■) H-WSBO-E-H_2 (experimental).

In this study, only smaller alkanes (C1 to C6) are produced from the aqueous fraction of the bio-oil. These alkanes are less valuable as fuel. The aqueous fraction of the bio-oil can essentially be used to produce larger gasoline range alkanes by carrying out some C-C bond formation reactions (e.g. aldol condensation) within it followed by APDH.[16, 17] Presence of various aldehydes and ketones makes the bio-oil aqueous fraction an excellent candidate for such a reactions.

5.7 Conclusion

The general conclusion from this study is that hydrogen and alkanes can be produced from the aqueous fraction of bio-oil by aqueous phase processing. Thus, previous work on aqueous phase processing of model biomass compounds[12,13,33] can be applied to processing of feedstocks derived from lignocellulosic biomass. This thus offers a new concept for the conversion of lignocellulosic biomass into fuels and chemicals. The first step in this process is to add water to the bio-oil and separate it into aqueous and organic phases. The aqueous phase is then sent to a low temperature hydrogenation unit where thermally unstable functionalities are hydrogenated to thermally stable compounds. In this hydrogenation step aldehydes are converted to alcohols, sugars to sugar alcohols, and aromatics are hydrogenated. Undesired methane is also formed from this reaction. A key need in this low temperature step is to reduce the amount of hydrogen that is consumed.

Hydrogen is produced at a hydrogen selectivity of 60% from the water soluble part of bio-oil. This selectivity is comparable to that observed for pure sorbitol at similar conversions. This makes bio-oil a feasible feedstock for the production of hydrogen. We have demonstrated here the feasibility to produce hydrogen from the water soluble bio-oil, but future research is needed to determine how the carbon conversion to gas phase can be increased maintaining the high selectivity. Concerns about catalyst stability must also be answered to efficiently use aqueous phase processing.

Alkanes are produced from the water soluble bio-oil by aqueous-phase dehydration/hydrogenation with a bifunctional catalyst. An alkane selectivity of 77% is obtained when hydrogen is co-fed with the bio-oil. Alternatively, an alkane selectivity of 45% is obtained when hydrogen is produced *insitu* from the bio-oil itself. The C_5 plus C_6 carbon selectivity ranges from 35 to 76% depending on the process conditions.

The advantage of this bio-oil processing approach is that we process the aqueous phase of the bio-oil differently than the organic phase. The aqueous phase is significantly different in composition than the organic phase. This will allow us to design catalysts that are well suited for conversion of both the aqueous and organic phases. We believe that in the future this will allow us to achieve higher overall yields for conversion of bio-oils into liquid fuels and chemicals. It would be advantageous to separate smaller molecules from the bio-oil prior to hydrotreating especially since these molecules form lighter gases during hydrotreating. These smaller molecules could then be sold as chemicals or reformed to hydrogen. Bio-oil composition changes depending on the feedstock. We envision that our process can handle any type of bio-oil. All the small aldehyde and ketonic functionalities in the aqueous fraction will be converted to corresponding polyols. These small polyols are excellent feedstock for the production of hydrogen and alkane. Bio-oil with high ash content can be a challenge to process as he Na, K, Ca and Mg salts in the ash can land up in the aqueous fraction and can de-activate the APP catalyst. For these reactions to become an industrial process the overall yield must be increased. Catalyst deactivation problems must be overcome and more active catalyst must be developed. However, in spite of these current difficulties it is highly likely that more

efficient catalytic processes will be developed for the conversion of pyrolysis oils through understanding the chemistry of this process and developing new generations of catalysts.

Chapter 6

HYDROPROCESSING OF BIO-OIL

6.1 Introduction

Pyrolysis oils needs to be deoxygenated to a mixture of organic molecules that are more compatible with current fuels and chemicals infrastructure.[30] The batch reactor hydrogenation studies described in Chapter 5 suggest that the aqueous fraction of the bio-oil (WSBO) can be an excellent feedstock to produce small oxygenated gasoline additives as well as valuable C2 to C6 diols. The challenge with WSBO hydrogenation is minimizing the hydrogen consumption and carbon loss to the gaseous products while achieving high selectivity to desired products. The low temperature hydrogenation (LTH) of the aqueous fraction of the bio-oil was further studied in detail in a trickle-bed reactor with both gas and liquid flowing in downward direction. For the hydrogenation reactions the trickle-bed reactor is expected to perform better due to the high hydrogen concentration in it as compared to batch reactor. In a batch reactor without a gas sparging impeller, hydrogen concentration is limited by its solubility in solvent. Hydrogen solubility in water is low.[64] Hence the flow reactor is expected to perform better than batch reactor. The main objective in LTH step is to reduce the carbon loss to gas phase while hydrogenating all the bio-oil functionalities. We were able to reduce all the WSBO functionalities except carboxylic acids to corresponding alcohols by LTH. The LTH product contains a significant amount of sorbitol, coming from the hydrogenation of glucose and levoglucosan. A high temperature hydrogenation (200-275 °C) step with Pt/C catalyst was added in series after low temperature hydrogenation to convert sorbitol

to the desired products. We could convert about half the carbon in the water soluble pine wood bio-oil to gasoline range oxygenated additives, and C2 to C6 diols. Whole bio-oil was also hydrotreated. The next section summarizes the past bio-oil hydroprocessing efforts.

6.2 Bio-oil Hydroprocessing: State of the Art

Several approaches toward the bio-oil upgrading are currently being studied including hydrotreating of bio-oils[30, 65, 66], zeolite conversion of bio-oils[32, 33, 60, 67], aqueous phase processing of bio-oils[29], and bio-oil model compounds hydrogenation studies[68-70]. However, none of these approaches are utilized commercially today primarily because they produce low yields of fungible products. The majority of the past bio-oil hydrotreating efforts have revolved around using γ-Al_2O_3 supported sulfided CoMo and NiMo catalysts. Elliott and Baker hydrotreated poplar wood bio-oil over sulfided CoMo catalyst at 355 °C and 2000 psi.[65] Only about 23 wt% bio-oil was converted to the deoxygenated product. Single stage hydrotreating of bio-oil over sulfided CoMo at temperatures over 310 °C resulted in heavy tar and coke plugging the reactor system.[30] A two stage hydrogenation process was hence developed. In the first stage, bio-oil was first stabilized by passing over Ni or sulfided CoMo catalyst at 2060 psi and temperatures in the range of 250-310 °C. The stabilized bio-oil was then hydrotreated over sulfided CoMo catalyst at 353 °C and 2060 psi to produce a deoxygenated liquid product containing 44% of the original bio-oil carbon. This process suffers from drawbacks such as: need to use sulfided catalysts which can contaminate the end product, severe reaction conditions, hydrothermal instability of γ-Al_2O_3 support, and

need to use low space velocities. Hydrogen consumption was about 8 g H_2/100 g carbon in feed. A relatively low LHSV of 0.07 volume of oil / volume of catalyst / h was used in the second step. A single stage non-isothermal bio-oil hydroprocessing over CoMo catalyst was also developed in the same group. The temperature at the reactor inlet was 250-260 °C and the temperature at the reactor outlet was 370-400 °C with the pressure of 2000 psi. The results for two different space velocities for hardwood vacuum pyrolysis bio-oil are shown in Table 6-1. The non-isothermal hydroprocessing works well only at low space velocities as seen in the Table 6-1. At low space velocity (0.13 vol oil/vol cat/h), hydrogen consumption is high and a large amount of carbon is lost to the gas phase. Several problems such as reactor plugging due to coking, difficulty in closing material balance, and accumulation of highly viscous tar-like material in the reactor were faced during these studies. Low temperature (< 100 °C) hydrogenation of the whole bio-oil was studied by Scholze on various metal based catalysts including Pd, Ni and Cu. Any hydrogenation above 80 °C resulted in phase separation in product. Also it was not established if hydrogenation increased the stability of bio-oil or not.[*(71)*]

Table 6-1 Non-isothermal hydroprocessing of vacuum pyrolysis bio-oil*

LHSV (vol oil / vol catalyst / h)	**0.28**	**0.13**
Inlet temperature (°C)	262	258
Outlet temperature (°C)	371	400
Pressure (psi)	2000	2000
H_2 consumption (L/L oil)	379	711
Oxygen in product (wt%)	9.0	0.8
Carbon conversion to gas (%)	23.9	35.5
Oil product yield (L/L feed)	0.29	0.42

* data taken from reference (*30*)

Bio-oil hydrodeoxygenation with conventional hydrotreating catalysts suffers with coking and catalyst deactivation problems. The hydrogen consumption is high and the process requires the use of severe operating conditions. The CoMo, NiMo based catalysts require presence of sulfur to maintain activity. Since the biomass based feedstock do not contain a considerable amount of sulfur it is best to avoid any external addition of sulfur to keep the process clean. Also the conventional CoMo, NiMo catalysts are supported typically on γ-alumina, which is unstable at high temperature in the presence of water. In fact Maggi and Delmon report that guaiacol and catechol form coke during hydrodeoxygenation on the catalyst support rather than on metal. Any compound with two or more oxygen atoms attached to benzene ring was found be the source of coke. They also found that activated carbon is better support with respect to selectivity than γ-alumina albeit with low activity.[68] The drawbacks of the sulfided $CoMo/Al_2O_3$ catalyst can be avoided by using supported noble metal catalyst. Elliott have studied the two step hydrotreating of bio-oils from different sources.[30] First step was on Pd/C catalyst at 310-360 °C and 2060 psi followed by a second hydrocracking step on conventional sulfided catalysts at 405 °C and 1500 psi. However, coking of catalyst and plugging of reactor system was observed for the first hydrogenation step.

6.3 Experimental

The materials and methods for this study is described in Sections 2.1, 2.4, 2.5, 2.6.2, and 2.8. Pine wood bio-oil and DOE bio-oil were used in these studies.

6.4 Homogeneous Reactions

Bio-oil is thermally unstable due to the presence of reactive functionalities such as aldehydes, ketones, acids, and sugars. Several chemical and physical changes occur in bio-oil when it is stored for long time or when it is heated. These changes are due the polymerization reactions occurring within various bio-oil components resulting in increase in viscosity and average molecular weight of bio-oil as described in Chapter 4. Water content of the bio-oil also increases upon storage and heating due the condensation polymerization reactions.

First we studied the homogeneous reaction of the aqueous fraction of bio-oil by hydrogenating it in the absence of any catalyst. The results are depicted in Figure 6-1. The homogeneous reactions are clearly present at 125 °C. Hydroxyacetaldehyde and sugars are especially reactive and we see a drop of more than 20% in their concentrations. No major products are observed indicating coke formation or polymerization reactions. At 150 °C, a 40% drop in the concentration is observed for Hydroxyacetaldehyde and sugars. Levoglucosan is highly reactive at 150 °C with about 90% disappearing due to homogeneous reactions. Acetic acid, hydroxyacetone, and phenolic compounds are quite stable with respect to homogeneous reactions up to 150 °C. Some of the sugars or levoglucosan might have converted to 5-HMF as we see increase in its concentration at 150 °C. The reactor plugged while running at 150 °C within 24 hours. Black tar like material was found in the reactor tube after the reaction, indicating coking. Due to the presence of homogeneous reactions all the catalytic experiments were done without any

void space in the reactor. The effect of temperature experiments does have a void space in reactor as these experiments were carried out before studying the homogeneous reactions in bio-oil.

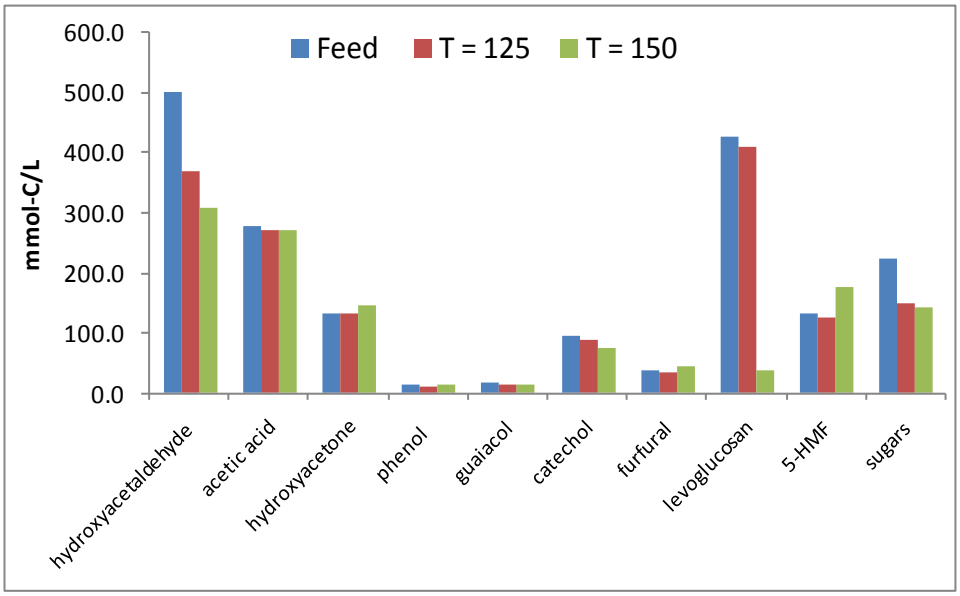

Figure 6-1 Reactivity of feed components during homogeneous reactions in aqueous fraction of pine wood bio-oil, P: 750 psi, feed flow rate: 0.04 ml min^{-1}, temperature is in °C.

Hydroxyacetaldehyde is stable to temperatures up to 350 °C.[72] Hence its observed disappearance during the homogeneous reactions at 125-150 °C can only be due to its reactions with other bio-oil components, possibly with sugars or lignin oligomers. Levoglucosan is also stable to temperatures up to 600 °C.[73] Its disappearance can be due to its reactions with other bio-oil components or it can also get converted to glucose by hydrolysis at 150 °C as aqueous fraction of the bio-oil is an acidic medium. Glucose can further react with lignin oligomers that can be present in WSBO. Xiang et al. have shown that glucose can decompose by reacting with acid soluble lignin in dilute-acid hydrolysis

environment at 200 °C.[74] These reactions can possibly proceed even at temperature as low as 125 °C.

6.5 Single Stage Hydrogenation of Water Soluble Pine Wood Bio-oil

6.5.1 Effect of Temperature

The Low Temperature Hydrogenation (LTH) step stabilizes the bio-oil by hydrogenating the carbonyl groups in it. In Section 5.4 we discussed the LTH data in a batch reactor. During the LTH, a fraction of carbon in WSBO is lost to the gas phase, predominantly in the form of methane. It is thus imperative to use lowest possible temperature so as to minimize the carbon loss to gas phase. We studied the effect of temperature in the range of 75-175 °C on the conversion of various components of the aqueous fraction of PWBO. The data obtained are depicted in Table 6-2. These experiments were done with void space (about 50%) in the reactor as this data is collected before studying the extent of homogeneous reactions in LTH of WS-PWBO. At 75 °C, only 2-furanone, furfural and 5-HMF show a significant activity towards hydrogenation. Only 4% conversion of total reactants is observed at 75 °C. At 100 °C, hydroxyacetaldehyde and 3-methyl-1,2-cyclopentadione start disappearing. Hydroxyacetone, phenol, guaiacol, catechol, levoglucosan, and sugars start reacting at 125 °C. About 90% conversion is observed for all the major reactants at 150 °C except acetic acid and phenol. Acetic acid is resilient to hydrogenation at temperatures below 175 °C. At 175 °C, reactor plugging was observed. The reactants and products concentration in feed and products of this experiment are shown in Table 6-3.

Table 6-2 Effect of temperature on reactant conversions for LTH of WS-PWBO

Compound	Conversion (%)				
	T: 75 °C	**100 °C**	**125 °C**	**150 °C**	**175 °C**
Hydroxyacetaldehyde	0	38	93	100	100
Acetic acid	0	0	16	13	10
Hydroxyacetone	0	0	58	96	100
2-Furanone	89	88	72	74	97
Phenol	2	1	37	39	33
3-Methyl-1,2-cyclopentadione	14	46	100	100	100
Guaiacol	6	13	100	100	100
Catechol	4	12	56	87	95
Furfural	71	73	100	100	100
5-Hydroxymethylfurfural	59	73	89	100	100
Levoglucosan	3	8	53	100	100
Sugars	11	14	N/A	97	99
Total	4	16	57	89	90

Catalyst: 5wt% Ru/C, WHSV: 3 h^{-1}, P: 750 psi, H_2 flow rate: 150 ml min^{-1}, feed: ~13wt% WS-PWBO solution in water

Table 6-3 Reactant and product concentration for low temperature hydrogenation of WS-PWBO at different temperatures

Compound	Product Concentration (mmol-C L^{-1})					
	Feed	Temperature (°C)				
		75	100	125	150	175
Reactants						
Hydroxyacetaldehyde	376.2	386.2	233.2	24.9	0.0	0.0
Acetic acid	191.9	205.2	203.9	161.9	166.6	172.1
Hydroxyacetone	160.9	196.4	203.8	67.4	5.8	0.0
2-Furanone	34.1	3.7	4.1	11.6	8.9	1.1
Phenol	2.2	2.2	2.2	1.4	1.4	1.5
3-Methyl-1,2-Cyclopentadione	43.4	37.2	23.3	0.0	0.0	0.0
Guaiacol	9.4	8.8	9.1	8.3	0.0	4.0
Catechol	247.1	237.4	218.2	108.1	33.1	13.5
Furfural	17.78	5.2	4.9	0.0	0.0	0.0
5-Hydroxymethylfurfural	57.4	23.6	15.6	6.4	0.0	0.0
Levoglucosan	602.4	582.5	553.2	280.8	0.0	0.0
Sugars	171.9	153.8	148.7	163.3	4.8	0.9
Products						
Methanol	15.1	34.0	40.6	23.1	22.1	16.0
Ethanol	0.0	3.1	3.6	8.9	10.1	10.8
1-Propanol	0.0	3.9	2.2	4.0	6.8	8.7
1-Butanol	0.0	0.0	0.0	2.6	3.2	4.3
1-Pentanol	0.0	0.0	0.0	0.0	0.0	2.7
Ethylene glycol	0.0	139.8	287.0	275.5	185.6	128.9
Cyclopentanol	0.0	0.0	0.0	2.0	5.6	7.7
Propylene glycol	0.0	4.4	6.1	96.5	153.8	139.5
Cyclohexanol	0.0	0.0	0.0	3.5	37.3	38.1
1,2-Butanediol	0.0	0.0	0.0	23.1	49.2	30.0
Tetrahydrofurfuryl alcohol	0.0	10.0	11.2	10.8	18.0	23.6
1,4-Butanediol	0.0	2.8	11.5	33.6	27.8	17.7
γ-Butyrolactone	0.0	54.2	57.3	55.0	72.7	60.5
γ-Valerolactone	0.0	0.0	0.0	4.1	7.0	8.7
Glycerol	0.0	13.4	16.7	10.0	11.6	5.4
1,2-Cyclohexanediol	0.0	0.0	0.0	2.6	32.0	33.0
Hydroxymethyl-γ-butyrolactone	0.0	22.1	22.7	29.2	27.7	17.0
Sorbitol	0.0	48.8	37.7	36.0	67.2	12.1
Total C identified	1929.7	2178.6	2116.7	1453.9	958.2	757.7
Carbon content by TOC	2633.3	2519.6	2539.0	2451.5	1971.2	1680.9
%C lost to gas phase	-	4	4	7	25	36

Catalyst: 5wt% Ru/C, WHSV: 3 h^{-1}, P: 750 psi, H_2 flow rate: 150 ml min^{-1}, feed: ~13wt% WS-PWBO solution in water

The major products from the LTH of WS-PWBO are ethylene glycol, propylene glycol, butanediols and γ-butyrolactone as shown in Table 6-3. The products concentration maximizes at 125 °C. More propylene glycol is observed at 150 °C but the ethylene glycol starts undergoing secondary reactions at that temperature. A large amount of carbon (25.2%) is lost to gas phase (mostly methane and ethane) at 150 °C. For the process to be economically attractive this carbon loss needs to be minimized. The carbon loss to gaseous compounds is moderate (7%) at 125 °C with all the bio-oil components showing reasonable hydrogenation activity. Ethylene glycol concentration is also a maximum at 125 °C. Due to all these reasons we chose 125 °C as the optimum temperature for any further LTH experiments. The experiments depicted in Tables 6-2 and 6-3 are carried out at comparatively high space velocity of 3 h^{-1}. In the next section we show that almost 100% conversion of all the reactants except acetic acid is achievable at 125 °C with lower space velocities. Also the catalyst was very stable with no signs of deactivation or coking. We studied the catalyst stability for 5 wt% Ru/C catalyst with WS-PWBO feed at WHSV of 1.5 h^{-1} for 78 hours. No catalyst activity loss was observed over the studied time period.

6.5.2 Effect of Space Velocity

The effect of space velocity on the LTH of WS-PWBO was studied at 125 °C and the data are shown in Table 6-4 and 6-5. The experiments were carried out at 125 °C as that was the optimum temperature for LTH as discussed in the previous section. At a space velocity of 6.0 h^{-1}, only guaiacol, furfural and 5-HMF are completely converted. Note that the concentrations of guaiacol and furfural in the feed were very low (Table 6-

5). Hydroxyacetaldehyde and hydroxyacetone show near complete conversion. The concentration of ethylene glycol in the product at WHSV of 3 h^{-1} is more than the concentration of hydroxyacetaldehyde in the feed. This implies that ethylene glycol is also formed some other feed component than hydroxyacetaldehyde. Sugars can produce ethylene glycol by hydrogenolysis.[75] The conversion 2-furanone shows a reverse than expected trend implying that it may be formed during LTH from some other bio-oil components. All of the components show 90% or more conversion at the lowest space velocity of 0.75 h^{-1} except for acetic acid and 2-furanone. Acetic acid hydrogenation requires high temperatures and pressures.[76] Elliott and Hart obtained 96% conversion for acetic acid on Ru/C catalyst at 250 °C and 2000 psi with only 4% selectivity to ethanol. Maximum ethanol selectivity of 34% was seen at the acetic acid conversion of 60%.[70]

Table 6-4 Effect of space velocity on conversion of reactants in LTH of WS-PWBO

Compound	**Conversion (%)**			
	WHSV: 0.75 h^{-}	**1.5 h^{-1}**	**3.0 h^{-1}**	**6.0 h^{-1}**
Hydroxyacetaldehyde	100.0	100.0	100.0	96.8
Acetic acid	12.6	9.8	16.8	13.3
Hydroxyacetone	100.0	100.0	100.0	92.8
2-Furanone	25.9	27.8	42.6	57.4
Phenol	100.0	100.0	100.0	92.4
3-Methyl-1,2-cyclopentadione	100.0	100.0	100.0	96.0
Guaiacol	100.0	100.0	100.0	100.0
Catechol	100.0	100.0	100.0	68.6
Furfural	100.0	100.0	100.0	100.0
5-Hydroxymethylfurfural	100.0	100.0	100.0	100.0
Levoglucosan	91.2	76.7	47.6	32.1
Sugars	89.3	54.5	65.3	0.7
Total	85.0	78.1	70.7	56.6

Catalyst: 5wt% Ru/C, T: 125 °C, P: 750 psi, H_2 flow rate: 150 ml min^{-1}, feed: ~13wt% WS-PWBO solution in water

Table 6-5 Reactant and product concentration for LTH of WS-PWBO at different space velocities

Compound	Concentration (mmol-C L^{-1})				
	Feed	Product			
		0.75 h^{-1}	1.5 h^{-1}	3.0 h^{-1}	6.0 h^{-1}
Reactants					
Hydroxyacetaldehyde	427.6	0.0	0.0	0.0	13.8
Acetic acid	244.1	213.4	220.2	203.2	211.7
Hydroxyacetone	199.3	0.0	0.0	0.0	14.3
2-Furanone	37.6	27.9	27.2	21.6	16.0
Phenol	2.5	0.0	0.0	0.0	0.2
3-Methyl-1,2-cyclopentadione	45.7	0.0	0.0	0.0	1.8
Guaiacol	10.3	0.0	0.0	0.0	0.0
Catechol	249.8	0.0	0.0	0.0	78.4
Furfural	20.9	0.0	0.0	0.0	0.0
5-Hydroxymethylfurfural	63.9	0.0	0.0	0.0	0.0
Levoglucosan	652.5	57.7	152.2	341.8	443.1
Sugars	124.4	13.4	56.7	43.1	123.6
Products					
Methanol	24.4	70.2	49.0	49.1	49.9
Ethanol	0.0	47.8	18.2	19.7	16.8
1-Propanol	7.9	37.1	8.3	9.7	8.0
1-Butanol	0.0	13.1	4.6	4.4	3.9
1-Pentanol	0.0	4.1	0.0	0.0	0.0
Ethylene glycol	0.0	450.6	413.2	498.0	495.7
Cyclopentanol	0.0	18.0	15.5	9.5	12.2
Propylene glycol	0.0	246.7	240.5	236.1	231.5
Cyclohexanol	0.0	120.0	122.2	124.6	74.2
1,2-Butanediol	0.0	56.4	74.0	32.1	23.5
Tetrahydrofurfuryl alcohol	0.0	29.8	18.8	1.0	2.7
1,4-Butanediol	0.0	32.8	48.8	54.2	52.5
γ-Butyrolactone	0.0	81.9	99.1	103.0	83.5
γ-Valerolactone	0.0	9.5	8.6	9.6	3.0
Glycerol	0.0	45.6	19.4	30.5	28.0
1,2-Cyclohexanediol	0.0	102.8	106.9	N/A	104.8
Hydroxymethyl-γ-butyrolactone	0.0	19.7	66.0	70.1	69.3
Sorbitol	43.8	497.4	602.4	386.9	186.2
Total C identified	2154.7	2195.9	2369.9	2355.4	2307.5
Carbon content by TOC	3879.3	3356.2	3634.7	3590.3	3669.3
% C identified		13.5	6.3	7.5	5.4

Catalyst: 5wt% Ru/C, T: 125 ℃, P: 750 psi, H_2 flow rate: 150 ml min^{-1}, feed: ~13wt% WS-PWBO solution in water

The product distribution in the LTH of the aqueous fraction of pine wood bio-oil at different space velocities is shown in Table 6-5. The concentration of various products maximizes at different space velocities. The monohydric alcohols (includes methanol, ethanol, 1-propanol, 1-butanol and 1-pentanol, cyclopentanol) concentration is highest at 0.75 h^{-1}. The concentration of diols such as ethylene glycol and butanediols maximizes at 3 h^{-1}. This implies that the monohydric alcohols mentioned above are formed from the secondary reactions of diols. At lower space velocity ethylene glycol seems to undergo secondary reactions. The possible secondary products are methane and ethanol. Hydroxyacetaldehyde in the feed is converted to ethylene glycol upon hydrogenation. Hydroxyacetaldehyde concentration in the feed is 427.6 mmol-C L^{-1}. Maximum ethylene glycol concentration observed is 498.0 mmol-C L^{-1}. This means that ethylene glycol is also produced from some other compound than hydroxyacetaldehyde. Ethylene glycol can be produced from sorbitol or glucose by hydrogenolysis.[77-79] Propylene glycol is produced by the hydrogenation of hydroxyacetone. Feed concentration of hydroxyacetone is 199.3 mmol-C L^{-1}, whereas maximum concentration of propylene glycol observed is 246.7 mmol-C L^{-1}. This gives an idea that all of the propylene glycol is produced from the hydroxyacetone. Propylene glycol and glycerol can be produced from sorbitol by hydrogenolysis.[77-79] A small amount of glycerol is seen in the product. Some propylene glycol may have been produced from sorbitol by hydrolysis but we cannot determine that based on the numbers we have as some propylene glycol may react further under the reaction conditions. Cyclohexanol and 1,2-cyclohexanediol are formed by the hydrogenation of guaiacol and catechol. This is different than what Elliott and Hart observed. They hydrogenated guaiacol over Ru/C catalyst at temperatures from 150-250

°C and obtained 2-methoxycyclohexanol (at 150 °C and 200 °C) and Cyclohexanol (at 250 °C) as major products.[70] Gamma-butyrolactone (γ-GBL) seems to have another source than 2-furanone as significantly more γ-GBL is produced than stoichiometrically possible from 2-furanone. This extra source of γ-GBL is unknown. The sorbitol concentration reaches a maximum at WHSV of 1.5 h^{-1}. Sorbitol undergoes secondary reactions at the space velocity of 0.75 h^{-1} with methane being the primary product. A significant amount of hexane is observed in the gas phase products but we are not sure of the identification of this peak in GC-FID.

At low space velocity (0.75 h^{-1}), 13.5% carbon is lost to the gas phase with methane being the major gas phase product. At the space velocities of 1.5 to 6 h^{-1}, the carbon loss to gas phase products is essentially the same at around 6%. The amount of carbon identified in gas phase by GC at low space velocities (0.75 and 1.5 h^{-1}) is more than what we found in gas phase by TOC analysis. This can be due to the calibration or product identification error in GC-FID.

6.6 Two-stage Hydrogenation of Water Soluble Pine Wood Bio-oil

The overall goal of the hydrogenation process is to produce valuable fuels and chemicals from the aqueous fraction of bio-oil. We divided the products obtained from the WSBO hydroprocessing in 10 different groups, C1 to C4 alkanes and other gas phase products, gasoline cut 1, gasoline cut 2, C2 to C6 diols, lactones, acetic acid, sorbitol,

other compounds, levoglucosan, and unidentified (see footnote of Table 6-6 for the list of components of each product group). Gasoline cut 1, gasoline cut 2, and C2 to C6 diols are considered as the valuable products. Gasoline cut 1 consists of monohydric alcohols boiling in the temperature range of 65-99 °C. Gasoline cut 2 consists of monohydric alcohols boiling in the temperature range of 115-175 °C. Figure 6-2 shows the product selectivity for the hydrogenation of WS-PWBO over Ru/C catalyst at 125 °C, 750 psi and at the WHSV of 3.0 h^{-1}. We achieved our best yield to the desired products at these reaction conditions. It can be seen in Figure 6-2 that less than 30% of the carbon in the feed is converted to gasoline cut 1, gasoline cut 2, and C2-C6 diols in the single stage process. The product of single stage hydrogenation of WS-PWBO still contains a considerable amount of sorbitol and levoglucosan. In order to improve the process economics it would be vital to convert these compounds to valuable products. A second high temperature hydrogenation stage is thus added after the low temperature stage to maximize the yield of valuable products from bio-oil. Two different catalysts were studied in the high temperature stage, 5wt% Ru/C and 5 wt% Pt/C. The first stage was operated at 125 °C with 5wt% Ru/C catalyst. Table 6-6 depicts the results for 2-stage hydrogenation of WSBO with Ru/C catalyst in both the stages. The single stage data is also shown in the last column of Table 6-6 for the comparison.

Table 6-6 Product yield and selectivity in 2-stage hydrogenation of WS-PWBO over Ru/C catalyst in both the stages. Pressure: 750 psi for both the stages, first stage catalyst: 5wt% Ru/C, temperature: 125 °C, second stage catalyst: 5 wt% Ru/C

Second Stage T (°C)	**200**	**220**	**250**	**250**	**Single Stage**
WHSV (hour^{-1})	3	3	3	6	3
Product Group	**Carbon Yield (%)**				
C1-C4 alkanes & other gas phase products	24.3	27.2	57.5	18.2	7.5
Gasoline cut 1	6.1	5.5	11.9	4.8	2.0
Gasoline cut 2	5.6	6.6	9.0	6.2	6.3
C2 to C6 diols	12.2	15.4	3.8	17.0	21.1
Lactones	1.5	3.5	0.4	4.1	2.9
Acetic acid	4.2	4.2	1.1	4.4	5.2
Sorbitol	9.4	4.1	0	6.4	10.0
Other chemicals	2.2	3.1	1.8	2.9	1.9
Levoglucosan	0	0	0	0	8.8
Unidentified	34.5	30.4	14.5	36.0	34.3

Individual compounds in different product groups are as follows,

1. C1-C4 alkanes & other gas phase compounds: methane, ethane, propane, butane and other gas phase compounds which have not been identified.
2. Gasoline cut 1 (boiling range: 65-99 °C): pentane, hexane, methanol, ethanol, 1-propanol, tetrahydrofuran, 2-butanol, and 2-methyltetrahydrofuran.
3. Gasoline cut 2 (boiling range: 115-175 °C): 1,2-cyclohexanediol, 2,5-dimethyltetrahydrofuran, 1-butanol, 2-pentanol, 1-pentanol, cyclopentanol, 2-hexanol, 3-methylcyclopentanol, cyclohexanol, 3-methylcyclohexanol, and 4-methylcyclohexanol.
4. C2 to C6 diols: 2,3-butanediol, propylene glycol, ethylene glycol, 1,2-hexanediol, 1,4-hexanediol, 1,4-butanediol, and 1,4-pentanediol.
5. Lactones: γ-butyrolactone and γ-valerolactone
6. Other chemicals: tetrahydrofurfuryl alcohol, 1,2,6-hexanetriol, 1,2,3-butanetriol, and glycerol

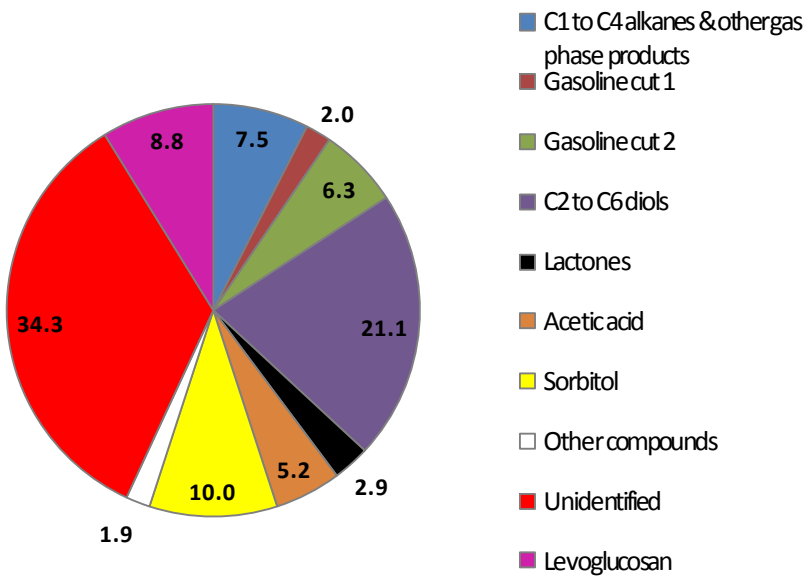

Figure 6-2 Product distribution from the hydrogenation of WS-PWBO over Ru/C catalyst at 125 °C, 750 psi and at the WHSV of 3.0 h^{-1}.

As seen in Table 6-6, addition of a second stage with Ru/C catalyst results in reduction in the total yield of valuable products. All of the levoglucosan disappeared even at the lowest temperature used (200 °C). In the hydrogenation process, levoglucosan is first converted to glucose by hydrolysis and then glucose is further converted to sorbitol by hydrogenation. The levoglucosan disappearance is not accompanied by corresponding increase in sorbitol concentration, implying that sorbitol is further converted to secondary products. Sorbitol can undergo hydrogenolysis under the reaction conditions used, resulting in products such as ethylene glycol, propylene glycol, butanediols, and glycerol. No such products are observed, implying sorbitol is directly reformed to gaseous products or the products obtained from sorbitol are further reformed to gaseous products. Methane is the predominant component in the gaseous products. About a quarter of carbon in the WSBO is lost to the gas phase upon 2-stage hydrogenation over Ru/C

catalyst at temperatures in the range of 200-225 °C. The carbon loss to gas phase increases to 57.5% at 250 °C and 750 psi pressure. Carbon loss to the gas phase can be reduced by operating at high space velocities. Carbon loss of only 18.2% was observed at 250 °C, 750 psi at the space velocity of 6 $hour^{-1}$. However only 28.0% carbon yield is observed to gasoline cut 1, gasoline cut 2, and C2-C6 diols combined at these reaction conditions, lower than the single stage process (29.5% carbon yield to valuable products). Hence Ru/C is not a good catalyst for the high temperature hydrogenation of water soluble bio-oil components.

To overcome the drawbacks associated with Ru/C, we studied the 2^{nd} stage of our process on 5 wt% Pt/C catalyst. The rate of C-C bond cleavage reactions on Pt is seven times less than that on Ru.[80] It was also shown in our group that Pt catalysts have high C-O hydrogenation and low C-C bond cleavage activity in hydrodeoxygenation of sorbitol.[75] Maris and Davis showed that Pt can catalyze glycerol hydrogenolysis to propylene glycol more selectively that Ru. Ru mainly produced ethylene glycol and methane due to its high activity for C-C bond cleavage.[81] The results for 2-stage hydrogenation are depicted in Table 6-7 and Figure 6-3 and in more detail in Table 6.8. The first hydrogenation stage was always carried out on Ru/C catalyst at 125 °C and 3 $hour^{-1}$. Figure 6-3 A-B depicts the product distribution at 220 °C at two different pressures. All of the levoglucosan is converted on Pt/C at 220 °C. Sorbitol being the major product from levoglucosan, its concentration increases in the hydrogenated product. Sorbitol also undergoes hydrogenolysis reactions at these operating conditions producing monohydric alcohols and diols. A significant amount of sorbitol is still present

in the product. The carbon yield to valuable products (gasoline cut 1 & 2, and C2 to C6 diols) has been improved to 35.4% (at 750 psi) upon second hydrogenation as compared to for the single stage process (Table 6.7, last column). The advantage of high pressure is a low carbon loss (8.9% at 1450 psi as compared to 15.9% at 750 psi) to gas phase products. A significant amount of sorbitol still remains in the liquid phase products. This sorbitol needs to be converted to valuable products to improve the process economics. The remaining sorbitol can be converted to valuable products by increasing the second stage temperature to 250 °C. At low pressure (750 psi) and 250 °C, about a quarter of the carbon is lost to gas phase with 41.2% total carbon yield to gasoline cut 1, gasoline cut 2, and C2 to C6 diols. (Figure 6-3C). All of the sorbitol has reacted at 250 °C. Carbon loss to gas phase can be reduced by operating the reactors at high pressure. At 1450 psi, carbon loss to gas phase products was found to be 11.7%. The carbon yield to desired products of 45.8% was achieved at these reaction conditions. Although there is only a 4.6% difference between the desired product yield at 750 psi and 1450 psi at 250 °C, the product distribution is significantly different (compare Figures 6-3C and 6-3D). At 750 psi, carbon yield to C2-C6 diols is 17.4%. At the same time yields of gasoline cut 1 and gasoline cut 2 are 13.2% and 10.6% respectively. Thus a significant amount of carbon is converted to gasoline cut 1 and 2 in the case of low pressure due to secondary hydrogenation reactions of C2-C6 diols to corresponding monohydric alcohols. On the other hand, 28.9% of the carbon is converted to C2-C6 diols at 1450 psi with only 8.8% and 8.1% carbon yields to gasoline cut 1 and 2 respectively. Hence the product spectrum can be manipulated by tuning the system total pressure so as to maximize yield to the desired products. Further increase in second stage temperature to 275 °C resulted in the

conversion of 32.4% carbon to gas phase products (Figure 6-3E). Yields of gasoline cut 2 and C2-C6 diols decreased at 275 °C due to secondary hydrogenation reactions producing more of gasoline cut 1 and C1-C4 alkanes.

Table 6-7 Product yield and selectivity in 2-stage hydrogenation of WS-PWBO.
First stage catalyst: 5wt% Ru/C, temperature: 125 °C, second stage catalyst: 5 wt% Pt/C, WHSV for both the stages: 3 $hour^{-1}$

Second Stage Temperature (°C)	**220**	**220**	**250**	**250**	**275**	**Single Stage**
Pressure (psi)	1450	750	750	1450	1450	750
Product Group			**Carbon Yield (%)**			
C1-C4 alkanes & other gas phase products	8.9	15.9	24.3	11.7	32.4	7.5
Gasoline cut 1	4.6	8.4	13.2	8.8	11.9	2.0
Gasoline cut 2	6.9	7.4	10.6	8.1	7.1	6.3
C2 to C6 diols	22.2	19.6	17.4	28.9	17.0	21.1
Lactones	5.1	3.4	2.7	4.2	3.8	2.9
Acetic acid	3.3	3.0	1.5	2.6	1.5	5.2
Sorbitol	14.8	12.7	0	0.5	0	10.0
Other chemicals	2.8	2.8	2.9	4.3	4.1	1.9
Levoglucosan	0	0	0	0	0	8.8
Unidentified	31.4	26.7	27.4	30.8	22.2	34.3

Table 6-8 Composition of the two-stage water soluble pine wood bio-oil (WS-PWBO) hydrogenation products. Feed: ~13 wt% WS-PWBO solution in water. Hydrogenation reaction conditions: first over 5wt% Ru/C catalyst (125 °C) then over 5 wt% Pt/C catalyst; P: 1450 psi, WHSV: 3 $hour^{-1}$

	Concentration (mmol carbon L^{-1})				
Pressure (psi)	1450	750	750	1450	1450
2^{nd} stage Temperature (°C)	220	220	250	250	275
Compound					
Pentane	4.5	15.9	19.8	14.5	18.0
Hexane	30.8	129.0	131.0	115.4	121.2
Acetic acid*	133.3	120.5	59.4	104.9	56.8
Levoglucosan*	0	4.4	0	0	0
Sugars*	4.4	6.6	4.4	6.5	4.1
Methanol	48.4	53.3	66.8	56.8	80.1
Ethanol	31.6	45.4	133.7	47.9	115.5
1-Propanol	18.7	34.1	80.2	42.5	59.8
Tetrahydrofuran	6.0	9.0	21.4	6.1	9.8
2-Butanol	7.6	8.6	13.1	15.0	17.9
2-Methyltetrahydrofuran	15.5	17.0	23.3	21.5	22.0
2,5-Dimethyltetrahydrofuran	14.4	18.9	25.6	19.7	17.0
1-Butanol	8.2	14.5	31.7	11.7	19.8
2-Pentanol	3.1	6.6	13.5	4.4	5.9
1-Pentanol	5.2	4.7	26.9	8.4	15.7
Ethylene glycol	414.8	355.5	192.2	465.1	189.6
Cyclopentanol	18.9	22.9	48.7	23.0	27.0
2-Hexanol	4.0	5.3	24.3	7.9	10.1
Propylene glycol	267.9	250.9	279.3	400.8	275.6
2,3-Butanediol	27.4	35.9	44.8	34.9	31.0
Cyclohexanol	51.9	75.8	77.0	51.3	41.1
1,2-Butanediol	83.0	75.3	100.6	137.4	111.1
Tetrahydrofurfuryl alcohol	18.8	40.4	94.8	72.7	132.9
1,4-Butanediol	58.3	41.5	34.4	68.6	33.9
γ-Butyrolactone	119.6	80.8	92.8	110.6	111.4
γ-Valerolactone	11.8	11.9	15.8	12.5	13.8
Glycerol	41.9	42.7	0.0	48.8	1.8
1,2-Cyclohexanediol	114.4	91.0	72.3	107.7	62.7
4-Hydroxymethyl-γ-butyrolactone	74.2	43.6	0.0	47.0	25.2
Sorbitol	591.8	510.6	0.0	21.8	0.0
3-Methylcyclopentanol	20.2	23.7	43.8	33.9	36.5
1,2,3-Butanetriol	23.7	10.2	15.9	29.2	27.1
1,4-Pentanediol	15.7	19.4	30.6	23.3	19.2
3-methylcyclohexanol	22.1	18.8	34.7	34.3	32.4

4-methylcyclohexanol	14.9	14.8	24.3	20.5	15.8
1,2-Hexanediol	21.4	7.8	16.1	27.7	19.3
1,2,6-Hexanetriol	15.5	12.4	0	14.2	0
Total carbon identified	2355.4	2158.2	1781.2	2171.5	1673.9
Total carbon in liquid as measured by TOC	3616.1	3223.8	2881.1	3405.4	2570.3
%C identified by GC and HPLC	65.1	66.9	61.8	63.4	65.1
% C to gas phase	9.7	19.5	28.1	15.0	35.8

* Acetic acid, levoglucosan, and sugars concentrations in feed are 144.8 mmol-C L^{-1}, 489.2 mmol-C L^{-1}, and 159.3 mmol-C L^{-1} respectively.

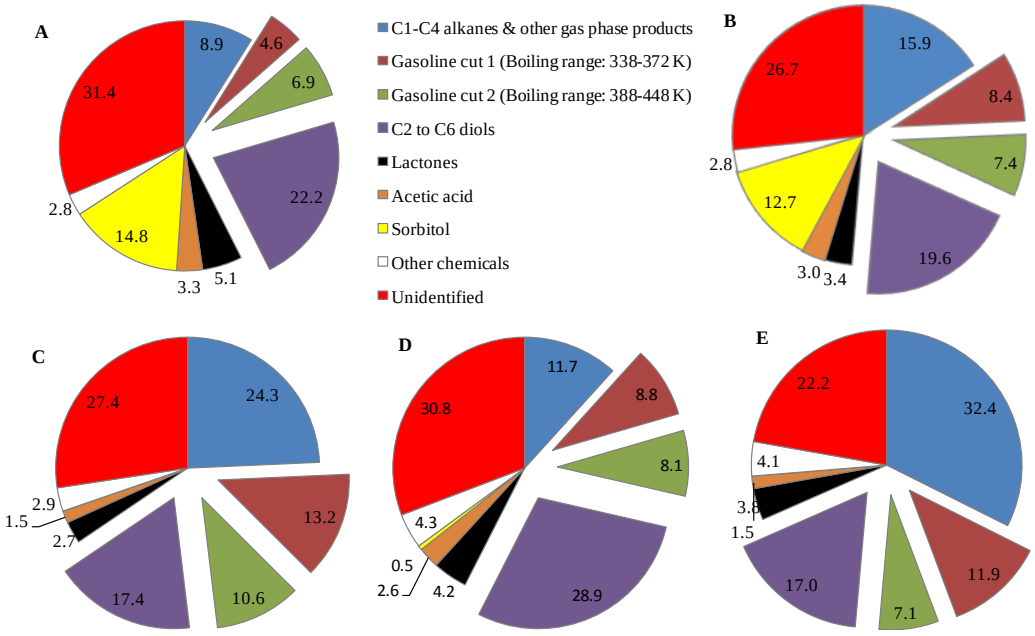

Figure 6-3 Product yield and selectivity in 2-stage hydrogenation of aqueous fraction of pine wood bio-oil over Ru/C and Pt/C catalyst. A: Ru/C-Pt/C, 125-220 °C, 1450 psi, B: Ru/C-Pt/C, 125-220 °C, 750 psi, C: Ru/C-Pt/C, 125-250 °C, 750 psi, D: Ru/C-Pt/C, 125-250 °C, 1450 psi, E: Ru/C-Pt/C, 125-275 °C, 1450 psi. All the experiments are carried out at the space velocity of 3 $hour^{-1}$.

The effect of the second stage temperature on the yield of desired product groups is shown in Figure 6-4. The optimum temperature for maximizing the desired product yield is *ca.* 250 °C. The C2-C6 diols yield decreases above 250 °C due to their further

hydrogenation reactions to produce gasoline cut 1 alcohols and C1-C4 gas phase alkanes. The C1-C4 alkanes and other gas phase products show an exponential rise in yield with temperature.

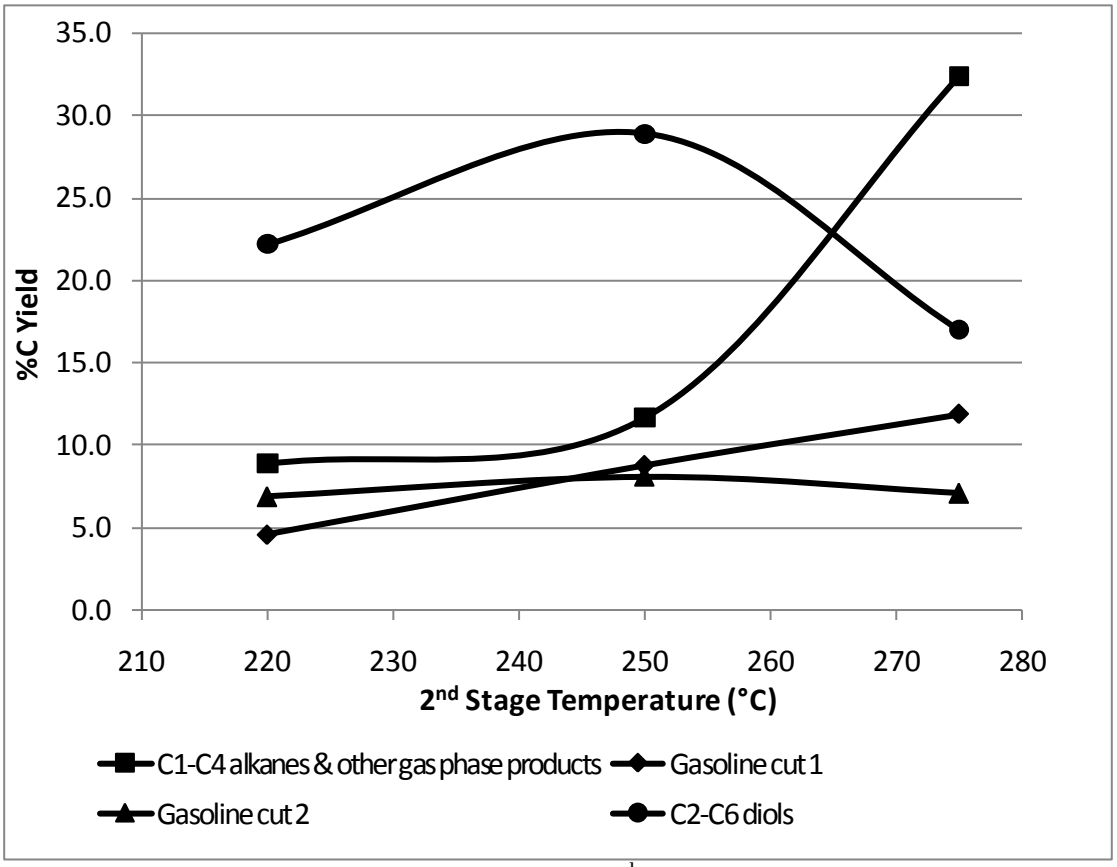

Figure 6-4 Product selectivity distribution with 2nd stage temperature in hydrogenation of PW-WSBO. First Stage: 125 °C, 5 wt% Ru/C catalyst, second Stage: 5 wt% Pt/C catalyst. P: 1450 psi for both stages, WHSV: 3 $hour^{-1}$ for both stages. Lines are guide to the eyes.

6.7 Hydroprocessing of Aqueous Fraction of DOE Bio-oil (WS-DOE-BO) and Use of Bimetallic Catalyst in Second Stage

The two stage hydrogenation process for the aqueous fraction of bio-oil described above can be used to produce oxygenated gasoline additives and valuable diols. It would be crucial to know if the same process (catalyst, reaction conditions etc.) can be used for different bio-oils. To test this, we subjected the water soluble DOE bio-oil to the single stage hydrogenation on Ru/C as well as to the 2-stage hydrogenation on Ru/C followed by Pt/C catalyst. The representative composition the WS-DOE-BO feed used in this study is shown in Table 6-9. The composition of WS-DOE-BO looks very similar to that of WS-PWBO except that the acetic acid concentration in WS-DOE-BO is almost 4 times than that in WS-PWBO. The extent of unidentifiable carbon in WS-DOE-BO is also less than that for WS-PWBO.

Table 6-9 Composition of the water soluble fraction of DOE bio-oil. The feed is made by mixing DOE-BO and water in 1:4 weight ratio.

Compounds	Concentration (mmolC L^{-1})
Methanol	30.0
Ethanol	0.0
1-Propanol	0.0
Hydroxyacetaldehyde	374.2
Acetic Acid	811.2
Hydroxyacetone	139.6
Propanoic Acid	45.0
Hexanoic Acid	42.1
1-Hydroxy-2-butanone	48.7
Furfural	19.0
2-Cyclopenten-1-one	29.5
γ-Butyrolactone	17.8
2(5H)-furanone	38.5
Phenol	0.6
3-Methyl-1,2-cyclopentadione	0.0
5-Hydroxymethylfurfural	42.6
Levoglucosan	1142.6
Sugars	247.8
Sorbitol	113.2
Total	3142.4
mmol C L^{-1} by TOC	4044.0
%C identified by GC and HPLC	77.7

Table 6-10 depicts the product composition of the single stage hydrogenation of WS-DOE-BO on 5 wt% Ru/C catalyst at 125 °C and 1450 psi. The product distribution is very similar to that for WS-PWBO (compare entries for WHSV of 3.0 h^{-1} in Table 6-5) with ethylene glycol and propylene glycol as major products. Levoglucosan and sugars are partially converted similar to WS-PWBO but the conversion is lower in WS-DOE-BO. Levoglucosan conversion of 65.3% was observed for water soluble pine wood bio-oil. Whereas, for the water soluble DOE bio-oil levoglucosan conversion of only 36.0% was obtained at the same reaction conditions. For the WS-DOE-BO the increase in

sorbitol concentration is less than the decrease in levoglucosan and sugar concentration, implying that sorbitol has undergone further hydrogenolysis to produce ethylene glycol, propylene glycol etc. This is not the case for water soluble pine wood bio-oil where a corresponding (to levoglucosan and sugar concentration decrease) increase in the sorbitol concentration was observed (Table 6-5, WHSV: 3.0 h^{-1}). The high hydrogenolysis activity for sorbitol in WS-DOE-BO can be due the high acetic acid concentration in the feed. Acetic acid can catalyze the retro-aldol condensation reactions of sorbitol producing C2 to C4 products which get hydrogenated to corresponding alcohols.

Table 6-10 Product composition of the single stage hydrogenation of WS-DOE-BO on 5 wt% Ru/C at 125 °C, 1450 psi, and 3 hour^{-1}. Feed: ~13 wt% WS-DOE-BO solution in water.

Product	Concentration (mmol-C L^{-1})
Methanol	57.5
Ethanol	12.0
2-Propanol	0.0
1-Propanol	11.0
2-Butanol	14.7
Acetic Acid	1001.8
1-Butanol	0.0
2-Pentanol	0.0
Propanoic Acid	50.4
1-Pentanol	0.0
Ethylene Glycol	462.6
Cyclopentanol	36.0
Propylene glycol	222.9
3-methylcyclopentanol	7.6
2,3-Butanediol	12.6
Cyclohexanol	70.3
1,2-Butanediol	21.1
Tetrahydrofurfuryl alcohol	18.5
1,4-Butanediol	29.0
γ-Butyrolactone	77.1
1,2-Cyclohexanediol	95.4
Levoglucosan	731.3
Glucose	126.5
Sorbitol	77.2
Total (mmolC L^{-1})	3196.6
Carbon in feed by TOC (mmol L^{-1})	4044.02
Carbon in product by TOC (mmolC L^{-1})	3646.2
%C to gas phase	9.8
%C identified by GC and HPLC	87.7

The single stage hydrogenation product of WS-DOE-BO was hydrogenated over 5 wt% Pt/C catalyst to completely convert the unreacted sugars, levoglucosan, and sorbitol to valuable alcohols and diols. The results are depicted in Table 6.11. The major

products are ethanol, ethylene glycol, propylene glycol, and methanol (all with concentration > 100 mmol carbon per liter). The product selectivity is significantly different for WS-DOE-BO and WS-PWBO (compare Tables 6-11 and 6-8). A notably higher concentration of monohydric alcohols was obtained for the WS-DOE-BO feed as compared to that for WS-PWBO feed. All of the levoglucosan, sorbitol, and sugars were converted. A significant drop in ethylene glycol and propylene glycol and a significant increase in ethanol and n-propanol concentration were observed. This indicates that the C2 to C6 diols are undergoing further C-O bond hydrogenolysis reaction to produce corresponding alcohols. This difference between the behavior of water soluble pine wood bio-oil and water soluble DOE bio-oil can be due to the high concentration of acetic acid which can catalyze the dehydration reactions in C2 to C6 diols, hence expediting the C-O bond hydrogenolysis reactions. Miyazawa et al. has shown that the rate of propylene glycol formation over Ru/C catalyst from glycerol (i.e. C-O bond hydrogenolysis) is enhanced by the presence of amberlyst resin.[82, 83] This indicates that the acids can catalyze the dehydration reaction in polyols such as glycerol (or in our case sorbitol) and hence enhance the C-O bond hydrogenolysis rate. The higher C-O bond cleavage rates in the WS-DOE-BO also resulted in high carbon loss to gas phase products, mainly in the form of C1 to C6 alkanes. The carbon loss to gas phase of 45.2% was observed for WS-DOE-BO as compared to 15.0% for WS-PWBO at the same reaction conditions.

Table 6-11 Feed and product composition for 2-stage hydrogenation of WS-DOE-BO. Feed: ~13 wt% WS-DOE-BO solution in water. P: 1450 psi, WHSV: 3 h^{-1}

Compound	Concentration (mmol-C L^{-1})		
	Feed	Ru/C, 125 °C - Pt/C, 250 °C	Ru/C, 125 °C – PtRe on Ceria-Zirconia, 250 °C
Reactants			
Methanol	28.2	111.7	99.3
1-Propanol	8.0	78.8	205.7
Hydroxyacetaldehyde	326.0	0.0	0.0
Acetic Acid	723.2	273.1	0.0
Hydroxyacetone	123.6	0.0	0.0
Propanoic acid	39.0	16.1	0.0
Hexanoic acid	0.0	0.0	0.0
1-Hydroxy-2-butanone	39.8	0.0	0.0
Furfural	15.9	0.0	0.0
2-Cyclopenten-1-one	22.2	0.0	0.0
γ-Butyrolactone	14.7	17.0	15.2
2(5H)-Furanone	28.2	0.0	0.0
Phenol	0.4	0.0	0.0
3-Methyl-1,2-cyclopentadione	21.7	0.0	0.0
5-Hydroxymethyl-furfural	28.1	0.0	0.0
Levoglucosan	988.1	0.0	0.0
Sugars	207.4	0.0	0.0
Sorbitol	0.0	0.0	0.0
Products			
Ethanol	0	249.6	703.9
2-Propanol	0	8.8	50.7
2-Butanol	0	5.6	27.1
1-Butanol	0	23.4	59.9
2-Pentanol	0	3.9	11.4
1-Pentanol	0	0.0	9.8
Ethylene glycol	0	210.3	0
Cyclopentanol	0	22.8	44.3
Propylene glycol	0	161.3	14.7
3-Methylcyclopentanol	0	30.7	20.8
2,3-Butanediol	0	19.6	20.8
Cyclohexanol	0	50.3	82.9
1,2-Butanediol	0	48.3	9.0
Tetrahydrofurfuryl alcohol	0	82.3	12.9
1,4-Butanediol	0	16.0	9.9
γ-Butyrolactone	0	17.0	15.2
1,2-Cyclohexanediol	0	49.9	41.9

Sorbitol	0	0.0	0.0
Total (mmol-C L^{-1})	3150.1	1479.1	1446.4
Carbon in feed by TOC (mmol L^{-1})	4044.02	3489.6	3642.4
Carbon in product by TOC (mmol-C L^{-1})	3646.2	1913.2	2206.5
%C to gas phase	9.8	45.2	39.4
%C identified by GC and HPLC	86.4	77.3	65.6

The Pt/C catalyst is active for hydrogenating all the major bio-oil functionalities to corresponding alcohols except carboxylic acids. It is desirable to completely reduce the acids in the aqueous fraction of the bio-oil with the economic standpoint of further processing of the hydrogenated product. Acetic acid hydrogenation proceeds through the acetyl (CH_3-CO-) intermediate. Acetyl intermediate is formed by the activation and the cleavage of C-OH bond of acetic acid. Pallassanna and Neurock showed that group VIII metals like Pt and Pd exhibit lower activation barriers for hydrogenation, but they tend to display poor activity for acetic C–O bond dissociation (hydrogenolysis).[*(84)*] They also showed that C-OH activation is more favored on metals to the left in periodic table such as Rhenium. They found by theoretical calculations that bimetallic PdRe catalyst exhibit higher activity for acetic acid hydrogenation to ethanol compared to monometallic Pd catalyst. Hence with same context we tested the PtRe catalyst supported on ceria-zirconia in the 2nd stage of the hydrogenation process. The results are shown in Table 6-11. A 100% acetic acid conversion was observed with the PtRe bimetallic catalyst. All of the levoglucosan, sugars, and sorbitol were also consumed. However, the product selectivity is significantly different than that for the monometallic Pt catalyst. The major products are ethanol (703.0 mmol-C L^{-1}), 1-propanol (205.7 mmol-C L^{-1}), methanol (99.3 mmol-C

L^{-1}), cyclohexanol (82.9 mmol-C L^{-1}), and 1-butanol (59.9 mmol-C L^{-1}). The PtRe bimetallic catalyst produced large amount of monohydric alcohols due to its ability to selectively activate the C-O bonds in compounds such as ethylene glycol and propylene glycol. No ethylene glycol was observed in the products and a very little propylene glycol was observed. The carbon loss to the gas phase for PtRe catalyst was 39.4%. The bimetallic catalyst hence can be a very good choice if you want to selectively produce gasoline cut 1 compounds (C2 to C4 monohydric alcohols) from the aqueous fraction of bio-oil. It also completely reduces the acetic acid and propanoic acid, hence simplifying the further processing of hydrogenated water soluble bio-oil.

6.8 Reactions in Hydroprocessing of Aqueous Fraction of Bio-oil

Based on the reactants present in WSBO and products obtained, the major reactions happening during the hydroprocessing of water soluble bio-oil are identified below,

- Hydrogenation of bio-oil components: These reactions take place in the low temperature hydrogenation step. The carbonyl functional groups in the bio-oil components are hydrogenated to corresponding alcohols. In guaiacol, methoxy functional group (-OCH_3) is hydrogenated to –OH group. Catechol undergoes ring hydrogenation to produce 1,2-cyclohexanediol which gets converted to cyclohexanol with elimination of a hydroxyl group. The reactions identified are listed below,

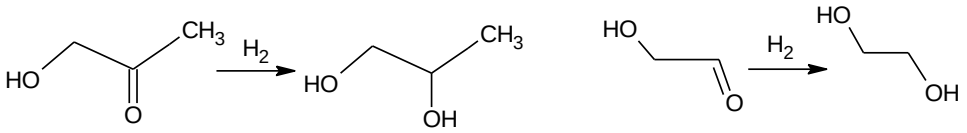

Hydroxyacetone Propylene glycol Hydroxyacetaldehyde Ethylene Glycol

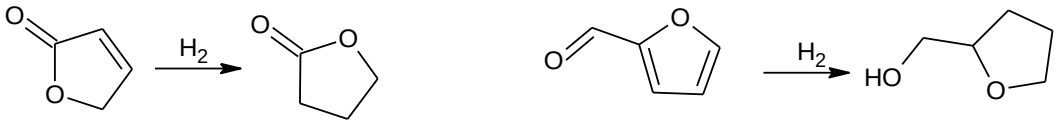

2(5H)-Furanone γ-Butyrolactone Furfural Tetrahydrofurfuryl alcohol

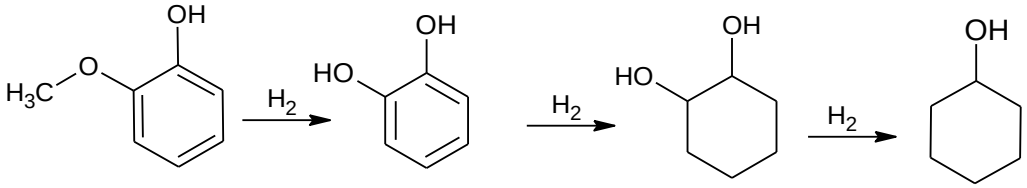

Guaiacol Catechol 1,2-Cyclohexanediol Cyclohexanol

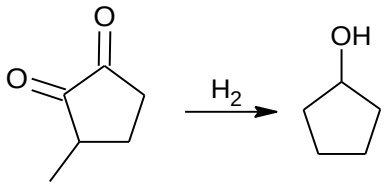

3-Methyl-1,2-cyclopentadione Cyclopentanol

- Hydrolysis followed by hydrogenation: These reactions take place in the low temperature hydrogenation stage. Levoglucosan in the bio-oil is converted to sorbitol in two steps. First is the hydrolysis of levoglucosan to glucose. This step is catalyzed by acids. Since we do not add any acid externally in our reaction

medium, this step is likely catalyzed by acetic acid in the WSBO feed. In the second step glucose is hydrogenated to sorbitol over metal catalyst.

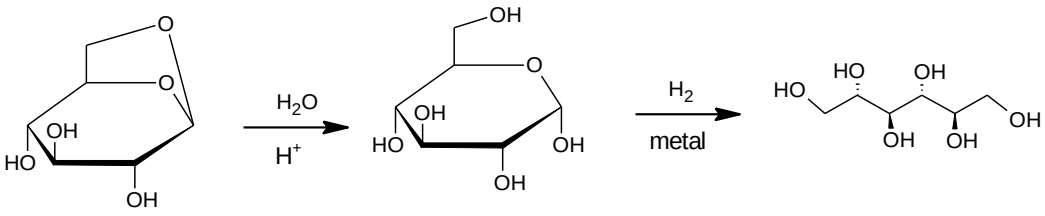

Levoglucosan Glucose Sorbitol

- Hydrogenolysis: In hydrogenolysis reaction as shown in the reaction scheme below, the larger polyols such as sorbitol undergo C-C bond cleavage reactions over metal in the presence of hydrogen to produce smaller polyols such as ethylene glycol, propylene glycol, and glycerol. The C-C bond cleavage reactions can be catalyzed solely by metals such as Ru and Pt but rates of these reactions increase in acidic and basic medium. This is because acids and bases can catalyze the retro-aldol condensation reactions. These reactions are very prominent in our process in 2nd hydrogenation step at high temperature. Although, there is an indication of hydrogenolysis reaction in the LTH step at low space velocities.

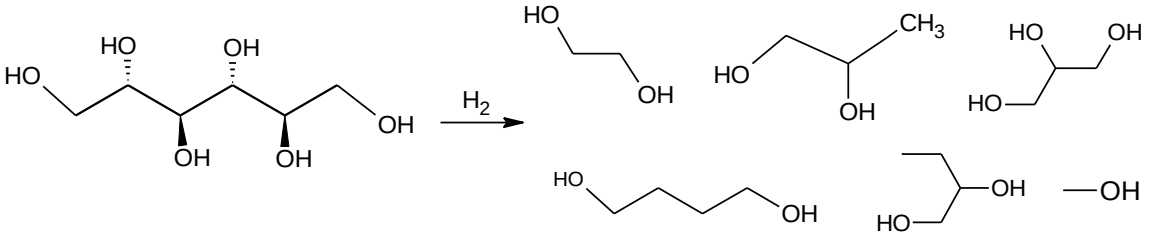

- Secondary hydrogenation reactions: These reactions occur in LTH as well as in HTH step. Secondary hydrogenation reactions are C-O bond cleavage reactions, where monohydric alcohols are produced from the diols. These reactions are catalyzed by metals and are expedited by presence of acids as we saw in case of WS-DOE-BO as feed.

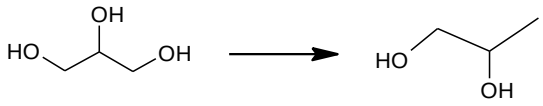

Glycerol Propylene glycol

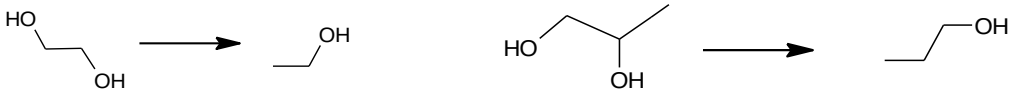

Ethylene glycol Ethanol Propylene glycol n-Propanol

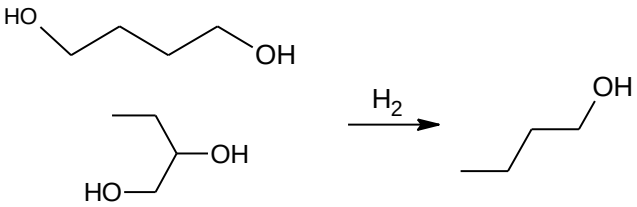

1,2 & 1,4-Butanediol 1-Butanol

In addition to these reactions, further hydrogenation of monohydric alcohols produce corresponding alkanes. CO is produced from decarbonylation of aldehydes. CO can further react with hydrogen to produce CH_4. CO_2 is produced from decarboxylation of carboxylic acids.

6.9 Low Temperature Hydrogenation of Whole Bio-oil

As described previously in this chapter, the aqueous fraction of the bio-oil contains mainly C2 to C6 oxygenated hydrocarbons and they can be converted to valuable gasoline additives and C2 to C6 diols by hydroprocessing over noble metal catalysts. The aqueous fraction contains only about half the energy of the bio-oil. The organic fraction of the bio-oil mainly contains lignin derived oligomers with ether linkages. It would be preferable to hydrotreat the entire bio-oil instead of just the aqueous fraction. Hence we subjected the DOE bio-oil to low temperature hydroprocessing over 5 wt% Ru/C catalyst at 1450 psi and temperatures in the range of 75 °C to 125 °C. The microfiltered (0.8 μm membrane) DOE bio-oil was used as feed. None of the bio-oil components showed significant reactivity up to the temperature up to 100 °C. The data for DOE-BO hydrogenation over Ru/C catalyst at 125 °C, 1450 psi at the space velocity of 1.6 $hour^{-1}$ is tabulated in Table 6-12. As seen in this table, different conversions are obtained for different feed components but no corresponding hydrogenation products were detected except for a small amount of sorbitol. Hence the disappearance in the reactants is most likely due to the homogeneous reactions that occur when bio-oil is heated to the hydrogenation reaction temperature. The same reactants that can be successfully hydrogenated when present in the aqueous fraction cannot be hydrogenated when present in the whole bio-oil. This indicates that the lignin-derived oligomers in the bio-oil might be permanently occupying and essentially deactivating the active catalytic sites.

Table 6-12 Composition of DOE-BO feed low temperature hydrogenated DOE-BO. Hydrogenation carried out over 5 wt% Ru/C catalyst, 125 °C, 1450 psi, 1.6 $hour^{-1}$

Compound	**mmol carbon min^{-1}**		**% Conversion**
	DOE-BO Feed	Hydrogenated DOE-BO	
Methanol	3.50×10^{-3}	3.47×10^{-3}	-
Methyl acetate	1.66×10^{-3}	3.17×10^{-3}	-
Hydroxyacetaldehyde	0.116	0	100
Acetic acid	0.109	0.127	0
Hydroxyacetone	2.11×10^{-2}	2.75×10^{-2}	0
Furfural	8.14×10^{-3}	5.60×10^{-3}	31.2
2-Furanone	6.50×10^{-3}	5.07×10^{-3}	31.4
3-Methyl-1,2-cyclopentadione	5.65×10^{-3}	0	100
Phenol	1.38×10^{-3}	4.45×10^{-3}	0
1-Hydroxy-2-butanone	6.72×10^{-3}	0	100
2-Cyclopenten-1-one	4.01×10^{-3}	0	100
γ-Butyrolactone	2.91×10^{-3}	5.07×10^{-3}	0
5-Hydroxymethylfurfural	8.33×10^{-3}	0	100
Levoglucosan	0.113	9.49×10^{-2}	16.4
Sugars	2.27×10^{-2}	1.73×10^{-2}	24.0
Sorbitol	0	2.20×10^{-3}	-
Total carbon identified	0.432	0.262	
Total carbon as determined by elemental analysis	1.294	1.269	
%C to gas phase products	-	1.9	

Since we could not gain much understanding from the gas chromatography data, we did the GPC analysis of all the hydrogenation samples. The data are depicted in Figure 6-5. The GPC curves for the hydrogenated products have shifted to right as compared to the feed, meaning there are polymerization reactions going on within bio-oil components when it is subjected to high temperature for hydrogenation. The weight average molecular weight data for the last peak in GPC curve and normalized area under curve (which is proportional to concentration of species with that molecular weight) for

these samples are tabulated in Table 6-13. The weight of average molecular weight of DOE bio-oil does not increase upon hydrogenation at 75 °C, however there is a substantial increase in the molecular weight when bio-oil is hydrogenated at 100 and 125 °C. The normalized concentration of high molecular weight oligomers also increase during hydrogenation and its temperature dependence is exponential. Hence we conclude that bio-oil is undergoing the self-polymerization reactions even in the reducing environment of hydrogenation. It might be beneficial to dilute the bio-oil using a solvent to minimize these self-polymerization reactions during the hydroprocessing.

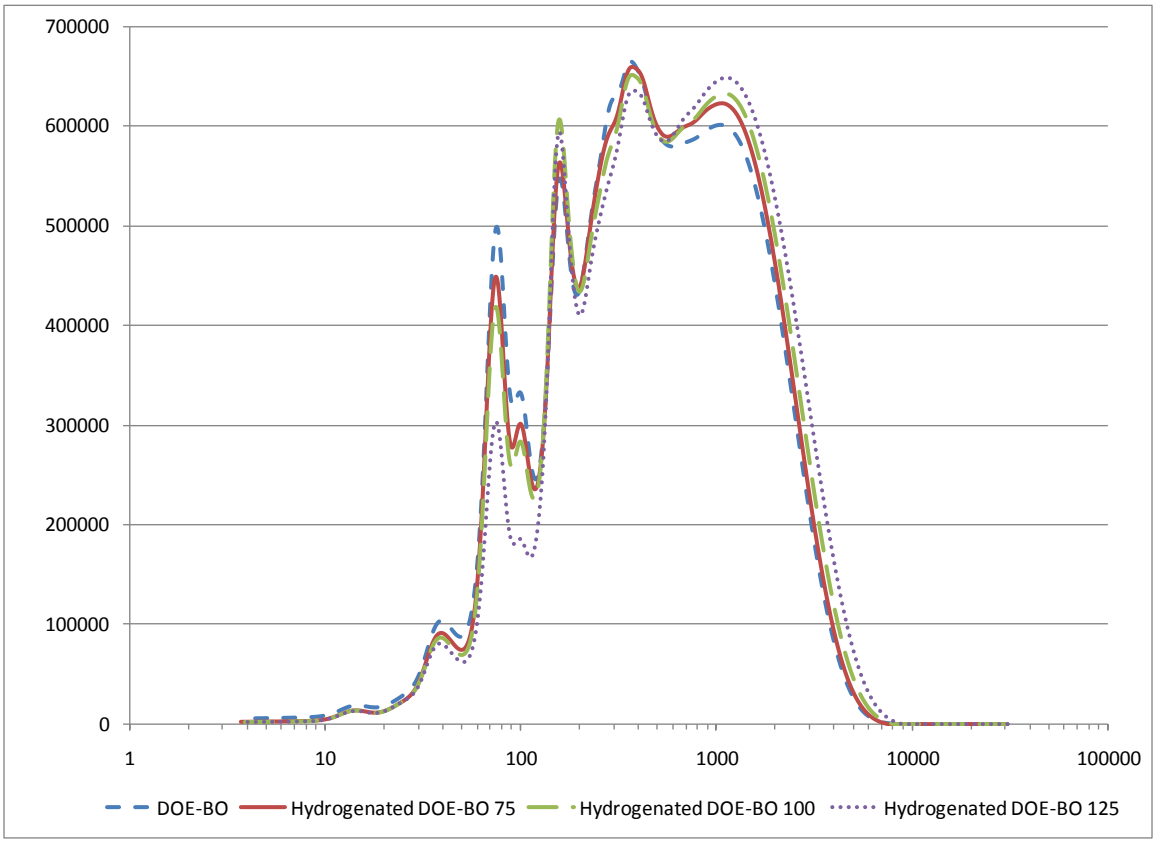

Figure 6-5 Molecular weight distribution for the DOE bio-oil feed and low temperature hydrogenation products. Hydrogenation carried out over 5 wt% Ru/C catalyst, 1450 psi, 1.6 hour^{-1}. Temperature shown in the figure is in °C.

Table 6-13 Molecular weight and concentration for DOE bio-oil and hydrogenated products. Hydrogenation was carried out over 5 wt% Ru/C catalyst, 1450 psi, 1.6 $hour^{-1}$.

	DOE bio-oil	Hydrogenated DOE bio-oil		
		Hydrogenation temperature (°C)		
		75	100	125
Weight average molecular weight for the last peak in GPC	1996.4	1992.0	2098.4	2274.11
Normalized concentration of last peak in GPC	100	107.1	116.4	132.2

6.10 Conclusion

The general conclusion from this study is that oxygenated gasoline additives and valuable C2 to C6 diols can be produced with high carbon yield from the aqueous fraction of the bio-oil (WSBO) in a 2-stage hydrogenation process. The aqueous fraction of the bio-oil contains C2 to C6 oxygenated hydrocarbons with various functionalities including aldehydes, ketones, acids, and carbohydrates. These functionalities are thermally unstable; hence a direct high temperature hydrogenation of bio-oil or WSBO is not feasible. The first hydrogenation step converts the aldehydes, ketones, and sugars to corresponding alcohols. The alcohols are thermally stable and can be treated at high temperature subsequently. The goal of the first step is to achieve complete hydrogenation of thermally unstable compounds while minimizing the carbon loss to gas phase. Ruthenium was found to be the most suitable catalyst for the low temperature hydrogenation step. Ruthenium is highly active for the C-C bond cleavage reactions and hence the minimum possible temperature should be used in the low temperature hydrogenation step. The optimum temperature was found to be 125 °C, where all the WSBO functionalities show a significant hydrogenation activity with only 7% carbon

loss the gas phase products. The carbon loss the gas phase increased exponentially with temperatures above 125 °C, with 25% carbon going to gas phase at 150 °C. Similarly the optimum space velocity was found to be around 1.5 to 3 $hour^{-1}$. Acetic acid is resilient to hydrogenation at the low temperatures used in the first step. The major products obtained are ethylene glycol, propylene glycol, and sorbitol.

The low temperature hydrogenation products contain a substantial amount of sorbitol which is a hydrogenation product of levoglucosan and glucose. A second high temperature stage was added to convert sorbitol to valuable products including diols and monohydric alcohols. Platinum was found to be the suitable catalyst. Up to 46% carbon of the WSBO was successfully converted to gasoline cut 1, gasoline cut 2, and C2 to C6 diols. The product distribution after 2-stage hydrogenation can be controlled using the pressure and 2^{nd} stage temperature. If desired, high yields of gasoline cut 1 and gasoline cut 2 can be obtained by operating at low total pressure or at high second stage temperature (*e.g.* 275 °C). High pressure is preferable in the 2-stage process to minimize the carbon loss to gas phase.

A sizeable difference between the product yields from two different aqueous fractions (WS-PWBO and WS-DOE-BO) was observed. WS-DOE-BO produced more monohydric alcohols compared to the WS-PWBO. This is due to the high acetic acid content of the WS-DOE-BO. Acetic acid can catalyze the secondary dehydration reactions in C2 to C6 diols, resulting in formation of corresponding monohydric alcohols by C-O bond cleavage. The bio-oil properties can hence affect the optimum reaction

conditions required to maximize the yield of desired products. In addition to Pt, we also tested the bimetallic PtRe catalyst in the 2nd hydrogenation step for WS-DOE-BO. PtRe catalyst completely hydrogenated acetic acid as opposed to Pt catalyst, which is beneficial for the further processing of the hydrogenated product. PtRe was found to have high C-O bond cleavage activity and hence gasoline-range monohydric alcohols were obtained as major products. The whole DOE bio-oil was also subjected to the low temperature hydrogenation over Ru/C catalyst at temperatures in the range of 75 to 125 °C. A quantifiable reactant disappearance was observed only at 125 °C but no corresponding hydrogenation products were observed. The average molecular weight of bio-oil increased upon hydrogenation due to bio-oil self-polymerization. It is possible that the lignin monomers present in the bio-oil are occupying the catalyst sites and the disappearance of reactants is only because of the homogenous thermal polymerization reactions.

To achieve the maximum yield to desired products from two-stage hydroprocessing of bio-oil, the catalyst in the first step should have high hydrogenation activity and low C-C bond cleavage activity, the catalyst in the second stage should have moderate C-C and C-O bond cleavage activity. The bio-oils with high water solubility and low acid content are desired.

CHAPTER 7

INTEGRATED HYDROPROCESSING AND ZEOLITE UPGRADING OF BIO-OIL

7.1 Introduction

As seen in the last chapter, past bio-oil hydrotreating efforts suffer several drawbacks. Another widely studied bio-oil upgrading route is the zeolite upgrading. Various researchers have studied the conversion of oxygenated hydrocarbons to aromatics and olefins over ZSM-5 catalyst. The most common example is the methanol to gasoline and methanol to olefins processes.[85] Chen et al. produced hydrocarbons from glucose, xylose, and furfural over HZSM-5 catalyst at 510 °C. Gayubo et al. have extensively studied the conversion of various aldehydes, ketones, phenols, acids, and alcohols and mixtures thereof over HZSM-5 catalyst to hydrocarbons.[86-88] Severe catalyst coking was observed. Recently Dumesic and co-workers demonstrated that aromatics can be produced from the mixture of monofunctional oxygenates including C5-C6 aldehyde, acids, and ketones over HZSM-5 catalyst at 400 °C.[17] Pyrolysis oil zeolite upgrading efforts have also revolved around using HZSM-5 catalyst. Adjaye and Bakhshi converted maple wood pyrolysis oil to organic product containing mainly aromatic hydrocarbons with 37% carbon yield in presence of hydrogen donor solvent tetralin.[32, 33] Similarly Chantal et al. observed the hydrocarbon yield of 17 wt% of bio-oil over HZSM-5 catalyst.[89] Studies have been performed to upgrade pyrolysis oil vapors over HZSM-5 even before the condensation. Milne et al. observed the yield of 18% at 475 °C in a quartz reactor.[90] The low hydrocarbon yield is due to the presence of functionalities such

as aldehydes and ketones in bio-oil, which are known to form large amounts of coke on HZSM-5 catalyst.[87]

A distinct strategy for bio-oil deoxygenation into high yield commodity chemicals including C2 to C6 monohydric alcohols and diols, C6 to C8 aromatic hydrocarbons, and C2 to C4 olefins with over 60% overall carbon yields was developed. Our approach involves hydroprocessing of the bio-oils over supported metal catalysts followed by conversion over zeolite catalysts. It is not possible to completely hydrodeoxygenate the pyrolysis oil in a packed bed reactor without frequent catalyst regeneration due to coke formation on the catalyst surface. Furthermore, complete hydrodeoxygenation requires large amounts of expensive hydrogen. In our process drawbacks associated with the prior bio-oil hydrogenation processes are overcome by operating at moderate temperatures (≤ 250 °C) where no catalyst coking or reactor plugging was observed. Furthermore, our process can produce products without the high hydrogen requirements. Employing a zeolite upgrading step at the end has an advantage that a fluidized bed reactor can be used, where the coked catalyst can be regenerated by burning off the coke and recycled back to the reactor. This study demonstrates how pyrolysis oil could practically be upgraded through catalytic processes into commodity chemicals.

The integrated catalytic process described here can be tuned to produce different targeted distributions of organic small molecules that fit seamlessly into the existing petrochemical infrastructure. The products can be tuned to change with different market conditions. The C6 to C8 aromatic hydrocarbons can be high-octane gasoline additives or

feedstocks to the chemical and polymer industries.[91] The C2 to C4 olefins can also be used directly for polymer synthesis, or can be modified to form other products including alkylated aromatics[92, 93] and longer linear alpha olefins[94]. The gasoline range alcohols can be high-octane gasoline additives. The C2 to C6 diols can serve as feedstocks for the chemical and polymer industries. The chemical industry relies on seven primary building blocks that are all derived from petroleum based processes including: benzene, toluene, xylene, ethylene, propylene, 1,3-butadiene, and methanol.[95] Five of these seven petrochemical feedstocks can be produced using the process described here, opening the door to a chemical industry based on renewable biomass feedstock.

7.2 H/C_{eff} Ratio

The hydrogen content of a particular feedstock can be expressed in terms of its hydrogen to carbon atomic effective ratio (H/C_{eff} ratio), as defined in Equation 7-1. The H/C_{eff} ratio is equal to the atoms of hydrogen minus twice the atoms of oxygen divided by the number of atoms of carbon in a feedstock.

$$H/C_{eff} = \frac{moles\,H - 2\times moles\,O}{moles\,C} \qquad (7\text{-}1)$$

The H/C_{eff} ratios for DOE-BO and low temperature hydrogenated DOE-BO were calculated based on the elemental analysis done at Galbraith Laboratories, Knoxville, Tennessee. The exact elemental composition cannot be determined for water soluble fraction of pine wood bio-oil (WSBO) (and its hydrogenated products) as it

contains a large amount of water, the amount of which could not be determined accurately. Hence the H/C_{eff} ratio for WSBO, low temperature hydrogenated WSBO and high temperature hydrogenated WSBO was estimated using their composition determined by GC-FID and HPLC. A small error in the H/C_{eff} ratio calculation will be introduced due to the unidentified carbon in WSBO and its hydrogenated products.

Lignocellulosic biomass and carbohydrate based feedstocks have H/C_{eff} ratios between 0 and 0.5. In contrast, petroleum based feedstocks have H/C_{eff} ratios from 1.0 to 2.0. Thus, biomass based feedstocks are hydrogen deficient due the presence of oxygen. For example, the bio-oil used in this study has an H/C_{eff} ratio of 0.06. During the conversion of biomass to chemicals, oxygen can be removed as a combination of CO, CO_2 and H_2O. If all the hydrogen comes from the biomass itself then oxygen will be removed as a combination of CO, CO_2 and H_2O. Whereas, if external hydrogen is used in these processes then more oxygen will be removed as H_2O. The exact ratio of CO, CO_2 and H_2O can be determined from the reaction stoichiometry between the feeds and the products. Thus, the addition of external hydrogen can increase the carbon yield of commodity chemicals produced from pyrolysis oils. This demonstrates how the biomass refining industry could be tied to the hydrogen economy.

7.3 Integrated Hydroprocessing and Zeolite Upgrading

In this study we converted eleven different biomass derived feedstocks, with a range of different functionalities over a ZSM-5 catalyst. This catalyst has the proper pore structure and active sites to effectively convert biomass derived molecules into aromatic

hydrocarbons and olefins.[13, 86, 96] Figure 7-1 depicts that the aromatic and olefin yield increases with the H/C_{eff} ratio of the feedstock (details in Table 7-1) and this relationship is applicable to a wide variety of biomass derived feedstocks. The theoretical yield, also shown in Figure 7-1, increases with the H/C_{eff} ratio as well. The increase in the aromatic and olefin yield with increasing H/C_{eff} ratio is due to two different phenomena, an increase in the thermal stability of the feedstock and an increase in the intrinsic amount of hydrogen in the feedstock. Increasing the H/C_{eff} ratio improves the thermal stability of the biomass-derived molecules by hydrogenating the functionalities (primarily aldehydes and ketones) that otherwise thermally decompose to char as shown in Table 7-2. For example, in thermogravimetric studies glucose produces 23.1 wt% coke when heated to 700 °C under helium atmosphere (Table 7-2). Sorbitol, a glucose derivative in which the aldehyde functionality has been hydrogenated to an alcohol, is significantly more thermally stable and produces only 6.1 wt% coke. Increasing the H/C_{eff} ratio also increases the intrinsic hydrogen content of the biomass derived feedstock, which allows higher theoretical yield of aromatic hydrocarbons and olefins from these feedstocks, as less carbon is used for the deoxygenation (Table 7-3). In zeolite upgrading of an oxygenated hydrocarbon C6-C8 aromatic hydrocarbons, C2-C4 olefins, CO, and water are the major products. Oxygen is removed from the feed in the form of CO or H_2O. In aromatics, toluene is the major component, whereas in olefins, propylene is the major component produced. Equations 7-2 and 7-3 show the overall stoichiometry for the conversion of glucose to toluene and propylene respectively.

$$C_6H_{12}O_6 \rightarrow (12/22)\ C_7H_8 + (26/22)\ CO + (84/22)\ H_2O \qquad (7\text{-}2)$$

$$C_6H_{12}O_6 \rightarrow C_3H_6 + 3CO + 3H_2O \quad (7\text{-}3)$$

Hence the theoretical carbon yield of toluene and propylene from glucose is 63.6% and 50.0% respectively. Similarly the stoichiometry for the conversion ethylene glycol over zeolite catalyst is shown in Equations 7-4 and 7-5.

$$C_2H_6O_2 \rightarrow (6/22)\ C_7H_8 + (2/22)\ CO + (42/22)\ H_2O \quad (7\text{-}4)$$

$$C_2H_6O_2 \rightarrow 0.5\ C_3H_6 + 0.5\ CO + 1.5\ H_2O \quad (7\text{-}5)$$

The theoretical carbon yields of toluene and propylene from ethylene glycol are 95.5% and 75.0% respectively. Based on the elemental composition of DOE-BO, low temperature hydrogenated DOE-BO and the measured compositions of WSBO and its hydrogenated products, similar maximum theoretical yield equations can be written. Table 7-3 depicts the theoretical yields to toluene and propylene from various oxygenated hydrocarbons of interest in this study. The table also depicts the observed aromatic + olefin yield as a percentage of theoretical toluene yield.

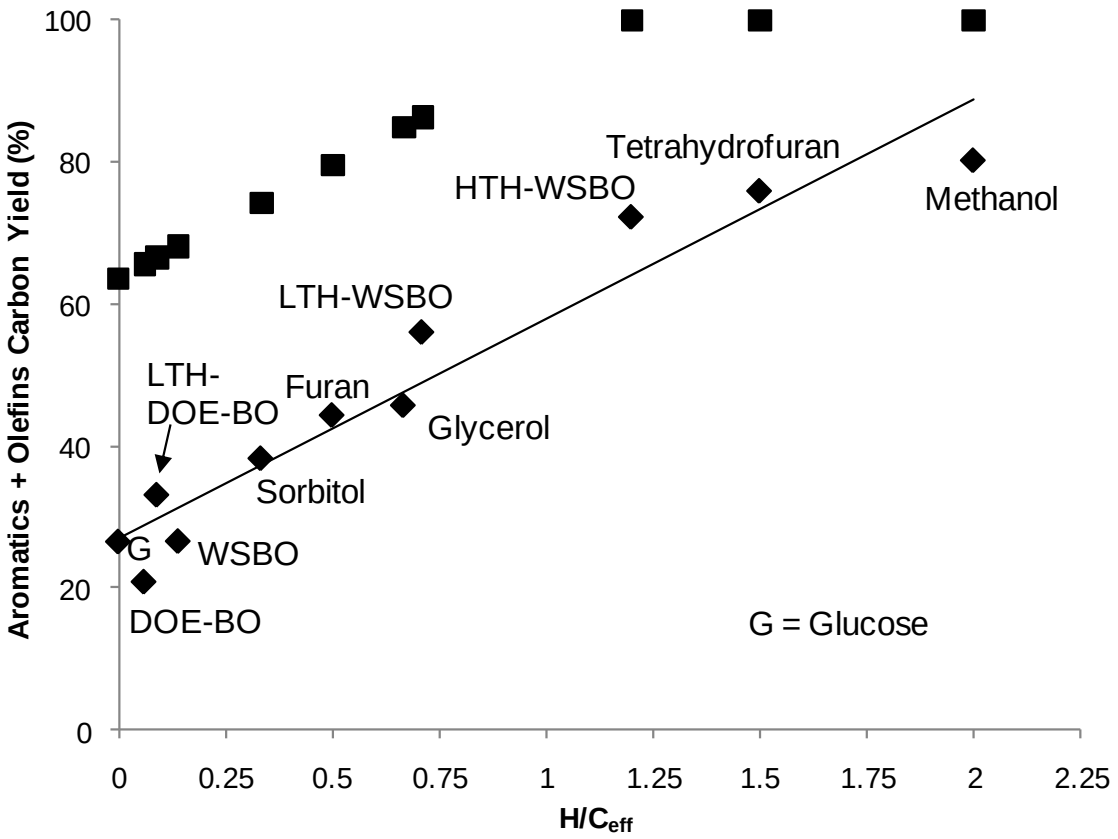

Figure 7-1 Carbon yield of olefins and aromatic hydrocarbons from the conversion of biomass derived feedstocks over HZSM-5 catalyst as a function of the hydrogen to carbon effective ratio (H/C_{eff}) of the feed. Legend: (◆) experimental yield, (■) theoretical yield. Theoretical yield is calculated for toluene. Key: WSBO is the water soluble fraction of the pine wood bio-oil, LTH-WSBO is WSBO hydrogenated over Ru/C (125 °C, 750 psi, 3 $hour^{-1}$), HTH-WSBO is WSBO hydrogenated first over Ru/C (125 °C, 1450 psi, 3 $hour^{-1}$), then over Pt/C (250 °C, 1450 psi, 3 $hour^{-1}$). DOE-BO is DOE bio-oil and LTH-DOE-BO is DOE-BO hydrogenated over Ru/C (125 °C, 1450 psi, 1.6 $hour^{-1}$).

Table 7-1 Carbon yields (%) for HZSM-5 upgrading of biomass-derived feedstocks. Catalyst: HZSM-5 (SiO_2/Al_2O_3 = 30), Reaction temperature = 600 °C, Helium carrier gas flow rate: 204 cm^3 min^{-1}. WS-PWBO is water soluble fraction of the pine wood bio-oil, LTH-WS-PWBO is low temperature hydrogenated WSBO, HTH-WS-PWBO is high temperature hydrogenated WSBO, LTH-DOE-BO is low temperature hydrogenated DOE-BO, THF is tetrahydrofuran.

	Carbon Yield (%) or Carbon Selectivity (%)										
Feed →	**WS-PWBO**	**LTH-WS-PWBO**	**HTH-WS-PWBO**	**DOE-BO**	**LTH-DOE-BO**	**Glucose**	**Sorbitol**	**Furan**	**Glycerol**	**THF**	**Methanol**
wt%	12.5	12.5	12.5	100	100	12.5	12.5	100	12.5	12.5	12.5
WHSV* ($hour^{-1}$)	11.7	11.7	11.7	11.7	11.7	11.7	11.7	1.97	11.7	11.7	11.7
H/C_{eff} ratio	0.14	0.71	1.20	0.06	0.09	0	0.33	0.50	0.66	1.50	2.00
CO	17.9	8.1	6.8	13.5	22.6	18.1	28.3	17.2	12.9	1.5	1.8
CO_2	5.8	6.9	5.7	4.8	4.4	5.2	5.8	3.5	8.4	0.9	2.0
Coke	32.3	18.9	14.8	49.5	35.3	32.6	14.2	34.8	9.4	5.7	2.3
Olefins	**18.5**	**32.7**	**50.6**	**11.2**	**18.4**	**14.3**	**24.4**	**17.7**	**28.1**	**51.5**	**55.5**
	Carbon Selectivity (%)										
Ethylene	41.6	31.8	32.0	51.8	52.7	39.9	45.1	54.2	55.5	12.2	42.2
Propylene	45.9	55.4	53.8	36.6	35.9	45.5	43.0	41.2	34.5	76.1	41.8
Butylene	12.4	12.8	14.2	11.6	11.4	14.7	11.9	4.5	10.0	11.7	16.0
Aromatics	**8.2**	**23.3**	**21.5**	**9.8**	**14.8**	**12.2**	**14.0**	**26.7**	**17.9**	**24.6**	**24.7**
	Carbon Selectivity (%)										
Benzene	26.8	17.6	27.0	17.3	16.9	23.8	25.7	37.1	18.4	33.7	5.7
Toluene	46.3	45.5	49.3	40.8	37.2	41.8	44.3	37.1	49.2	44.7	21.1
Xylenes	20.7	31.3	19.1	23.5	38.5	23.0	20.0	10.5	25.1	16.7	66.8
Ethylbenzene	1.2	2.6	2.3	2.0	3.4	3.3	2.9	0.0	2.2	1.6	2.0
Styrene	2.4	1.7	1.4	4.1	2.7	4.1	2.1	5.6	2.2	1.2	2.0
Indene	1.2	1.3	0.5	8.2	0.0	2.5	3.6	7.5	2.8	1.6	1.6
Naphthalene	1.2	0.0	0.5	4.1	1.4	1.6	1.4	2.2	0.0	0.4	0.8
Total identified carbon (%)	82.7	89.9	99.4	88.8	95.5	82.4	86.7	99.9	85.7	84.2	86.3

* WHSV for WSBO, LTH-WS-PWBO, and HTH-WS-PWBO is on the water soluble bio-oil content basis, excluding the water that is added externally in the feed.

Table 7-2 Homogeneous coke yield for different feedstocks

Feed	H/C_{eff} ratio	Coke (%wt)
Glucose	0	23.1
DOE-BO	0.06	19.0
LTH-DOE-BO	0.09	13.6
WS-PWBO	0.14	12.8
Sorbitol	0.33	6.1
Furan	0.50	0
Glycerol	0.67	0.4
LTH-WS-PWBO	0.71	2.8
HTH-WS-PWBO	1.20	0.2
Tetrahydrofuran	1.50	0
Methanol	2.00	0

Table 7-3 Theoretical toluene and propylene yields and percentage of theoretical toluene yield for different feedstocks

Feed	H/C_{eff} ratio	Theoretical carbon yield (%)		Experimental aromatic + olefin carbon yield (%)	Percentage of theoretical toluene yield*
		Toluene	Propylene		
Glucose	0	63.6	50.0	26.6	41.8
DOE-BO	0.06	65.6	51.6	21.0	32.0
LTH-DOE-BO	0.09	66.5	52.3	33.2	49.9
WS-PWBO	0.14	68.1	53.5	26.7	39.1
Sorbitol	0.33	74.2	58.3	38.3	51.6
Furan	0.50	79.5	62.5	44.4	55.8
Glycerol	0.67	84.8	66.7	45.8	54.0
LTH-WS-PWBO	0.71	86.3	67.8	56.0	64.9
Ethylene glycol	1.00	95.5	75.0	-	-
HTH-WS-PWBO	1.20	100	80.1	72.3	72.3
Propylene glycol	1.33	100	83.3	-	-
Tetrahydrofuran	1.50	100	87.5	75.9	75.9
Methanol	2.00	100	100	80.2	80.2
Ethanol	2.00	100	100	-	-
1-Propanol	2.00	100	100	-	-

*Percentage of theoretical toluene yield is calculated by dividing the experimental aromatic + olefin carbon yield (%) by theoretical carbon yield to toluene (%).

In the same respect as glucose to sorbitol, bio-oil and its aqueous fraction can be stabilized by hydroprocessing and at the same time an increase in intrinsic hydrogen content results in higher aromatic and olefin yields. Figure 7-2 shows a generic reaction scheme for the conversion of bio-oil (or the water soluble fraction of bio-oil) by hydroprocessing and zeolite upgrading to various products. The thermally unstable carbonyl functionalities in bio-oil directly go to coke on zeolite catalyst, bypassing the desired commodity chemicals including aromatic hydrocarbons, olefins, and alcohols. The carbonyl functionalities are converted to thermally stable corresponding alcohols upon hydrogenation and the coke yield decreases in zeolite upgrading. A second hydrogenation step further increases the H/C_{eff} ratio of feed resulting in even lower coke yields in zeolite upgrading.

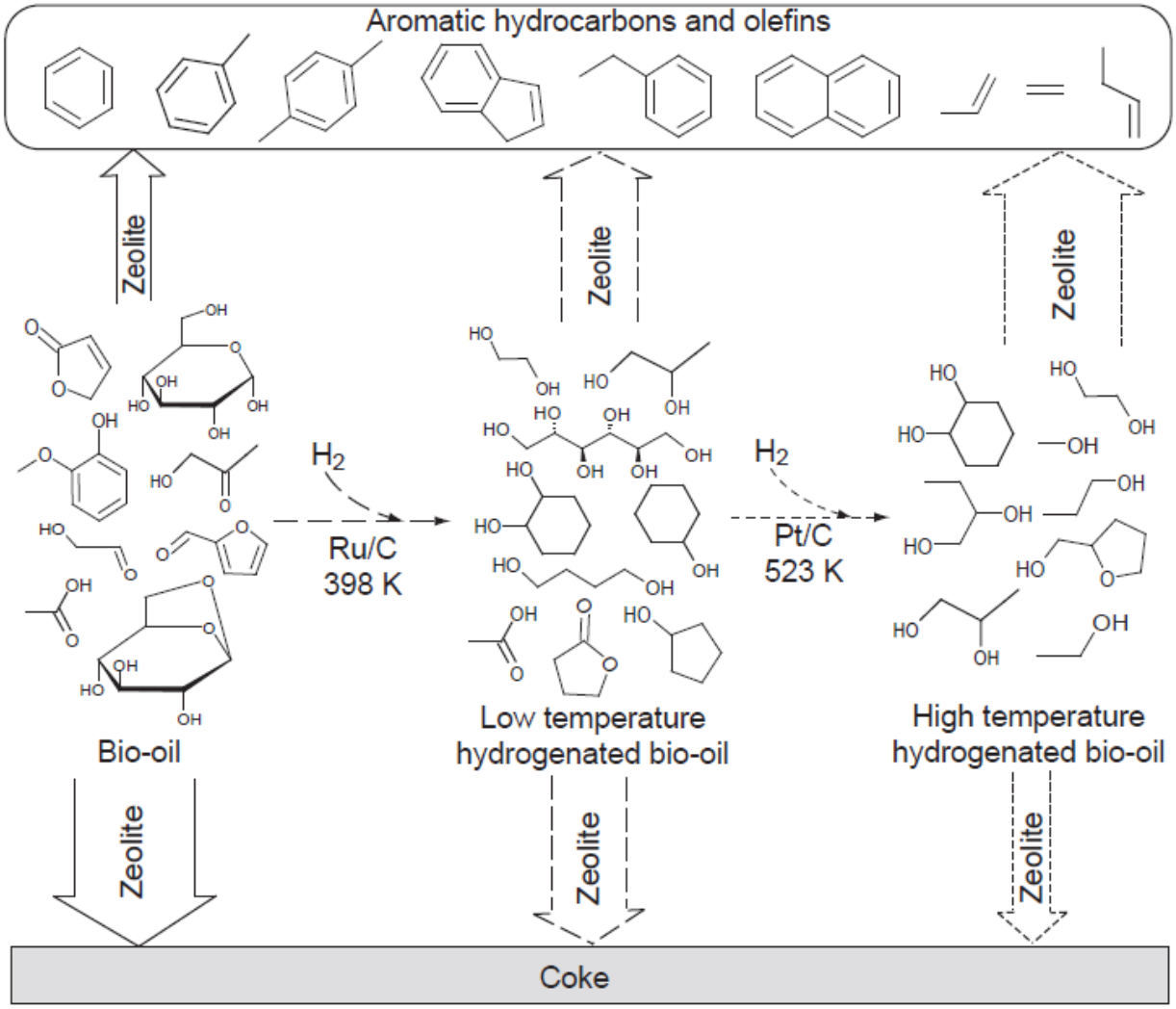

Figure 7-2 Reaction schematic for the integrated hydroprocessing and zeolite upgrading of pyrolysis oil. Solid arrows: pyrolysis oil is directly passed over zeolite catalyst, long-dashed arrows: pyrolysis oil is hydrogenated over Ru/C at 125 °C (398 K) and then passed over zeolite catalyst, short-dashed arrows: pyrolysis oil is first hydrogenated over Ru/C at 125 °C (398 K), then over Pt/C at 250 °C (523 K) and then passed over zeolite catalyst. Width of the vertical arrows represents the product carbon yield from a particular field. In addition to the product streams shown in the figure, oxygen is removed at the zeolite stage as a mixture of CO, CO_2, and H_2O. Boosting the hydrogen content of the zeolite feed (left to right) increases the thermal stability of the feed resulting in reduction in amount of coke and increase in the yields of aromatic hydrocarbons and olefins. Addition of hydrogen also raises the proportion of oxygen lost as water relative to CO and CO_2, and thereby further raises the proportion of carbon incorporated into marketable compounds.

Figure 7-3 shows different process options we used in this study for the conversion of pyrolysis oil. The crude pyrolysis oil can be subjected directly to our process or it can first be phase separated into an aqueous and an organic phase by addition of water. Thus we have five different options including: Option 1a: direct conversion of pyrolysis oils over a zeolite catalyst, Option 1b: low temperature hydrogenation of pyrolysis oil followed by the conversion over a zeolite catalyst, Option 2a conversion of aqueous phase of bio-oil over a zeolite catalyst, Option 2b: low temperature hydrogenation of the aqueous phase of bio-oil followed by conversion with a zeolite catalyst, and Option 2c: low and high temperature hydrogenation of the aqueous phase of bio-oil followed by zeolite conversion. The organic phase of the bio-oil mainly contains high molecular weight lignin derived phenolic oligomers.[24] These lignin oligomers can be used to make phenol-formaldehyde resins[97] or as a low cost feedstock for the base catalyzed depolymerization processes[98-100] to produce phenolic chemicals or aromatic fuel.[101-103] To exploit the advantages of hydroprocessing and zeolite upgrading for the upgrading of pyrolysis oil we opted to study three different processing steps that can be operated in series: a low temperature hydrogenation step using a Ru based catalyst, a higher temperature hydrogenation step using a Pt based catalyst following the Ru based step and a zeolite conversion step. The Ru catalyst was chosen based on previous experimental and theoretical studies on aqueous phase acetic acid hydrogenation over monometallic catalysts.[104] The conclusion from this study was that Ru was the most active and selective monometallic catalysts for aqueous phase acetic acid hydrogenation at low temperatures. Pt was chosen as the catalyst for the high temperature hydrogenation because previous studies for hydrodeoxygenation of sorbitol have

indicated that Pt catalysts have high C-O hydrogenation and low C-C bond cleavage activity.[75] Pt also has seven times less C-C bond cleavage activity as compared to Ru.[80] We explored these conversion options with two different pyrolysis oil feeds: crude bio-oil obtained from the U.S. Department of Energy's National Renewable Energy Laboratory (DOE-BO), and the water soluble fraction of a pine wood bio-oil (WS-PWBO). WS-PWBO sample was made by mixing pine wood bio-oil and water in 1:4 weight ratio. For the DOE bio-oil sample, we compared the outcomes of zeolite upgrading with and without preceding low temperature hydrogenation. For the WS-PWBO sample, we examined these two protocols as well as the third, incorporating a high temperature hydrogenation step between the low temperature hydrogenation and zeolite upgrading steps.

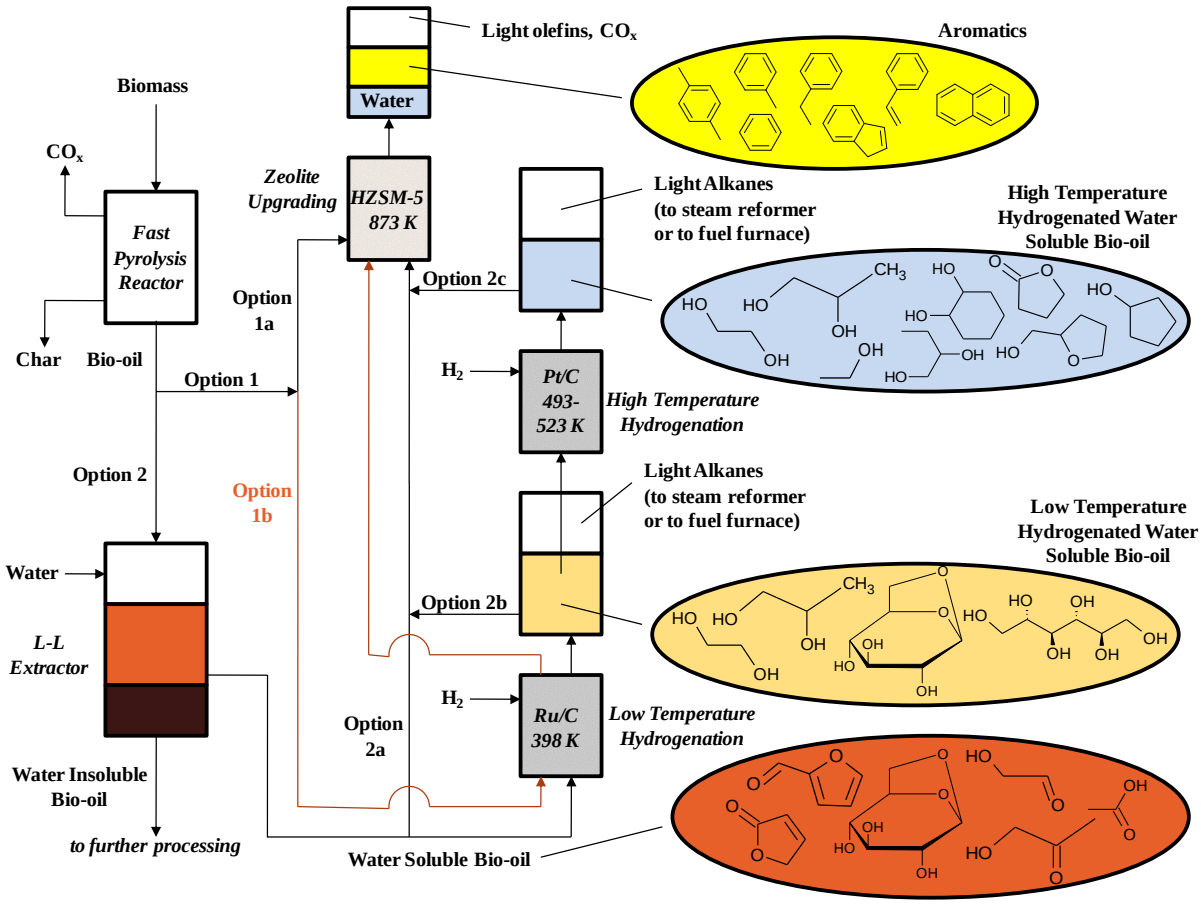

Figure 7-3 Production of olefins, aromatic hydrocarbons, diols, and gasoline range alcohols from the integrated catalytic processing of pyrolysis oil.

7.4 Hydroprocessing of Bio-oil: Feed and Product Analysis

Gas chromatography (GC) and high performance liquid chromatography (HPLC) of the DOE bio-oil (Table 6-12) identified hydroxyacetaldehyde (9.0% of the total bio-oil carbon content), levoglucosan (8.8% of total bio-oil carbon), acetic acid (8.4% of total bio-oil carbon), sugars (1.8% of total bio-oil carbon) and hydroxyacetone (1.6% of total bio-oil carbon) as major components. Only 1/3rd of the carbon content quantified by elemental analysis could be identified using these techniques. The remaining 2/3rd of the

carbon can be attributed to non-quantified compounds present in small quantities and GC and HPLC undetectable lignin and sugar oligomers. Gel permeation chromatography (GPC) (Figure 6-4) of DOE bio-oil confirmed the presence of oligomers ranging in molecular weight from 300 to 7000 Da. Analysis of the WS-PWBO by GC and HPLC identified the compounds comprising 56.5% of the total carbon content (Figure 7-4A and Table 7-4). The most abundant functionalities in the WSBO include carbonyl compounds (24.7% of total WS-PWBO carbon), carbohydrates (20% of total WS-PWBO carbon, includes sugars and levoglucosan), and phenolics (7.9% of total WSBO carbon). The WS-PWBO has an H/C_{eff} ratio of 0.14. The unidentified carbon in the WS-PWBO is most likely present as undetectable lignin and sugar oligomers.

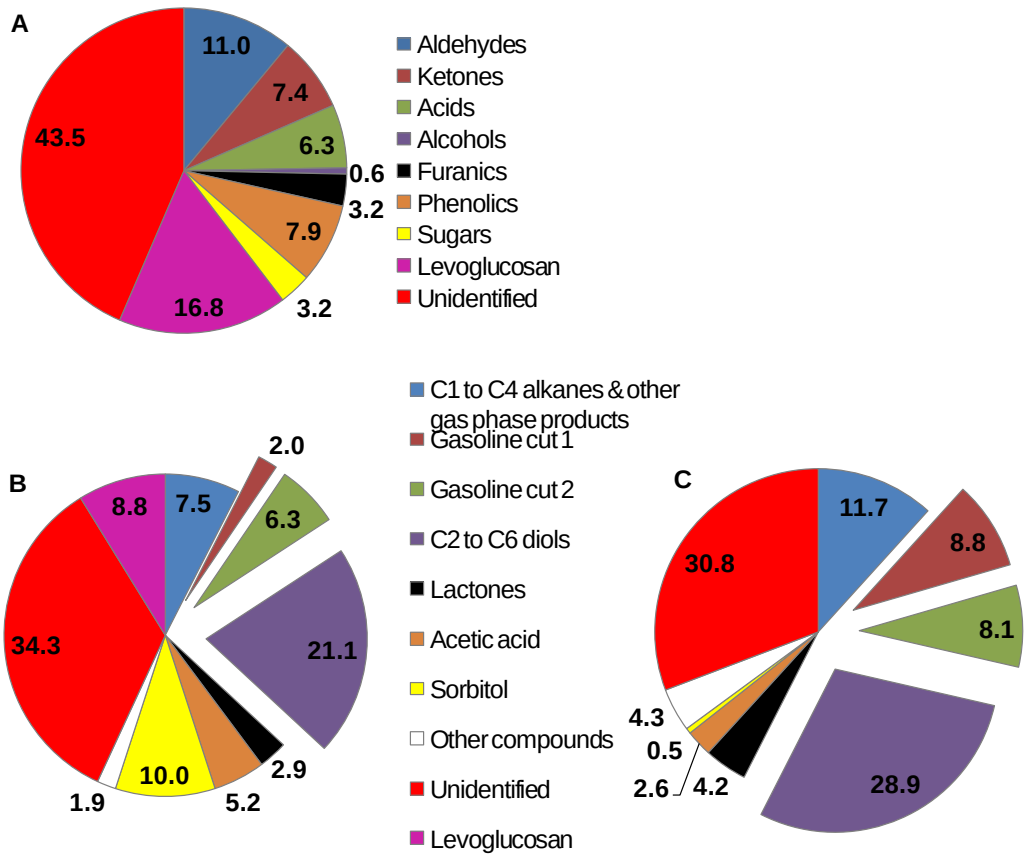

Figure 7-4 Feed and product carbon distribution (in %C) for the hydrogenation of WS-PWBO and for the zeolite upgrading. (A) WS-PWBO feed, (B) Product distribution from single stage hydrogenation of WS-PWBO over Ru/C at 125 °C, 750 psi, 3 hour^{-1}, (C) Product distribution from 2-Stage hydrogenation of WS-PWBO, first over Ru/C at 125 °C, 1450 psi, 3 hour^{-1}, then over Pt/C at 250 °C, 1450 psi, 3 hour^{-1}.

Individual compounds in different product groups are as follows,

1. C1-C4 alkanes & other gas phase compounds: methane, ethane, propane, butane and other gas phase compounds which have not been identified.
2. Gasoline cut 1 (boiling range: 65-99 °C): pentane, hexane, methanol, ethanol, 1-propanol, tetrahydrofuran, 2-butanol, and 2-methyltetrahydrofuran.
3. Gasoline cut 2 (boiling range: 115-175 °C): 1,2-cyclohexanediol, 2,5-dimethyltetrahydrofuran, 1-butanol, 2-pentanol, 1-pentanol, cyclopentanol, 2-hexanol, 3-methylcyclopentanol, cyclohexanol, 3-methylcyclohexanol, and 4-methylcyclohexanol.
4. C2 to C6 diols: 2,3-butanediol, propylene glycol, ethylene glycol, 1,2-hexanediol, 1,4-hexanediol, 1,4-butanediol, and 1,4-pentanediol.
5. Lactones: γ-butyrolactone and γ-valerolactone
6. Other chemicals: tetrahydrofurfuryl alcohol, 1,2,6-hexanetriol, 1,2,3-butanetriol, and glycerol

Table 7-4 Composition of WS-PWBO feed*

Compound	mmol carbon L^{-1}	Classification
Hydroxyacetaldehyde	427.6	Aldehyde
Acetic acid	244.1	Acid
Hydroxyacetone	199.3	Ketone
2-Furanone	37.6	Ketone
Phenol	2.5	Phenolic
3-Methyl-1,2-cyclopentadione	45.7	Ketone
Guaiacol	10.3	Phenolic
Catechol	249.8	Phenolic
1-Hydroxy-2-butanone	20.2	Ketone
Furfural	20.9	Aldehyde
2-Cyclopenten-1-one	21.9	Ketone
5-Hydroxymethylfurfural	63.9	Aldehyde
4-Methylcatechol	47.5	Phenolic
Levoglucosan	652.5	Sugar
Sugars	124.4	Sugar
Methanol	24.4	Alcohol
Total carbon identified	2192.6	
Total carbon as measured by TOC	3879.4	

*made by mixing 7 gm pine wood bio-oil with 28 gm water. The WS-PWBO has 3879.4 mmol carbon L^{-1}, hence the carbon concentration of each component is given in mmol carbon L^{-1} for that compound in WS-PWBO. Fraction carbon contribution of each compound can be found by dividing mmol carbon L^{-1} for that compound by 3879.4 mmol carbon L^{-1}.

We next examined the composition of the product stream from low temperature hydrogenation of the DOE-BO. The H/C_{eff} ratio rose from 0.06 to 0.09 with about 0.9 g hydrogen consumed per 100 g carbon in the feed during this step. The water content of the bio-oil also increased from 24.8 wt% to 27 wt% during the low temperature hydrogenation step. At the same time, the proportion of carbon content identifiable by GC and HPLC went down (Table 6-12), perhaps as a result of homogeneous thermal polymerization reactions among the bio-oil components. The GPC analysis of the hydrogenated DOE bio-oil (Figure 6-4) shows higher concentrations of oligomers with

molecular weights greater than 400 Da compared to the feed. The amount of thermal coke formed from DOE bio-oil is reduced from 19.0 wt% to 13.6% upon low temperature hydrogenation (Table 7-2). This implies that the product of low temperature hydrogenation of DOE-BO is more thermally stable than the feed.

In the case of the water soluble fraction of the pine wood bio-oil (WS-PWBO), the H/C_{eff} ratio increased from 0.14 to 0.71 after low temperature hydrogenation, and rose further to 1.20 upon high temperature hydrogenation. Low temperature hydrogenation was carried out 125 °C as it was found to be the lowest temperature at which all the pyrolysis oil functionalities started showing significant activity towards hydrogenation. The compositions of the low temperature hydrogenated WS-PWBO and high temperature hydrogenated WS-PWBO based on chromatographic analysis are shown in Figure 7-4 B-C and in more detail in Table 7-5. In the low temperature hydrogenation we were able to convert 29.4% of the WSBO feed carbon to gasoline cut 1, gasoline cut 2, and C2 to C6 diols (Figure 7-4B), which can be marketed as products in their own right. Gasoline cut 1 comprises mainly of small (up to 3 carbon atoms) monohydric alcohols boiling in the temperature range of 65-100 °C. Gasoline cut 2 mainly contains C4 to C6 monohydric alcohols boiling in the temperature range of 115-174 °C. The C2 to C6 diols boil above 178 °C with ethylene glycol and propylene glycol being the major components. These product groups can easily be separated by distillation. Gasoline cut 1 and gasoline cut 2 can be added to gasoline as renewable high octane additives. Glycols can be further purified and sold. The thermal stability of the WS-PWBO increases significantly after hydrogenation, with a homogeneous thermal coke yield decreasing from 12.8 wt% for the

WS-PWBO to 2.8 wt% for the WS-PWBO after a low temperature hydrogenation. The hydrogen consumption for the low temperature hydrogenation process was 4.8 g H_2/100 g carbon in the feed.

However, the product distribution still contains significant amounts of hydrogen deficient compounds such as acetic acid (H/C_{eff} ratio = 0), levoglucosan (H/C_{eff} ratio = 0), and sorbitol (H/C_{eff} ratio = 0.33). By feeding this stream through a high temperature hydrogenation reactor at 250 °C and 1450 psi, the total carbon yield of gasoline cut 1, gasoline cut 2, and C2 to C6 diols increased to 45.8% (Figure 7-4C and Table 7-5). In this process the product distribution can be customized by modifying the reaction condition, for example, if there is a larger market for gasoline cut 1, its yield can be increased by operating the second stage at higher temperatures or lower space velocities. At higher temperatures, C2 to C6 diols undergo further C-O and C-C bond cleavage reactions producing small monohydric alcohols. High temperature hydrogenation was carried out at 250 °C so as to achieve high sorbitol and levoglucosan conversion. In the high temperature hydrogenation step a 100% levoglucosan conversion and a 95% sorbitol conversion was obtained. An increase in carbon yield to the desired product groups of gasoline cut 1, gasoline cut 2, and C2 to C6 diols was observed corresponding to the 80% of the levoglucosan and sorbitol carbon. Sorbitol can be converted over a supported Pt catalyst to a mixture of alcohols and polyols through reactions including hydrogenation, dehydration, decarbonylation, and retro-aldol condensation. While sorbitol is significantly more thermally stable than glucose it still has a low overall H/C_{eff} ratio of 0.33 in comparison to the H/C_{eff} ratios of the possible products from hydrogenolysis of

sorbitol, including propylene glycol (H/C_{eff} ratio = 1.33), propanol (H/C_{eff} ratio = 2), and butanediols (H/C_{eff} ratio = 1.5). The net hydrogen consumption for the combined low and high temperature hydrogenation process was 8.1 g H_2/100 g carbon in the feed. The WS-PWBO had high thermal stability after the high temperature hydrogenation with the homogeneous thermal coke yield decreasing from 12.8 wt% for the WS-PWBO to 0.2 wt% after high temperature hydrogenation. High pressure hydrogen is necessary in the high temperature step to minimize carbon loss to less valuable C1 to C4 alkanes.[25, 75]

Table 7-5 Composition of the WS-PWBO hydrogenation products. Low temperature hydrogenation reaction conditions: over 5 wt% Ru/C catalyst ; T: 125 °C; P: 750 psi; WHSV: 3 $hour^{-1}$, high temperature hydrogenation reaction conditions: first over 5wt% Ru/C catalyst (125 °C) then over 5 wt% Pt/C catalyst (250 °C); P: 1450 psi, WHSV: 3 $hour^{-1}$

Compound	mmol carbon L^{-1}	
	LTH-WS-PWBO*	HTH-WS-PWBO†
Pentane	0	14.5
Hexane	0	115.4
Acetic acid	203.2	104.9
Levoglucosan	341.8	0
Sugars	43.1	6.5
Methanol	49.1	56.8
Ethanol	19.7	47.9
1-Propanol	9.7	42.5
Tetrahydrofuran	0	6.1
2-Butanol	0	15.0
2-Methyltetrahydrofuran	0	21.5
2,5-Dimethyltetrahydrofuran	0	19.7
1-Butanol	4.4	11.7
2-Pentanol	0	4.4
1-Pentanol	0	8.4
Ethylene glycol	498.0	465.1
Cyclopentanol	9.5	23.0
2-Hexanol	0	7.9
Propylene glycol	236.1	400.8
2,3-Butanediol	0	34.9
Cyclohexanol	124.6	51.3
1,2-Butanediol	32.1	137.4
Tetrahydrofurfuryl alcohol	1.0	72.7
1,4-Butanediol	54.2	68.6
γ-Butyrolactone	103.0	110.6
γ-Valerolactone	9.6	12.5
Glycerol	0	48.8
1,2-Cyclohexanediol	106.9	107.7
4-Hydroxymethyl-γ-butyrolactone	70.1	47.0
Sorbitol	386.9	21.8
3-Methylcyclopentanol	0	33.9
1,2,3-Butanetriol	0	29.2
1,4-Pentanediol	0	23.3
3-methylcyclohexanol	0	34.3
4-methylcyclohexanol	0	20.5
1,2-Hexanediol	0	27.7

1,2,6-Hexanetriol	0	14.2
Total carbon identified	2355.4	2171.5
Total carbon in liquid as measured by TOC	3590.3	3405.4

*low temperature hydrogenation product of WS-PWBO, †high temperature hydrogenation product of WS-PWBO, see footnote of Table 7-4 for concentration units

7.5 Zeolite Upgrading of Non-hydrogenated and Hydrogenated Bio-oil-derived Feeds

The hydrogenated feeds were then added to the zeolite step (step yields in Figure 7-5 and overall yields in Table 7-6). Only 20% of the DOE bio-oil carbon was converted to olefins and aromatics if fed directly to the zeolite without any hydrotreatment, with 50% of the carbon forming coke. The remaining 30% of the carbon was converted to CO, CO_2, and unidentified oxygenates. Low temperature hydrogenation raises the yield of olefins and aromatics after zeolite upgrading to 32.6% (Table 7-6). The low temperature hydrogenation step only used a small amount of hydrogen but resulted in a significant increase in the yield of desired products. The improvement in olefins and aromatics yield from DOE-BO to LTH-DOE-BO is more than what we expected from the corresponding H/C_{eff} increase. This can be due to the sizeable reduction in coke yield (35.3%) for LTH-DOE-BO. It can also be noted in Table 7-1 that CO yield considerably increases from DOE-BO (13.5% carbon) to LTH-DOE-BO (22.6% carbon). This behavior is similar to what we observed for glucose (H/C_{eff} =0) and sorbitol (H/C_{eff} =0.33). Carbon monoxide is produced by decarbonylation reactions, whereas coke is produced by homogeneous or catalytic coking reactions. These reactions are competing parallel reactions. Glucose (or

DOE-BO) is thermally unstable and hence has higher coking tendency as compared to sorbitol (or LTH-DOE-BO), resulting in the coking reactions dominating the decarbonylation reactions. Decarbonylation reactions are one of the two main routes for deoxygenation of the feed molecule to produce olefins and aromatics (other route is dehydration). Hence as the feed molecule is thermally stabilized the coking reactions reduce, decarbonylation increases and olefins and aromatics yield increases as observed from DOE-BO to LTH-DOE-BO.

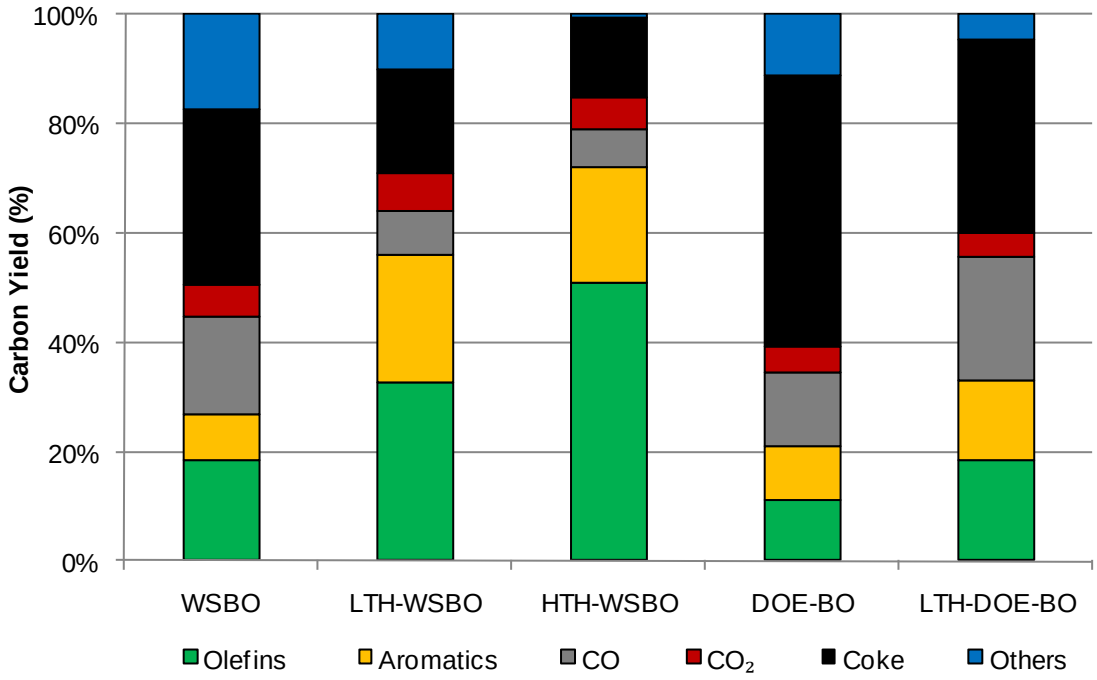

Figure 7-5 Carbon yields for the conversion of bio-oil derived feedstocks over HZSM-5 at 873 K. Key: WSBO is the water soluble fraction of the pine wood bio-oil, LTH-WSBO is WSBO hydrogenated over Ru/C (125 °C, 750 psi, 3 $hour^{-1}$), HTH-WSBO is WSBO hydrogenated first over Ru/C (125 °C, 1450 psi, 3 $hour^{-1}$), then over Pt/C (250 °C, 1450 psi, 3 $hour^{-1}$). DOE-BO is DOE bio-oil and LTH-DOE-BO is DOE bio-oil hydrogenated over Ru/C (125 °C, 1450 psi, 1.6 $hour^{-1}$). The category others encompasses phenol, alkyl phenols, naphthol and alkyl naphthols.

Table 7-6 Overall carbon yield for the integrated catalytic process for the conversion of pyrolysis oils and the aqueous fraction of pyrolysis oil.

Feed	Process	Hydrogen Consumption (g/100 g carbon in feed)	Final Products (% carbon yield) or Carbon Selectivity* (%)					
			C1-C6 Alkanes	CO_x	Aromatics	Olefins	Coke	Unidentified
DOE-BO	Zeolite	None	0	18.3	9.8 Carbon Selectivity (%) Benzene: 17.3 Toluene: 40.8 Xylene: 23.5 EtBenz†: 2.0	11.2 Ethylene: 51.8 Propylene: 36.6 Butylene: 11.6	49.5	11.2
DOE-BO	Ru/H_2 + Zeolite	0.9	2	26.5	14.4 Carbon Selectivity (%) Benzene: 16.9 Toluene: 37.2 Xylene: 38.5 EtBenz: 3.4	18.2 Ethylene: 52.2 Propylene: 35.9 Butylene: 11.4	34.6	4.3
WS-PWBO	Zeolite	None	0	23.7	8.2 Carbon Selectivity (%) Benzene: 26.8 Toluene: 46.3 Xylene: 20.7 EtBenz: 1.2	18.5 Ethylene: 41.6 Propylene: 45.9 Butylene: 12.4	32.3	17.3
WS-PWBO	Ru/H_2 + Zeolite	4.8	7.5	13.9	21.6 Carbon Selectivity (%) Benzene: 17.6 Toluene: 45.5 Xylene: 31.3 EtBenz: 2.6	30.2 Ethylene: 31.8 Propylene: 55.4 Butylene: 12.8	17.4	9.4
WS-PWBO	Ru/H_2 + Pt/H_2 + Zeolite	8.1	15.0	10.7	18.3 Carbon Selectivity (%) Benzene: 27.0 Toluene: 49.3 Xylene: 19.1 EtBenz: 2.3	43.0 Ethylene: 32.0 Propylene: 53.8 Butylene: 14.2	12.6	0.4

***** carbon selectivity values are reported for individual components benzene, toluene, xylene, ethylbenzene, ethylene, propylene, and butylene. † EtBenz = Ethylbenzene

Similar results were observed with the water soluble fraction of the pine wood bio-oil (WS-PWBO). Direct zeolite upgrading of WS-PWBO affords 26.7% carbon yield of olefins and aromatics. Low temperature hydrogenation prior to zeolite upgrading raised the yield to 51.8%, while the high temperature hydrogenation leads to 61.3% olefins and aromatics yield. The high temperature hydrogenation process converts 15.0% carbon in WS-PWBO to light alkanes, twice that of low temperature hydrogenation process. All these points are shown in Figure 7-1 along with the theoretical yield with toluene as the major product. The difference between experimental and theoretical yields is reduced with increasing H/C_{eff} ratio of the WS-PWBO feed indicating that the hydrogen added is used primarily for increasing the olefin and aromatic yield from the process. As seen in Table 7-3, the percentage of theoretical toluene yield for water soluble fraction of the pine wood bio-oil (WS-PWBO) increased from 39.1% to 64.9% upon low temperature hydrogenation, and increased further to 72.3% upon high temperature hydrogenation.

The major products obtained in the zeolite upgrading of DOE-BO and WS-PWBO are C2 to C4 olefins and C6 to C8 aromatic hydrocarbons. Under the reaction conditions used in this study the olefins selectivity for the DOE bio-oil was 50% to ethylene, 35% to propylene, with the balance being butylenes. The aromatic selectivity for the DOE bio-oil decreased with toluene (37-40% selectivity) > xylenes (23.5-38.5% selectivity) > benzene (17% selectivity). The olefin selectivity for the WS-PWBO was different than the DOE bio-oil with an olefin selectivity of 55% to propylene, 32% to ethylene, with the balance being butylenes. The aromatic selectivity for the WSBO

decreased with toluene (45-50% selectivity) > xylenes (20-30% selectivity) > benzene (17-27% selectivity). The ratios of these products can be tuned by adjusting both the reaction conditions and catalytic process. For example, in the zeolite upgrading of high temperature hydrogenated WSBO the aromatic hydrocarbons to olefin ratio increases from 1:2.8 to 1:1.1 as the temperature is reduced from 650 °C to 400 °C (Table 7-7). Olefins can also be converted to aromatics by recycling the olefins back to the zeolite reactor. Several existing processes can also be used to convert olefins to aromatics including olefin aromatization and alkylation of the aromatics using olefins.[105, 106] These results indicate that the olefin to aromatic ratio and the types of olefins and aromatics produced can be adjusted according to the market demand using several approaches.

Table 7-7 Effect of temperature on the product carbon yields (%) for zeolite upgrading of HTH-WS-PWBO on HZSM-5. WHSV: 11.7 $hour^{-1}$, Helium carrier gas flow rate: 204 ml min^{-1}, HTH-WS-PWBO was obtained by 2-stage hydrogenation of WS-PWBO. Hydrogenation reaction conditions, 1st stage: 5 wt% Ru/C catalyst, 125 °C, 1450 psi, WHSV: 3 $hour^{-1}$, 2nd stage: 5 wt% Pt/C catalyst, 250 °C, 1450 psi, WHSV: 3 $hour^{-1}$.

Product	**Temperature (°C)**			
	400	**500**	**600**	**650**
CO	2.2	6.5	6.8	10.5
CO_2	1.3	4.0	5.7	6.6
Coke	27.5	20.2	14.8	13.8
Ethylene	10.9	12.7	16.2	19.0
Propylene	14.7	21.2	27.2	25.7
Butylene	4.6	6.6	7.2	6.1
Olefins	30.3	40.5	50.6	50.7
Benzene	2.7	3.4	5.8	6.5
Toluene	9.9	10.5	10.6	8.9
Xylene	10.9	6.7	4.1	2.6
Ethyl-benzene	3.3	1.44	0.5	0.2
Styrene	0	0.1	0.3	0.2
Indene	0	0	0.1	0.1
Naphthalene	0	0	0.1	0.1
Aromatics	26.8	22.6	21.5	18.4
Total identified carbon (%)	88.1	93.4	99.4	99.9

7.6 Process Economics

The cost of hydrogen is important in determining how much hydroprocessing should be done before deoxygenation with the zeolite catalyst. Figure 7-6 depicts the economic potential of our integrated catalytic process as a function of H/C_{eff} ratio of the feed to zeolite step for four different hydrogen costs. The economic potential of the process is calculated by subtracting the cost of process feeds (biomass and hydrogen) from the selling price of the products. Importantly, the economic potential only includes

the costs of the raw material and does not include any other operating costs or capital costs. The market price of hydrogen varies widely depending on location, mode of supply and natural gas prices. The cheapest hydrogen is from large steam reformers and typically costs $1.50 to $2.50 per kg.[107] Whereas, the hydrogen shipped in tube trailers can cost as much as $12 per kg.[108] The optimum H/C_{eff} ratio, where the economic potential of the process is highest, decreases with increasing hydrogen cost. For example, if hydrogen cost is $2 per kg then the maximum economic potential occurs at an H/C_{eff} of 1.4. Whereas, when the hydrogen cost is $4.20 per kg, the maximum economic potential occurs when pyrolysis oil is fed directly to the zeolite catalyst without any hydrogenation. Combining the hydrogenation steps with a zeolite conversion step reduces the overall hydrogen requirements as compared to using hydrogen for a complete deoxygenation of pyrolysis oil. A complete deoxygenation of pyrolysis oil by hydrodeoxygenation with a 100% carbon yield to their corresponding hydrocarbons (*i.e.* alkanes from C1-C6 non-phenolic oxygenates and aromatics from phenolic compounds) requires 14 to 15 g H_2/100 g carbon in the feed, if the catalyst coking problems are overcome. In comparison, increasing the H/C_{eff} ratio of pyrolysis oil from 0 to 1.4 requires 11.7 g H_2/100 g carbon in the feed reducing the hydrogen requirements compared to complete hydrodeoxygenation by 20%. Furthermore, during the hydrotreating process large amounts of undesired methane is produced which also can significantly increase the hydrogen requirements. Hydrogen required in these processes should preferably be obtained from renewable sources such as by reforming of biomass derived feedstock.[15, 29, 109] Alternatively, hydrogen can be obtained from coal gasification or from water

splitting driven by carbon-free energy sources such as solar, nuclear and wind energy, as suggested by Agrawal et al.[110]

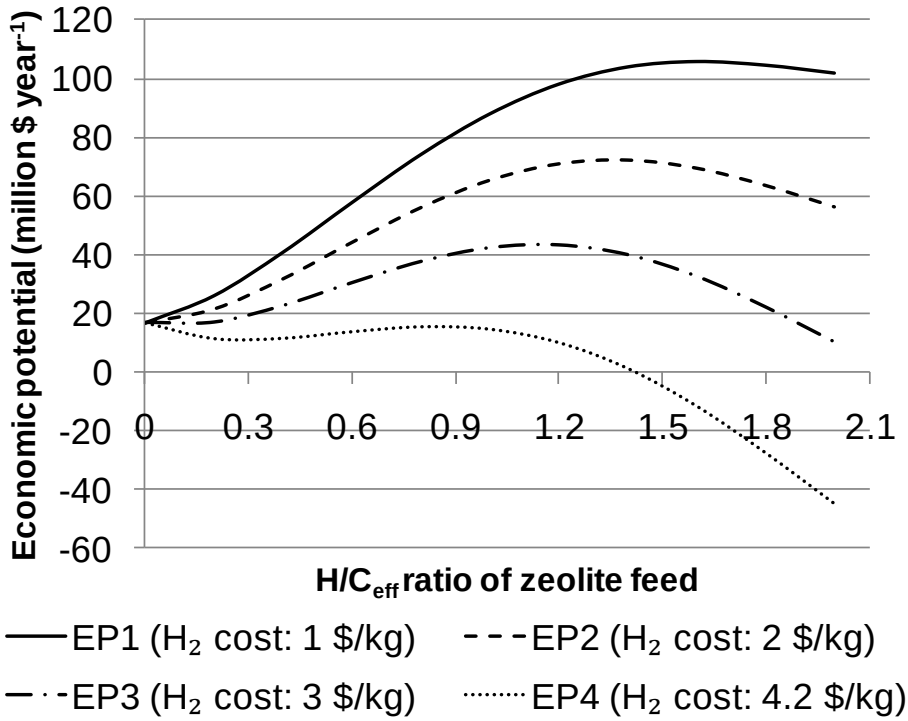

Figure 7-6 Annual economic potential for the integrated hydroprocessing and zeolite upgrading of pyrolysis oil as a function of H/C_{eff} ratio of feed to zeolite catalyst. Data in Figure 7-1 was used for calculating the economic potential values. The plant capacity was assumed to be 100 ton $hour^{-1}$ of biomass. Pyrolysis oil yield was assumed to be 70 wt% of biomass. It was assumed that in the zeolite upgrading step all olefins produced are converted to aromatics. July 2010 spot price of benzene of 2.60 \$ $gallon^{-1}$ was used as aromatic hydrocarbon selling price. Biomass cost was assumed to be \$50 per metric ton.

7.7 Conclusion

The study shows that the aromatic hydrocarbons and olefins can be produced with high yields from the bio-oil and its aqueous fraction. The yield of aromatics and olefins from the zeolite upgrading increases with increasing H/C_{eff} ratio of the feed. Bio-oil and

WSBO is hydrogen deficient and hence hydrogen needs to be added to these feeds to achieve high yields of valuable products. There exists an optimum H/C_{eff} ratio for bio-oil derived feeds where the economic potential of the process will be maximum. The optimum H/C_{eff} ratio depends mainly on the cost of hydrogen.

Three classes of chemistry are needed for efficient conversion of biomass into petrochemicals are: (1) pyrolysis of biomass into bio-oil using thermal decomposition processes; (2) hydrotreatment of bio-oils using supported metal catalysts and hydrogen; and (3) production of aromatics and olefins from the hydrotreated bio-oils with zeolite catalysts. By optimizing these three processes a range of petrochemicals can be produced. The goals of the reaction chemistry in the hydrogenation steps are to add hydrogen to the biomass derived molecules with (1) controlled cleavage of C-C and C-O bonds, and (2) complete hydrogenation of thermally unstable aldehyde, ketone, carboxyl, and sugar functionalities to corresponding alcohols. Cleavage of C-C bond is desired such that hydrogen deficient molecules like sorbitol are converted to hydrogen rich molecules such as ethylene glycol and propylene glycol. Further C-C bond cleavage to lighter alkanes (*e.g.* methane) is undesired. A controlled C-O bond cleavage is preferred when a further increase in H/C_{eff} ratio is desired or when a high yield of gasoline cut 1 is desired. An example of C-O bond cleavage reaction occurring in the hydrotreatment step is the conversion of ethylene glycol to ethanol. A further C-O cleavage in ethanol is not desired as it will produce undesired ethane.

Zeolite catalysts convert the biomass feedstocks into aromatics and olefins which can fit easily into the existing infrastructure. Increasing the yield of petrochemical products from biomass therefore requires hydrogen. Thus there exists an optimum solution for the economical maximum yield of petrochemical feedstocks products that is dictated by the cost of hydrogen. It is expected that future advances in the field of metal and zeolite catalysts combined with reaction engineering will allow us to design even more efficient and economical processes to convert biomass resources to renewable chemical industry feedstocks.

CHAPTER 8

CONCLUSIONS AND FUTURE WORK

8.1 Conclusions

We have used a combination of characterization techniques to understand the physical and chemical nature of bio-oils. Bio-oil was found to contain GC and HPLC detectable C2 to C6 oxygenated hydrocarbon with various functionalities including aldehydes, ketones, acids, and carbohydrates. The most abundant components of the bio-oil were found to be levoglucosan, acetic acid, hydroxyacetaldehyde, and hydroxyacetone. Only about 40% carbon in the bio-oil was detectable by GC and HPLC, with the balance being GC and HPLC non-detectable oligomers. Using gel permeation chromatography it was determined that the bio-oil also contained GC and HPLC undetectable high molecular weight oligomers with molecular weights from 200 to up to 10000 Da. Bio-oil was found to be up to 62 wt% soluble in water, with water soluble fraction mainly containing the C2 to C6 oxygenated hydrocarbons. Bio-oil phase separated readily in water soluble (WSBO) and water insoluble (WIBO) phases upon addition of water. Up to 60% carbon in the water soluble bio-oil can be detected by GC and HPLC as opposed to about 40% in bio-oil and less than 20% in water insoluble bio-oil.

The stability analysis of the bio-oil showed that the viscosity and molecular weight of bio-oil and its fractions increases when incubated at 90 °C. The rate of viscosity increase upon aging is higher for the water insoluble fraction of bio-oil (WIBO)

than that for bio-oil than that for the water soluble fraction of bio-oil. The WIBO contains a high concentration of high molecular weight lignin oligomers, implying that these oligomers are largely responsible for the bio-oil instability. The aqueous fraction of the bio-oil was completely stabilized by hydrogenation over Ru/C catalyst at 125 °C. Char can be removed from the bio-oil by microfiltration using ceramic membranes with pore sizes less than 1 μm. Removal of char does not affect the bio-oil stability but is desired as char can cause difficulty in further processing of the bio-oil. The high molecular weight (HMW) lignin was found to be the major contributor towards the absolute viscosity of bio-oil as well as towards the increase in bio-oil viscosity during the incubation at 90 °C. The viscosity increase in the bio-oil was due to two reasons: increase in the average molecular weight and increase in the concentration of high molecular weight oligomers. Nanofiltration by 5 nm membrane was found to reduce the rate of viscosity increase and molecular weight increase in bio-oil.

We produced hydrogen and alkanes from the aqueous fraction of the bio-oil (WSBO). The key step in that process is the low temperature hydrogenation (LTH) of WSBO over Ru/C catalyst. The LTH step reduced the thermally unstable bio-oil functionalities to corresponding alcohols, which are thermally stable. The challenge in the LTH step is to minimize the carbon loss to gas phase products. Hydrogen was produced with 60% selectivity whereas alkanes were produced with up to 97% selectivity. WSBO is less active for reforming as compared to pure sorbitol. The alkane selectivity obtained from water soluble bio-oil is towards the higher alkanes (C5 and C6 alkanes) as compared to pure sorbitol. Alkane selectivity can be increased by supplying

hydrogen externally or by addition of strong acid such as HCl to the feed. The external hydrogen suppresses the reforming reactions that are otherwise necessary to produce hydrogen required in hydrogenation/dehydration. The addition of HCl in the feed expedites the dehydration reaction resulting in higher alkanes yield.

Ideally pyrolysis oils needs to be deoxygenated to a mixture of organic molecules that are more compatible with current fuels and chemicals infrastructure. Oxygenated gasoline additives and valuable C2 to C6 diols can be produced with high carbon yield from the aqueous fraction of the bio-oil (WSBO) in a 2-stage process. The goal of the first step is to stabilize WSBO for high temperature processing by completely hydrogenating the thermally unstable compounds while minimizing the carbon loss to gas phase. The major products obtained are ethylene glycol, propylene glycol, and sorbitol. The optimum temperature (where maximum product yield is observed) was found to be 125 °C with optimum space velocity of about 1.5 to 3 $hour^{-1}$. In the second stage, sorbitol is converted over Pt/C catalyst to more diols and monohydric alcohols. Up to 46% carbon of the WSBO was successfully converted to gasoline cut 1, gasoline cut 2, and C2 to C6 diols. The product selectivity can be controlled by manipulating pressure and temperature of the second stage. The product selectivity is a function of feed composition. C2 to C6 diols were obtained as major product from WS-PWBO, whereas, monohydric alcohols were the major products from WS-DOE-BO. The rate of C-O bond cleavage is higher in WS-DOE-BO due to high acetic acid concentration as it can catalyze the dehydration reactions. To achieve the maximum yield to desired products from two-stage hydroprocessing of bio-oil, the catalyst in the first step should have high hydrogenation

activity and low C-C bond cleavage activity, the catalyst in the second stage should have moderate C-C and C-O bond cleavage activity. The bio-oils with high water solubility and low acid content are desired.

In addition to water soluble bio-oil, we also hydrogenated whole bio-oil in single stage over Ru/C catalyst. A quantifiable reactant disappearance was observed only at 125 °C but no corresponding hydrogenation products were observed. The average molecular weight of bio-oil increased upon hydrogenation due to bio-oil self-polymerization. It is possible that the lignin oligomers present in the bio-oil are occupying the catalyst sites and the disappearance of reactants is only because of the homogenous thermal polymerization reactions.

In addition to the production of alcohols and diols, we have also shown that hydroprocessing can be combined with zeolite upgrading to produce aromatics and olefins in high yields from WSBO and bio-oil. The yield of aromatics and olefins from the zeolite upgrading increases with increasing H/C_{eff} ratio of the feed. The product selectivity can be manipulated by changing the temperature of zeolite upgrading reactor. Bio-oil and WSBO is hydrogen deficient and hence hydrogen needs to be added to these feeds to achieve high yields of valuable products. Combing the hydroprocessing with zeolite upgrading requires less hydrogen as compared to a complete hydrodeoxygenation by hydrotreating. The increase in the olefins and aromatics yield after the addition of hydrogen to the feed is due to two reasons:

1. Addition of hydrogen increases the thermal stability of feed resulting in less coke.

Addition of hydrogen increases the intrinsic hydrogen content of feed resulting in less CO and CO_2.

2. Zeolite catalysts convert the biomass feedstocks into aromatics and olefins which can fit easily into the existing chemicals infrastructure. Increasing the yield of petrochemical products from biomass therefore requires hydrogen. Thus there exists an optimum solution for the economical maximum yield of petrochemical feedstocks products that is dictated by the cost of hydrogen. It is expected that future advances in the field of metal and zeolite catalysts combined with reaction engineering will allow us to design even more efficient and economical processes to convert biomass resources to renewable chemical industry feedstocks.

This work has significant practical implications. Bio-oil to date has no market due to the drawbacks associated with it. The aqueous phase processing of water soluble bio-oil can be used to produce hydrogen and alkanes from bio-oil. The hydroprocessing and zeolite upgrading can be used to produce a wide range of products including gasoline-range alcohols, C2 to C6 diols, aromatics, and olefins. The processes that we have developed are flexible such that the desired products can be produced depending on the market demand. These processes can hence form a core of a biorefinery based on catalytic fast pyrolysis of biomass. Five of the seven (benzene, toluene, xylene, ethylene, propylene) chemical industry building blocks can be produced using the processes described here, opening the door to a chemical industry based on renewable biomass feedstock.

8.2 Future Work

In this work we have shown that the high molecular weight lignin is mainly responsible for the bio-oil instability. More work needs to be done on modifying the pyrolysis process such that the concentration of HMW lignin in bio-oils is reduced. It is possible that lignin is depolymerized during pyrolysis but it repolymerizes during the char separation and condensation resulting in the formation of high molecular weight oligomers. To eliminate HMW lignin it would be crucial to know if it is coming from non-depolymerized lignin or from the repolymerization of depolymerized lignin. The bio-oil vapors can possibly be selectively condensed such that HMW lignin is condensed separately from other bio-oil components due to its high boiling point. This strategy needs to be studied in detail.

In the bio-oil hydroprocessing, a completely different product distribution was obtained for WS-PWBO and WS-DOE-BO. We attributed this to high acid content of the DOE-BO. This phenomenon needs to be studied in detail. Bio-oil from various sources such as hardwood, softwood, switch grass, and corn stover can be tested. Bimetallic PtRe catalyst fared better towards hydrogenating acetic acid as compared to monometallic Pt catalyst. The carbon loss to gas phase was also less for PtRe catalyst compared to Pt catalyst. More bimetallic catalysts need to be tested in these processes. Other factors such as ratio of Pt to Re in the bimetallic catalyst can also be studied.

We were able to hydrogenate the components of the water soluble fraction of bio-oil successfully. Whereas, in the case of low temperature hydrogenation of bio-oil we observed that the reactants disappeared but did not detect any corresponding alcohols products as discussed in Section 6.9. The average molecular weight of bio-oil increased upon hydrogenation due to bio-oil self-polymerization. It is possible that the lignin oligomers present in the bio-oil are occupying the catalyst active sites and the disappearance of reactants is only because of the homogenous thermal polymerization reactions. Bio-oil lignin oligomer model compound hydrogenation studies can be carried out to study this in detail. These studies will also help in designing the processes for the hydrogenation of whole bio-oil. Previous lignin model hydrodeoxygenation efforts have revolved around simpler model compounds such as guaiacol, phenol, catechol, and anisole over conventional CoMo-NiMo as well as on noble metal catalysts.[*69, 70, 111-113*] These monomers are not realistic lignin model compounds as the water insoluble bio-oil contains high molecular weight oligomers. Hence the hydrodeoxygenation of simple oligomers like a trimer shown below should be studied in future.

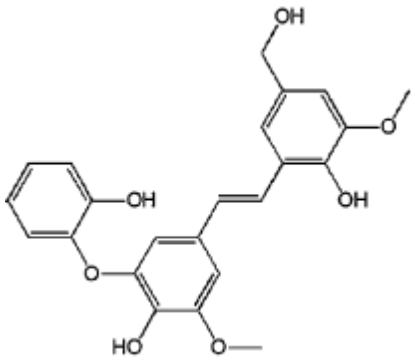

Optimum reaction conditions (temperature, pressure), catalyst screening and catalyst deactivation studies need to be done for hydrodeoxygenation of such model compounds.

BIBLIOGRAPHY

1. G. W. Huber, S. Iborra, A. Corma, *Chem. Rev.* **106**, 4044 (2006).

2. Y. Roman-Leshkov, C. J. Barrett, Z. Y. Liu, J. A. Dumesic, *Nature* **447**, 982 (2007).

3. D. L. Klass, *Biomass for renewable energy, fuels and chemicals*. (Academic Press, San Diego, 1998).

4. C. E. Wyman, *Annu. Rev. Energy Env.* **24**, 189 (1999).

5. C. E. Wyman *et al.*, *Bioresour. Technol.* **96**, 1959 (2005).

6. R. D. Perlack *et al.*, "Biomass as Feedstock for a Bioenergy and Bioproducts Industry: The Technical Feasibility of a Billion-Ton Annual Supply" *DOE/GO-102995-2135* (Oak Ridge National Laboratory, 2005).

7. S. Czernik, A. V. Bridgwater, *Energy Fuels* **18**, 590 (2004).

8. A. V. Bridgwater, G. V. C. Peacocke, *Renewable Sustainable Energy Rev.* **4**, 1 (2000).

9. A. V. Bridgwater, D. Meier, D. Radlein, *Org. Geochem.* **30**, 1479 (1999).

10. D. Mohan, C. U. Pittman, P. H. Steele, *Energy Fuels* **20**, 848 (2006).

11. P. J. Dauenhauer, B. J. Dreyer, N. J. Degenstein, L. D. Schmidt, *Angew. Chem., Int. Ed.* **46**, 5864 (2007).

12. M. J. A. Tijmensen, A. P. C. Faaij, C. N. Hamelinck, M. R. M. v. Hardeveld, *Biomass Bioenergy* **23**, 129 (2002).

13. T. R. Carlson, T. P. Vispute, G. W. Huber, *ChemSusChem* **1**, 397 (2008).

14. T. R. Carlson, J. Jae, Y. C. Lin, G. A. Tompsett, G. W. Huber, *J. of Catal.* **270**, 110 (2010).

15. R. D. Cortright, R. R. Davda, J. A. Dumesic, *Nature* **418**, 964 (2002).

16. G. W. Huber, J. N. Chheda, C. J. Barrett, J. A. Dumesic, *Science* **308**, 1446 (2005).

17. E. L. Kunkes *et al.*, *Science* **322**, 417 (2008).

18. A. V. Bridgwater, *Chem. Eng. J.* **91**, 87 (2003).
19. A. V. Bridgwater, M. L. Cottam, *Energy Fuels* **6**, 113 (1992).

20. M. Wright, R. C. Brown, *Biofuels, Bioprod. Bioref.* **1**, 191 (2007).

21. J. P. Diebold, "A Review of the Chemical and Physical Mechanisms of the Storage Stability of Fast Pyrolysis Bio-Oils" *NREL/SR-570-27613* (National Renewable Energy Laboratory, 2000).

22. F. A. Agblevor, S. Besler, D. Montane, R. J. Evans, *Abstracts of Papers of American Chemical Society* **209**, 8 (1995).

23. D. Radlein, in *The Fast Pyrolysis of Biomass: A Handbook,* A. V. Bridgwater *et al.*, Eds. (CPL Press, Newbury, UK, 1999), pp. 164-188.

24. R. Bayerbach, D. Meier, *J. Anal. Appl. Pyrolysis* **85**, 98 (2009).

25. G. W. Huber, R. D. Cortright, J. A. Dumesic, *Angew. Chem., Int. Ed.* **43**, 1549 (2004).

26. G. W. Huber, J. W. Shabaker, S. T. Evans, J. A. Dumesic, *Appl. Catal. B* **62**, 226 (2006).

27. R. R. Davda, J. W. Shabaker, G. W. Huber, R. D. Cortright, J. A. Dumesic, *Appl. Catal. B* **56**, 171 (2005).

28. G. W. Huber, J. A. Dumesic, *Catal. Today* **111**, 119 (2006).

29. T. P. Vispute, G. W. Huber, *Green Chem.* **11**, 1433 (2009).

30. D. C. Elliott, *Energy Fuels* **21**, 1792 (2007).

31. S. P. Zhang, Y. J. Yan, J. W. Ren, T. C. Li, *Energy Sources* **25**, 57 (2003).

32. J. D. Adjaye, N. N. Bakhshi, *Fuel Process. Technol.* **45**, 161 (1995).

33. J. D. Adjaye, N. N. Bakhshi, *Fuel Process. Technol.* **45**, 185 (1995).

34. P. Badger, U.S. Patent Application No. 11/480 914.

35. P. Badger, P. Fransham. U.S. Patent Application No. 11/480 915.

36. S. Elmaleh, W. Naceur, *J. Mem. Sci.* **66**, 227 (1992).

37. L. V. Cremades, E. Rodriguez-Grau, R. Mulero, J. A. Cusido, *Water SA* **33**, 253 (2007).

38. G. V. C. Peacocke, P. A. Russel, J. D. Jenkins, A. V. Bridgwater, *Biomass Bioenergy* **7**, 169 (1994).

39. B. Scholze, D. Meier, *Journal of Analytical and Applied Pyrolysis* **60**, 41 (2001).

40. K. Sipila, E. Kuoppala, L. Fagernas, A. Oasmaa, *Biomass Bioenergy* **14**, 103 (1998).

41. A. Oasmaa, S. Czernik, *Energy Fuels* **13**, 914 (1999).

42. J. Piskorz, D. S. Scott, D. Radlien, in *Pyrolysis Oils from Biomass: Producing Analyzing and Upgrading*, E. J. Soltes, T. A. Milne, Eds. (American Chemical Society, Washington DC, 1988), pp. 167-178.

43. S. Helle, N. M. Bennett, K. Lau, J. H. Matsui, S. J. B. Duff, *Carbohydrate Res.* **342**, 2365 (2007).

44. Z. Y. Luo *et al.*, *Biomass Bioenergy* **26**, 455 (2004).

45. M. Garcia-Perez *et al.*, *Energy Fuels* **20**, 364 (2006).

46. M. E. Boucher, A. Chaala, H. Pakdel, C. Roy, *Biomass Bioenergy* **19**, 351 (2000).

47. B. Scholze, D. Meier, *Journal of Analytical and Applied Pyrolysis* **60**, 41 (20011).
48. S. T. Srinivas, A. K. Dalai, N. N. Bakhshi, *Can. J. Chem. Eng.* **78**, 343 (2000).

49. J. P. Diebold, S. Czernik, *Energy Fuels* **11**, 1081 (1997).

50. E. Fratini *et al.*, *Langmuir* **22**, 306 (2006).

51. S. Czernik, D. K. Johnson, S. Black, *Biomass Bioenergy* **7**, 187 (1994).

52. A. Oasmaa, E. Kuoppala, Y. Solantausta, *Energy Fuels* **17**, 433 (2003).

53. A. Oasmaa, E. Kuoppala, *Energy Fuels* **17**, 1075 (2003).

54. A. Oasmaa, E. Kuoppala, S. Gust, Y. Solantausta, *Energy Fuels* **17**, 1 (2003).

55. A. Holmqvist, O. Wallberg, A. S. Jonsson, *Chem. Eng. Res. and Des.* **83**, 994 (2005).

56. A. S. Jonsson, A. K. Nordin, O. Wallberg, *Chem. Eng. Res. Des.* **86**, 1271 (2008).

57. T. Tzanetakis, N. Ashgriz, D. F. James, M. J. Thomson, *Energy Fuels* **22**, 2725 (2008).

58. Q. Lu, W. Z. Li, X. F. Zhu, *Energy Convers. Manage.* **50**, 1376 (2009).

59. T. A. Milne, C. C. Elam, R. J. Evans, "Hydrogen from Biomass: State of the Art and Research Challenges" (Report No. IEA/H2/TR-02/001, International Energy Agency, 2002).

60. R. K. Sharma, N. N. Bakhshi, *Energy Fuels* **7**, 306 (1993).

61. P. Gallezot, N. Nicolaus, G. Flèche, P. Fuertes, A. Perrard, *J. Catal.* **180**, 51 (1998).

62. J. Wisniak, R. Simon, *Ind. Eng. Chem. Prod. Res. Dev.* **18**, 50 (1979).

63. Z. Zhang, J. E. Jackson, D. J. Miller, *Appl. Catal., A* **219**, 89 (2001).

64. H. A. Pray, C. E. Schweichert, B. H. Minnich, *Ind. Eng. Chem.* **44**, 1146 (1952).

65. D. C. Elliott, E. G. Baker, "Biomass Liquifaction Product Analysis and Upgrading", (Report No. 23130, NRCC, Sherbrooke, Quebec, Canada, 1983).

66. T. L. Marker *et al.*, "Opportunities for Biorenewables in Petroleum Refineries" (Final Report DE-FG36-05GO15085, UOP LLC, Des Plaines, IL, 2005); http://www.osti.gov/bridge/servlets/purl/861458-Wv5uum/861458.pdf.

67. J. D. Adjaye, S. P. R. Katikaneni, N. N. Bakhshi, *Fuel Process. Technol.* **48**, 115 (1996).

68. R. Maggi, B. Delmon, in *Hydrotreatment and Hydroprocessing of Oil Fractions*, G. F. Froment, B. Delmon, P. Grange, Eds. (Elsevier Science B. V., 1997).

69. E. Furimsky, *Appl. Catal. A* **199**, 147 (2000).

70. D. C. Elliott, T. R. Hart, *Energy Fuels* **23**, 631 (2009).

71. B. Scholze, Long-term stability, catalytic upgrading, and application of pyrolysis oilssImproving the properties of a potential substitute for fossil fuels, thesis, University of Hamburg (2002).

72. D. Wang, D. Montane, E. Chornet, *Appl. Catal., A* **143**, 245 (1996).

73. P. R. Patwardhan, J. A. Satrio, R. C. Brown, B. H. Shanks, *J. Anal. Appl. Pyrolysis* **86**, 323 (2009).

74. Q. Xiang, Y. Y. Lee, R. W. Torget, *Appl. Biochem. Biotechnol.* **115**, 1127 (04/01, 2004).

75. N. Li, G. W. Huber, *J. Catal.* **270**, 48 (2010).

76. J. E. Carnahan, T. A. Ford, W. F. Gresham, W. E. Grigsby, G. F. Hager, *J. Am. Chem. Soc.* **77**, 766 (1955).

77. M. Schlaf, *Dalton Trans.*, 4645 (2006).

78. D. K. Sohounloue, C. Montassier, J. Barbier, *React. Kinet. Catal. Let.* **22**, 391 (1983).

79. S. P. Crabtree, R. C. Lawrence, M. W. Tuck, D. V. Tyres, *Hydrocarbon Process.* **85**, 87 (2006).

80. R. R. Davda, J. W. Shabaker, G. W. Huber, R. D. Cortright, J. A. Dumesic, *Appl. Catal., B* **43**, 13 (2003).

81. E. P. Maris, R. J. Davis, *J. Catal.* **249** 328 (2007).

82. T. Miyazawa, Y. Kusunoki, K. Kunimori, K. Tomishige, *J. Catal.* **240**, 213 (2006).

83. T. Miyazawa, S. Koso, K. Kunimori, K. Tomishige, *J. of Catal.* **318**, 244 (2007).

84. V. Pallassana, M. Neurock, *J. Catal.* **209**, 289 (2002).

85. M. Stöcker, *Microporous Mesoporous Mat.* **29**, 3 (1999).

86. A. G. Gayubo, A. T. Aguayo, A. Atutxa, R. Aguado, J. Bilbao, *Ind. Eng. Chem. Res.* **43**, 2610 (2004).

87. A. G. Gayubo *et al.*, *Ind. Eng. Chem. Res.* **43**, 2619 (2004).

88. A. G. Gayubo, A. T. Aguayo, A. Atutxa, B. Valle, J. Bilbao, *J. Chem. Technol. Biotechnol.* **80**, 1244 (2005).

89. P. Chantal, S. Kaliaguine, J. L. Grandmaison, A. Mahay, *Appl. Catal.* **10**, 317 (1984).

90. T. A. Milne, R. J. Evans, J. Filley, in *Research in Thermochemical Biomass Conversion* A. V. Bridgwater, J. L. Kuester, Eds. (Elsevier Appl. Sci., London, 1988).

91. C. H. Bartholomew, R. J. Farrauto, *Fundamentals of Industrial Catalytic Processes*. (Wiley, Hoboken, NJ, 2006).

92. J. T. F. Degnan, M. Smith, C. R. Venkat, *Appl. Catal., A* **221**, 283 (2001).

93. C. Perego, P. Ingallina, *Catal. Today* **73**, 3 (2002).

94. *Alpha Olefins Applications Handbook* G. R. Lappin, J. D. Sauer, Eds., (Marcel Dekker, New York, NY, 1989).

95. H. H. Szmant, *Organic Building Blocks of the Chemical Industry*. (John Wiley, New York, NY, 1989).

96. N. Y. Chen, J. T. F. Degnan, L. R. Koenig, *Chemtech* **16**, 506 (1986).

97. T. A. Milne, F. Agblevor, M. Davis, S. Deutch, D. Johnson, in *Developments in Thermal Biomass Conversion*, A. V. Bridgwater, D. G. B. Boocock, Eds. (Blackie Academic and Professional, London, UK, 1997), pp. 409-424.

98. J. S. Shabtai, W. W. Zmierczak, E. Chornet, *US Patent 5959167*. (The University of Utah Research Foundation, USA, 1999).

99. J. S. Shabtai, W. W. Zmierczak, E. Chornet, *US Patent 6172272 B1*. (The University of Utah, USA, 2001).

100. J. E. Miller, L. Evans, A. Littlewolf, D. E. Trudell, *Fuel* **78**, 1363 (1999).

101. C. Zhao, Y. Kou, A. A. Lemonidou, X. Li, J. A. Lercher, *Angew. Chem., Int. Ed.* **48**, 3987 (2009).

102. S. Crossley, J. Faria, M. Shen, D. E. Resasco, *Science* **327**, 68 (2010).

103. C. Zhao, Y. Kou, A. A. Lemonidou, X. B. Li, J. A. Lercher, *Chem. Comm.* **46**, 412 (2010).

104. H. Olcay, L. Xu, Y. Xu, G. W. Huber, *ChemCatChem*, (2010).

105. M. Guisnet, N. S. Gnep, F. Alario, *Appl. Catal., A* **89**, 1 (1992).

106. V. R. Choudhary, P. Devadas, S. Banerjee, A. K. Kinage, *Microporous Mesoporous Mat.* **47**, 253 (2001).

107. C. E. G. Padro, V. Putsche, "Survey of the economics of hydrogen technologies" *NREL/TP-570-27079* (National Renewable Energy Laboratory, 1999).

108. National Research Council and National Academy of Engineering, "*The Hydrogen Economy: Opportunities, Costs, Barriers, and R&D Needs"* (National Academies Press, Washington DC, 2004).

109. G. W. Huber, J. W. Shabaker, J. A. Dumesic, *Science* **300**, 2075 (2003).

110. R. Agrawal, N. R. Singh, F. H. Ribeiro, W. N. Delgass, *Proc. Natl. Acad. Sci. U.S.A.* **104**, 4828 (2007).

111. R. K. M. R. Kallury, T. T. Tidwell, D. G. B. Boocock, D. H. L. Chow, *Can. J. Chem.* **62**, 2540 (1984).

112. E. Laurent, B. Delmon, *Appl. Catal. A* **109**, 77 (1994).

113. A. Gutierrez, R. K. Kaila, M. L. Honkela, R. Slioor, A. O. I. Krause, *Catal. Today* **147**, 239 (2009).